Thin film composite nanofiltration membranes for extreme conditions

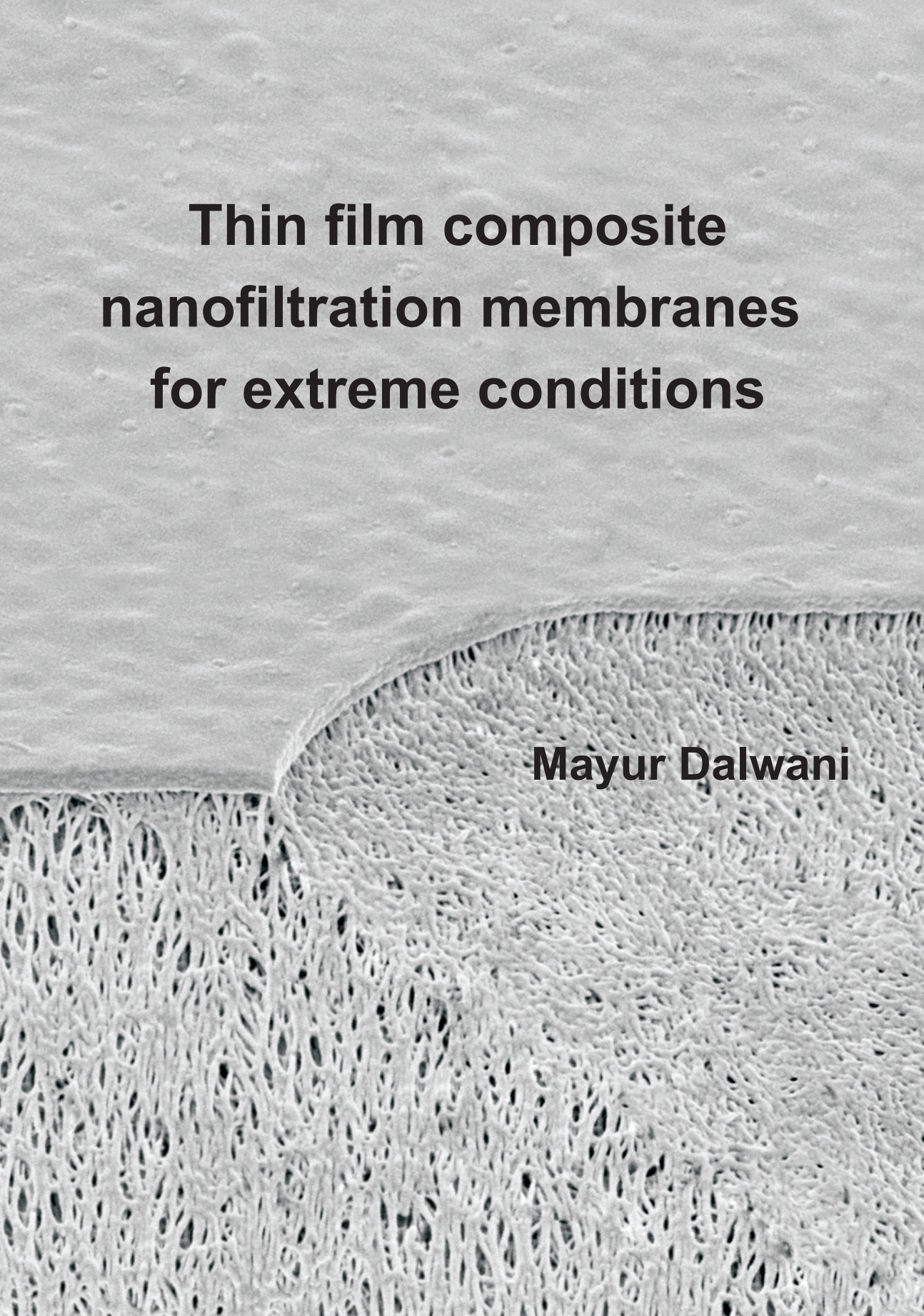

Mayur Dalwani

THIN FILM COMPOSITE NANOFILTRATION MEMBRANES FOR EXTREME CONDITIONS

This is an Institute for Sustainable Process Technology (ISPT) project.

Promotion committee

Prof. Dr.-Ing. M. Wessling (promotor)	University of Twente
Dr. Ir. N.E. Benes (co-promotor)	University of Twente
Prof. Dr. Ir. R.G.H. Lammertink	University of Twente
Prof. Dr. Ir. A. Nijmeijer	University of Twente
Prof. I. Vankelecom	Katholieke Universiteit Leuven
Dr. D. Stamatialis	University of Twente
Ir. G. Bargeman	AkzoNobel Chemicals BV

Thin film composite nanofiltration membranes for extreme conditions

ISBN: 978-90-365-3276-1

DOI: http://dx.doi.org/10.3990/1.9789036532761

Printed by Gildeprint Drukkerij, Enschede, The Netherlands

THIN FILM COMPOSITE NANOFILTRATION MEMBRANES FOR EXTREME CONDITIONS

DISSERTATION

To obtain
the degree of doctor at the University of Twente,
on the authority of the rector magnificus,
Prof. Dr. H. Brinksma,
on account of the decision of the graduation committee,
to be publicly defended on
Friday the 11th of November, 2011, at 16:45

by

Mayur Ramesh Dalwani

Born on January 22nd, 1981
In Mumbai, India

This dissertation has been approved by:

Prof. Dr.-Ing. M. Wessling (promotor)

Dr. Ir. N.E. Benes (co-promotor)

CONTENTS

General Introduction

A membrane is a permselective barrier between two phases that facilitates separation of components on application of a driving force. This thesis focuses on pressure driven membrane separation of solutes from dilute liquid solutions [1]. This type of separation can be classified as microfiltration, ultrafiltration, nanofiltration or reverse osmosis, depending on size and charge of the solutes to be separated.

After the significant commercial success of reverse osmosis and ultrafiltration, membranes with separation characteristics in between these two technologies are foreseen to have a promising market [2, 3]. Such membranes are referred to as nanofiltration (NF) membranes [1, 4]. Typically, NF involves separation of monovalent and divalent salts, or organic solutes with molecular weight in the range 200 to 1000 g mol^{-1} [5]. Although most commercial polymeric NF membranes are suitable for treating aqueous streams at pH levels between 2 and 10, many potential applications in the chemical industry involve much more aggressive conditions [2, 5]. A non-exhaustive list of applications includes treatment of effluents from the pulp and paper [6] and the textile industry [2], separation of hemicellulose from concentrated alkaline process liquors [7], purification of acids [8, 9], removal of metals like copper and gold from process streams with a high sulfuric acid concentration [10] and the removal of sulfate ions from effluents in the mining industry [11]. This thesis focuses on the development and performance characterization of stable membranes for these harsh applications.

1.1 pH dependent performance

It has been demonstrated that the feed pH during NF has a prominent effect on the separation performance. Mänttäri and coworkers have shown that the solution pH alters retention and flux of diverse commercial membranes differently and is strongly dependent on charge or chemistry of the polymer network [12]. As per their claim, if membranes possess dissociable groups then they demonstrate a more open structure in alkaline conditions, leading to a higher flux and a consequent lower retention [12]. Meihong and coworkers [13] also observed a

similar increase in flux at alkaline pH on their in-house prepared polyamide membranes. Further, dissociation of the carboxylic groups at elevated pH facilitated improved sodium sulfate removal from concentrated brine solutions of the chloralkali industry [13]. On the other hand, Tang et al. [14] and Lianchao et al. [15] have reported significant decrease of polyamide membrane flux with increasing pH. It is reasoned that as the pH in the feed decreases, amino groups on the polyamide membrane surface are changed into RH_3N^+ or R_3HN^+, which results in either an increase in the hydrophilicity of the membrane [14], or an enlarged pore surface [15]. Whereas at elevated pH electrostatic repulsion between the negatively charged $-COO^-$ group on the membrane surface and OH^- in the feed solution causes shrinkage of the pores. Furthermore, pH of the feed solution affects significantly the fouling potential of the membranes [16, 17]. Polyamide membranes show a greater tendency to foul in acidic environments than at higher pH conditions [16]. Hwang et al. [17] studied the effect of feed pH during filtration of an aqueous mixture containing humic acid and sodium chloride. By increasing the pH from 5 to 11 an increase in flux and sodium chloride rejection was observed. This increase in flux is attributed to reduced membrane fouling by humic acid at high pH. They elaborate that a rise in feed pH could cause an enhanced anionic charge on the humic acid molecule. This increased negative charge developed on the molecule leads to its higher repulsion from the anionic membrane surface due to the Donnan exclusion mechanism, consequently reducing its fouling potential. All these studies thereby suggest that apart from extensive stability tests at relevant pH, a comprehensive evaluation of membrane performance as a function of pH is particularly essential.

1.2 Thin film composite membranes

Generally a thin film composite (TFC) membrane consists of three layers (Fig. 1). The ultra-thin top layer is the actual selective barrier in the composite, and is responsible for the molecular selectivity. This top layer is supported by a porous sub layer; usually an asymmetric ultrafiltration or microfiltration membrane that

provides a sufficiently smooth surface to accommodate a defect free thin top layer. The third layer is a non-woven reinforcing fabric that provides for the main part of the mechanical strength of the composite structure.

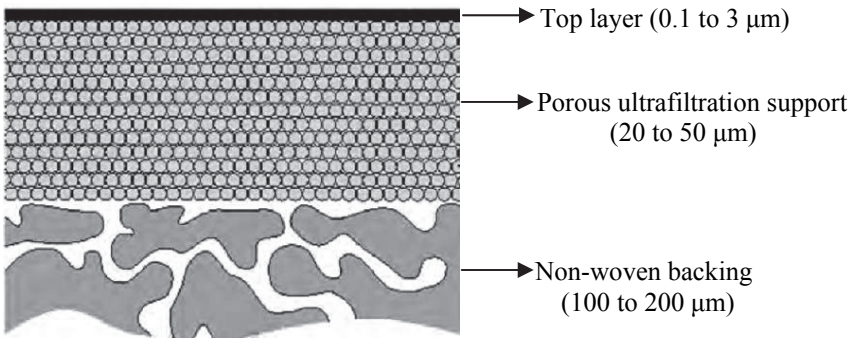

Fig. 1 : Schematic of a thin film composte membrane

Since their commercial recognition in the 1980's thin film composite (TFC) membranes have dominated most of the nanofiltration / reverse osmosis market. TFC membranes offer some key advantages relative to traditional asymmetric membranes. In a TFC the specific features of each individual layer can be tailored independently to obtain a composite with desirable properties. In contrast, in asymmetric membranes consisting of a single material, compromises must be made with respect to contradicting demands on materials properties of the dense top layer and the porous sub structure. The top layer of a TFC can be chosen independently from a vast variety of chemical structures, including crosslinked polymeric compositions that can be formed into thin films. The hydrophilicity, and thus the flux, and chemical resistance can be tuned independent of the TFC sub layers. The ultra-porous sub layer is generally prepared on top of the non-woven fabric via the phase inversion technique [1]. This sub layer can also be tailored independently, aiming at minimum resistance to permeate flow combined with enhanced compression resistance.

In a TFC the top layer is formed by a variety of techniques ranging from simple solution casting (spin coating, dip coating and spray coating) to intricate polymerizations (interfacial polymerization, in-situ polymerization, plasma polymerization and grafting). In this thesis two of the above mentioned methods have been utilized to fabricate TFCs: the spin coating technique (**chapter 4**) and

the interfacial polymerization technique (**chapter 3 and 5**). The important parameters involved in these two techniques are briefly addressed below.

1.2.1 Spin Coating

Spin coating is a quick and easy laboratory method to generate thin and homogeneous organic films out of solutions. In brief, an excess amount of solution is placed on an ultraporous substrate that is then rotated at high speed. The liquid spreads due to centrifugal forces and a uniform liquid layer forms on the substrate. Evaporation of solvent results a uniform solid polymer coating. Fig. 2 is a schematic presentation of a spin coater [18].

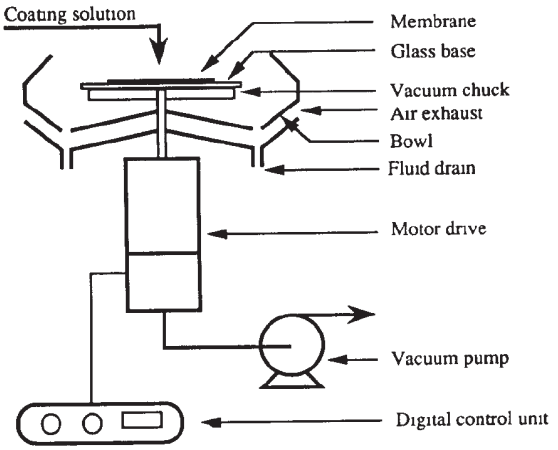

Fig. 2 : Schematic of a spin coater

The quality of the thin coating layer depends mainly on the spinning speed [19], solvent evaporation rate [20, 21], viscosity or concentration of the polymer solution [22] and the pore and surface characteristics of the support [18]. By keeping in mind these physical parameters, a thin polymer film of almost any composition can be coated on a suitable support. Spin coating has limited application in the field of membrane technology on a commercial scale, due to restricted product size, but benefits from the minimal amount of required polymer solution. On the laboratorial or research level it allows quick preparation of numerous variations, which at a later stage could easily be up-scaled via analogous dip-coating technique to facilitate larger membrane areas.

1.2.2 Interfacial polymerization

Although the Interfacial Polymerization (IP) technique involves relatively many more intricate parameters compared to spin coating, it is a very popular technique to manufacture thin film composite (TFC) membranes [4]. This technique has been widely used to fabricate RO and NF membranes [23-37]. An elaborate discussion of several developed IP membranes along with the chemistry of the IP layers can be found in the exhaustive overview by Peterson [4]. In IP, polymerization is carried out between two highly reactive monomers dissolved in two immiscible solvents. The two solvents represent two separate phases, in contact only at a distinct interface. This allows the reactive monomers present in the phases to react only at this distinct interface. The IP process consists of a sequence of steps, depicted in Fig. 3. In the first step an ultraporous support is pretreated to make it suitable for the IP process. Typically, in this step the wetting behavior of the support is adjusted by a surfactant. In the second step the substrate is impregnated with one of the solvents, usually the aqueous, containing one of the reactants. The impregnated support is then immersed in the second phase, containing the second reactant. Since the two phases are immiscible with each other an interface is created between them. Given that the two monomers / reactants are highly reactive with each other, one of the monomers travels through the interface and reacts with the other monomer to form a polymerized product. Due to the limited partition coefficient of the reactants in the opposite phase and the barrier created at the interface, a very thin polymer layer is formed. Due to the very high reactivity of the two monomers the IP layer is generally dense. The combination of a thin and dense film potentially allows for a high flux and high selectivity in membrane applications. Finally, after allowing a certain reaction time, the two phases are drained out from the membrane leaving behind the thin selective film on the support.

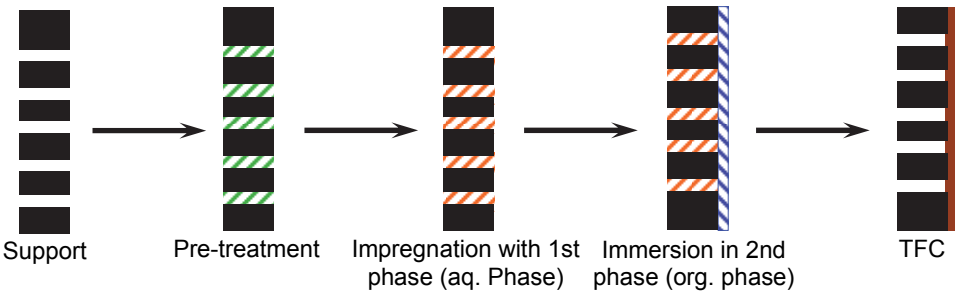

Fig. 3 : Interfacial polymerization process

There are several parameters which can be varied during fabrication of TFC membranes via the IP route, in order to engineer the ultimate membrane morphology and performance [4, 30, 35, 38-42]. Researchers have studied many parameters such as different monomer types [5, 15, 27, 34, 36, 39, 43-54], viscosity of the phases [38], and temperature [40]. The most important parameters relevant to this study are discussed below.

- **Aqueous phase reactant:** Predominantly, amines are used as the aqueous phase reactant. As compared to aliphatic diamines, membranes made from aromatic diamines generally form denser polymer layers, and thus allow higher selectivity at the cost of a lower flux [5]. Correspondingly, aromatic diamines (e.g., m-phenylene diamine, p-phenylene diamine) are used to make dense RO membranes and aliphatic diamines (e.g., piperazine , amine substituted piperazines) are used to make NF membranes. The membrane performance can be engineered by blending different amines and using them together in the aqueous phase [23].
- **Organic phase reactant:** As previously mentioned acyl chlorides are usually employed as the monomer in the organic phase. Similar to amines in the aqueous phase, different classes or types of acyl chlorides [55] [45] or blending [52] strongly influence the membrane performance.
- **Reactant concentration and reaction time:** In general high monomer concentration [30, 32, 34, 56], high reaction rates [47] and longer polymerization times[32, 34, 39] results in thicker layers with higher rejections but lower fluxes [49].

- **Additives:** Many additives are reported to be employed in the IP technique. The most important additives used are phase transfer catalysts. These do not only increase the polymerization rate by enlarging the contact surface between the phases, but also limit the influx of amine into the organic phase. The reduced transport rate of amine reduces the film thickness [35, 57]. Wettability of the often hydrophobic support is enhanced by agents such as Sodium dodecyl sulfate (SDS) and Poly (ethylene glycol) [34]. Hydrophilicity of the formed IP layer can be improved introducing non-polymerizable carboxylic groups [46]. Some researchers claim to enhance chemical resistance of the membrane by adding additives like hydroquinone in the aqueous phase [58].

1.2.3 Hybrid membranes

The benefits of using polymeric-inorganic hybrid materials in the field of membrane technology have been adequately demonstrated [59-77]. In this field, numerous inorganic fillers like zeolite [59, 60, 62], titanium oxide [61], silica [64], carbon molecular sieves [65], sodium alginate [66] etc have been employed for the fabrication of hybrid thin films, generally classified as mixed matrix membranes. Vankelecom and co-workers have successfully fabricated TFC membranes consisting of a PDMS selective layer in which inorganic fillers are dispersed, with a polyacrlonitrile and polyimide support [67, 68]. These composites have been demonstrated as efficient PDMS based solvent resistant nanofiltration membranes [59, 67]. Further they have extended the concept to polyimide based NF membranes for applications involving aprotic solvents [69]. Studies have also demonstrated advantages of incorporating fillers like zeolite [70, 73, 74], titanium dioxide [75], silver [72, 76] and silica [71, 77] within the interfacial polymerization layer. In these studies inorganic nanoparticles were first dispersed in one of the phases and then interfacial polymerization is carried out on an ultraporous support similar to the procedure illustrated in section 1.2.2. In all these cases the inorganic nanoparticles are primarily inert fillers which do not participate in IP

reaction, but are just physically dispersed within the matrix. Consequently the problem of leaking via interfacial voids created between the particles and the IP layer cannot be ruled out [73, 74] especially at high particle loadings. Thus techniques allowing particles to be covalently linked and homogenously distributed in the polymer matrix could be beneficial for fabrication of hybrid membranes.

1.3 Scope of the thesis

This thesis focuses on fabrication and performance evaluation of thin film composite membranes during nanofiltration with special attention to extreme pH applications.

Chapter 2 presents a new method based on gel permeation chromatography for molecular weight cut off analysis of NF membranes as a function of pH.

Chapter 3 utilizes this method to characterize in-house developed piperazine-trimesoyl chloride TFC membranes as a function of pH. Donnan steric partitioning pore model is used to relate the pH induced performance changes to morphological changes in the membrane matrix. Following an investigation of optimal fabrication parameters the performance of the developed membranes is compared to commercial NF membranes popularly used in the industry currently.

Chapter 4 explores the applicability of sulfonated poly (ether ether ketone) (SPEEK) based TFC membranes during filtration at extreme filtration conditions. The optimal fabrication parameters required for obtaining stable membranes is discussed. Apart from extensive stability tests the performance of the new membranes is compared to commercially available membranes. Additionally a technique to crosslink SPEEK to enhance membrane retention is briefly addressed.

In **Chapter 5** the technique of IP is exploited for fabrication of novel hybrid membranes which contain polyhedral oligomeric silsesquioxanes (POSS) as the primary building blocks. The concept is illustrated using a water soluble quaternary ammonium chloride salt functionalized POSS as the aqueous phase monomer, and trimesoyl chloride as the organic phase monomer. Fourier

transform infrared spectrometry and X-ray photoelectron spectroscopy are used to confirm and analyze the reaction mechanism. Further important fabrication parameters and vital reaction conditions are discussed.

References

[1] M. Mulder, Basic Principles of Membrane Technology, Kluver Academic publishers 2003.

[2] A.I. Schafer; A.G. Fane; T.D. Waite, Nanofiltration — Principles and Applications, Elsevier 2005.

[3] S.P. Nunes; K.V. Peinemann, Membrane Technology in the Chemical Industry, Wiley-VCH, Weinhim 2001.

[4] R.J. Petersen, Composite reverse osmosis and nanofiltration membranes, Journal of Membrane Science 83 (1993) 81-150.

[5] P. Vandezande; L.E.M. Gevers; I.F.J. Vankelecom, Solvent resistant nanofiltration: separating on a molecular level, Chemical Society Reviews (2008) -.

[6] M. Nyström; L. Kaipia; S. Luque, Fouling and retention of nanofiltration membranes, Journal of Membrane Science 98 (1995) 249-262.

[7] R. Schlesinger; G. Gotzinger; H. Sixta; A. Friedl; M. Harasek, Evaluation of alkali resistant nanofiltration membranes for the separation of hemicellulose from concentrated alkaline process liquors, Desalination 192 (2006) 303-314.

[8] M.P. González; R. Navarro; I. Saucedo; M. Avila; J. Revilla; C. Bouchard, Purification of phosphoric acid solutions by reverse osmosis and nanofiltration, Desalination 147 (2002) 315-320.

[9] D. Jakobs; G. Baumgarten, Nanofiltration of nitric acidic solutions from picture tube production, Desalination 145 (2002) 65-68.

[10] S. Platt; M. Nyström; A. Bottino; G. Capannelli, Stability of NF membranes under extreme acidic conditions, Journal of Membrane Science 239 (2004) 91-103.

[11] T.J.K. Visser; S.J. Modise; H.M. Krieg; K. Keizer, The removal of acid sulphate pollution by nanofiltration, Desalination 140 (2001) 79-86.

[12] M. Mänttäri; A. Pihlajamäki; M. Nyström, Effect of pH on hydrophilicity and charge and their effect on the filtration efficiency of NF membranes at different pH, Journal of Membrane Science 280 (2006) 311-320.

[13] M. Liu; S. Yu; Y. Zhou; C. Gao, Study on the thin-film composite nanofiltration membrane for the removal of sulfate from concentrated salt aqueous: Preparation and performance, Journal of Membrane Science 310 (2008) 289-295.

[14] B. Tang; Z. Huo; P. Wu, Study on a novel polyester composite nanofiltration membrane by interfacial polymerization of triethanolamine (TEOA) and trimesoyl chloride (TMC): I. Preparation, characterization and nanofiltration properties test of membrane, Journal of Membrane Science 320 (2008) 198-205.

[15] L. Li; B. Wang; H. Tan; T. Chen; J. Xu, A novel nanofiltration membrane prepared with PAMAM and TMC by in situ interfacial polymerization on PEK-C ultrafiltration membrane, Journal of Membrane Science 269 (2006) 84-93.

[16] D. Nanda; K.-L. Tung; Y.-L. Li; N.-J. Lin; C.-J. Chuang, Effect of pH on membrane morphology, fouling potential, and filtration performance of nanofiltration membrane for water softening, Journal of Membrane Science 349 (2010) 411-420.

[17] J.-E. Hwang; J. Jegal; K.-H. Lee, Separation of humic acid with nanofiltration polyamide composite membranes, Journal of Applied Polymer Science 86 (2002) 2847-2853.

[18] J.D. Le Roux; D.R. Paul, Preparation of composite membranes by a spin coating process, Journal of Membrane Science 74 (1992) 233-252.

[19] K.J. Skrobis; D.D. Denton; A.V. Skrobis, Effect of early solvent evaporation on the mechanism of the spin-coating of polymeric solutions, Polymer Engineering & Science 30 (1990) 193-196.

[20] B.T. Chen, Investigation of the solvent-evaporation effect on spin coating of thin films, Polymer Engineering & Science 23 (1983) 399-403.

[21] J.H. Lai, An investigation of spin coating of electron resists, Polymer Engineering & Science 19 (1979) 1117-1121.

[22] L.L. Spangler; J.M. Torkelson; J.S. Royal, Influence of solvent and molecular weight on thickness and surface topography of spin-coated polymer films, Polymer Engineering & Science 30 (1990) 644-653.

[23] P.L. Riley; C.E. Milstead; A.L. Lloyd; M.W. Seroy; M. Tagami, Spiral-wound thin-film composite membrane systems for brackish and seawater desalination by reverse osmosis, Desalination 23 (1966) 331-355.

[24] R.L. Riley; R.L. Fox; C.R. Lyons; C.E. Milstead; M.W. Seroy; M. Tagami, Spiral-wound poly (ether/amide) thin-film composite membrane systems, Desalination 19 (1976) 113-126.

[25] A. Prakash Rao; N.V. Desai; R. Rangarajan, Interfacially synthesized thin film composite RO membranes for seawater desalination, Journal of Membrane Science 124 (1997) 263-272.

[26] J.E. Cadotte; R.J. Petersen; R.E. Larson; E.E. Erickson, A new thin-film composite seawater reverse osmosis membrane, Desalination 32 (1980) 25-31.

[27] J.Z. Runhong Du, Positively charged composite nanofiltration membrane prepared by poly(-dimethylaminoethyl methacrylate)/polysulfone, Journal of Applied Polymer Science 91 (2004) 2721-2728.

[28] J. Cadotte; R. Forester; M. Kim; R. Petersen; T. Stocker, Nanofiltration membranes broaden the use of membrane separation technology, Desalination 70 (1988) 77-88.

[29] United States Patent 4767645 1988.

[30] S. Verissimo; K.V. Peinemann; J. Bordado, Thin-film composite hollow fiber membranes: An optimized manufacturing method, Journal of Membrane Science 264 (2005) 48-55.

[31] S. Verissimo; K.V. Peinemann; J. Bordado, Influence of the diamine structure on the nanofiltration performance, surface morphology and surface charge of the composite polyamide membranes, Journal of Membrane Science 279 (2006) 266-275.

[32] A.L. Ahmad; B.S. Ooi, Properties-performance of thin film composites membrane: study on trimesoyl chloride content and polymerization time, Journal of Membrane Science 255 (2005) 67-77.

[33] A.L. Ahmad; B.S. Ooi, Optimization of composite nanofiltration membrane through pH control: Application in CuSO4 removal, Separation and Purification Technology 47 (2006) 162-172.

[34] S.-H. Chen; D.-J. Chang; R.-M. Liou; C.-S. Hsu; S.-S. Lin, Preparation and separation properties of polyamide nanofiltration membrane, Journal of Applied Polymer Science 83 (2002) 1112-1118.

[35] S.G.M.K.-H.L. Jonggeon Jegal, Factors affecting the interfacial polymerization of polyamide active layers for the formation of polyamide composite membranes, Journal of Applied Polymer Science 86 (2002) 2781-2787.

[36] X.-Z. Wei; L.-P. Zhu; H.-Y. Deng; Y.-Y. Xu; B.-K. Zhu; Z.-M. Huang, New type of nanofiltration membrane based on crosslinked hyperbranched polymers, Journal of Membrane Science 323 (2008) 278-287.

[37] United States Patent 5755964 1996.

[38] A.K. Ghosh; B.-H. Jeong; X. Huang; E.M.V. Hoek, Impacts of reaction and curing conditions on polyamide composite reverse osmosis membrane properties, Journal of Membrane Science 311 (2008) 34-45.

[39] F.L.B.S. Yujun Song, Preparation, characterization, and application of thin film composite nanofiltration membranes, Journal of Applied Polymer Science 95 (2005) 1251-1261.

[40] A. Prakash Rao; S.V. Joshi; J.J. Trivedi; C.V. Devmurari; V.J. Shah, Structure-performance correlation of polyamide thin film composite membranes: effect of coating conditions on film formation, Journal of Membrane Science 211 (2003) 13-24.

[41] I.J. Roh; J.-J. Kim; S.Y. Park, Mechanical properties and reverse osmosis performance of interfacially polymerized polyamide thin films, Journal of Membrane Science 197 (2002) 199-210.

[42] United States Patent 6132804 2000.

[43] P.R. Buch; A.V.R. Reddy, Synthesis, characterization and thermal properties of soluble aromatic poly(amide imide)s, Polymer 46 (2005) 5524-5532.

[44] S.G.J.Y.S.Y.D.W.I. Seung-Yeop Kwak, Details of surface features in aromatic polyamide reverse osmosis membranes characterized by scanning electron and atomic force microscopy, Journal of Polymer Science Part B: Polymer Physics 37 (1999) 1429-1440.

[45] S.Y.P.J.J.K.C.K.K. I. J. Roh, Effects of the polyamide molecular structure on the performance of reverse osmosis membranes, Journal of Polymer Science Part B: Polymer Physics 36 (1998) 1821-1830.

[46] Z. Yong; Y. Sanchuan; L. Meihong; G. Congjie, Polyamide thin film composite membrane prepared from m-phenylenediamine and m-phenylenediamine-5-sulfonic acid, Journal of Membrane Science 270 (2006) 162-168.

[47] C.K. Kim; J.H. Kim; I.J. Roh; J.J. Kim, The changes of membrane performance with polyamide molecular structure in the reverse osmosis process, Journal of Membrane Science 165 (2000) 189-199.

[48] S. Sridhar; B. Smitha; S. Mayor; B. Prathab; T. Aminabhavi, Gas permeation properties of polyamide membrane prepared by interfacial polymerization, Journal of Materials Science 42 (2007) 9392-9401.

[49] Y. Song; P. Sun; L.L. Henry; B. Sun, Mechanisms of structure and performance controlled thin film composite membrane formation via interfacial polymerization process, Journal of Membrane Science 251 (2005) 67-79.

[50] L. Li; S. Zhang; X. Zhang; G. Zheng, Polyamide Thin Film Composite Membranes Prepared From Isomeric Biphenyl Tetraacyl Chloride and m-Phenylenediamine, Journal of Membrane Science In Press, Accepted Manuscript.

[51] Y. Shang; Y. Peng, UF membrane of PVA modified with TDI, Desalination 221 (2008) 324-330.

[52] United States patent 5274047 1992.

[53] European Patent EP0311912 1991.

[54] United States Patent 6536605 2003.

[55] M. Liu; D. Wu; S. Yu; C. Gao, Influence of the polyacyl chloride structure on the reverse osmosis performance, surface properties, chlorine stability of the thin film composite polyamide membranes, Journal of Membrane Science In Press, Accepted Manuscript.

[56] G.-Y. Chai; W.B. Krantz, Formation and characterization of polyamide membranes via interfacial polymerization, Journal of Membrane Science 93 (1994) 175-192.

[57] United States Patent 5693227 1997.

[58] M.M. Jayarani; S.S. Kulkarni, Thin-film composite poly(esteramide)-based membranes, Desalination 130 (2000) 17-30.

[59] L.E.M. Gevers; I.F.J. Vankelecom; P.A. Jacobs, Zeolite filled polydimethylsiloxane (PDMS) as an improved membrane for solvent-resistant nanofiltration (SRNF), Chemical Communications (2005) 2500-2502.

[60] M. Jia; K.-V. Peinemann; R.-D. Behling, Molecular sieving effect of the zeolite-filled silicone rubber membranes in gas permeation, Journal of Membrane Science 57 (1991) 289-292.

[61] K. Ebert; D. Fritsch; J. Koll; C. Tjahjawiguna, Influence of inorganic fillers on the compaction behaviour of porous polymer based membranes, Journal of Membrane Science 233 (2004) 71-78.

[62] Xin Chen; H. Yang; Z. Gu; Z. Shao, Preparation and characterization of HY zeolite-filled chitosan membranes for pervaporation separation, Journal of Applied Polymer Science 79 (2001) 1144-1149.

[63] Y.-T.F.J.-R.C.S.-Y.T. Bor-Kuan Chen, Effects of meta and para diamines on the properties of polyetherimide nanocomposite films prepared by the sol-gel process, Journal of Applied Polymer Science 105 (2007) 1093-1100.

[64] M. Sadeghi; G. Khanbabaei; A.H.S. Dehaghani; M. Sadeghi; M.A. Aravand; M. Akbarzade; S. Khatti, Gas permeation properties of ethylene vinyl acetate-silica nanocomposite membranes, Journal of Membrane Science 322 (2008) 423-428.

[65] D.Q. Vu; W.J. Koros; S.J. Miller, Mixed matrix membranes using carbon molecular sieves: I. Preparation and experimental results, Journal of Membrane Science 211 (2003) 311-334.

[66] S.G. Adoor; B. Prathab; L.S. Manjeshwar; T.M. Aminabhavi, Mixed matrix membranes of sodium alginate and poly(vinyl alcohol) for pervaporation

dehydration of isopropanol at different temperatures, Polymer 48 (2007) 5417-5430.

[67] L.E.M. Gevers; I.F.J. Vankelecom; P.A. Jacobs, Solvent-resistant nanofiltration with filled polydimethylsiloxane (PDMS) membranes, Journal of Membrane Science 278 (2006) 199-204.

[68] WO2005/058465 2005.

[69] K. Vanherck; P. Vandezande; S.O. Aldea; I.F.J. Vankelecom, Cross-linked polyimide membranes for solvent resistant nanofiltration in aprotic solvents, Journal of Membrane Science 320 (2008) 468-476.

[70] B.-H. Jeong; E.M.V. Hoek; Y. Yan; A. Subramani; X. Huang; G. Hurwitz; A.K. Ghosh; A. Jawor, Interfacial polymerization of thin film nanocomposites: A new concept for reverse osmosis membranes, Journal of Membrane Science 294 (2007) 1-7.

[71] P.S. Singh; V.K. Aswal, Characterization of physical structure of silica nanoparticles encapsulated in polymeric structure of polyamide films, Journal of Colloid and Interface Science 326 (2008) 176-185.

[72] P. Dallas; D. Niarchos; D. Vrbanic; N. Boukos; S. Pejovnik; C. Trapalis; D. Petridis, Interfacial polymerization of pyrrole and in situ synthesis of polypyrrole/silver nanocomposites, Polymer 48 (2007) 2007-2013.

[73] M. Fathizadeh; A. Aroujalian; A. Raisi, Effect of added NaX nano-zeolite into polyamide as a top thin layer of membrane on water flux and salt rejection in a reverse osmosis process, Journal of Membrane Science 375 (2011) 88-95.

[74] M.L. Lind; A.K. Ghosh; A. Jawor; X. Huang; W. Hou; Y. Yang; E.M.V. Hoek, Influence of Zeolite Crystal Size on Zeolite-Polyamide Thin Film Nanocomposite Membranes, Langmuir 25 (2009) 10139-10145.

[75] H.S. Lee; S.J. Im; J.H. Kim; H.J. Kim; J.P. Kim; B.R. Min, Polyamide thin-film nanofiltration membranes containing TiO2 nanoparticles, Desalination 219 (2008) 48-56.

[76] S.Y. Lee; H.J. Kim; R. Patel; S.J. Im; J.H. Kim; B.R. Min, Silver nanoparticles immobilized on thin film composite polyamide membrane: characterization, nanofiltration, antifouling properties, Polymers for Advanced Technologies 18 (2007) 562-568.

[77] G.L. Jadav; P.S. Singh, Synthesis of novel silica-polyamide nanocomposite membrane with enhanced properties, Journal of Membrane Science 328 (2009) 257-267.

A method for characterizing membranes during nanofiltration at extreme pH

THIS CHAPTER HAS BEEN PUBLISHED:

M. Dalwani; N.E. Benes; G. Bargeman; D. Stamatialis; M. Wessling, A method for characterizing membranes during nanofiltration at extreme pH, Journal of Membrane Science 363 (2010) 188-194.

ABSTRACT

This work presents a method for molecular weight cut off (MWCO) characterization of nanofiltration membranes, in a broad range of acidic and alkaline environments. Polyethylene glycols (PEG) have been identified as suitable marker molecules with sufficient chemical stability under the harsh conditions of interest. PEG molecular weight distributions have been analyzed using gel permeation chromatography (GPC). To allow quantitative GPC analysis, a protocol is presented to overcome the problem of an overlapping salt peak in the GPC elugram. The method is applied to a well-known commercial nanofiltration membrane (NF-270, DOW FILMTEC™) in the pH range 2-12. This membrane has similar MWCO (~270 g mol-1) and permeance (~10 L m-2 hr-1 bar-1) in acid environment and at neutral conditions. At pH=12 a reversible increase was observed for the MWCO (~380 g mol-1) and the permeance (~12 L m-2 hr-1 bar-1). This demonstrates the added value of our method to observe the change of MWCO as a function of pH during nanofiltration at the relevant conditions.

2.1 Introduction

Nanofiltration (NF) membranes have separation characteristics between those of ultrafiltration and reverse osmosis membranes [1, 2]. Typically, NF involves separation of monovalent and divalent salts, or organic solutes with molecular weight in the range 200 to 1000 g mol^{-1} [3]. At present, most commercial NF membranes are known to be suitable for treatment of aqueous streams at pH levels between 2 and 10. However, many potential applications in the chemical industry involve much more aggressive conditions [3, 4]. Advances in the development of stable membranes will aid the use of membranes in such applications. An essential requirement in this respect is a general molecular weight cut off (MWCO) determination method that enables comparison of membranes from different sources [5, 6]. The MWCO corresponds to the molecular weight that is rejected 90% by the membrane [1, 7]. Our work in fact focuses on developing a method for MWCO characterization during nanofiltration at extreme pH conditions.

The choice of a suitable marker molecule is crucial for such a method. A suitable marker molecule should combine the following: sufficient stability and solubility in the conditions of interest, uncharged (neutral), and a broad molecular weight distribution. Various solute molecules have been proposed as marker. The most commonly used are dyes whose concentration can be measured using a UV spectrophotometer. Analysis of retention of such a dye is very quick, easy and effective [8-11]. Ideally, MWCO analysis based on dyes would involve dyes with the same basic units, but differing in the molecular weight. Such dyes will have a peak absorbance at a similar wavelength, thus sequential retention measurements of dyes with different molecular weight will be required to determine the MWCO. Deriving the MWCO from a mixture of dyes with different chemical structure has two drawbacks. Firstly, the interaction of each type of dye with the membrane will be different due to the different charge, rigidity and shape of the dyes. Since the dyes are charged dielectric exclusion effects and interactions with charges on the membrane surface would also have to be taken into account. Secondly, it is

difficult to find a suitable variety of dyes, with varying molecular weights and distinctly separated peak absorption wavelengths [5].

An alternative is using oligomers, or broadly distributed mixtures thereof, combined with gas chromatography [12-14], total organic content analysis [15-18], gel permeation chromatography (GPC) [19-27] or high pressure liquid chromatography [5, 28]. Polyethylene glycols (PEG) are cheap oligomers that are easily available with a molecular weight ranging from 62 g mol^{-1} (ethylene glycol monomer) up to ~40,000 g mol^{-1}. PEGs are inherently neutral molecules soluble in water and a wide range of organic solvents. This makes them ideal markers for MWCO analysis in aqueous [17, 19, 23-26, 29] as well as organic feeds like ethanol, methanol, isopropanol and dimethylformamide [28]. Furthermore, PEGs are available in fractions corresponding with the NF range (e.g., PEG 200, 300, 400, 600, 1000, 1500), each fraction in turn having a broad molecular weight distribution [28].

In this work we present a method to determine the MWCO of membranes in acidic and alkaline solutions, using PEG molecules as markers. Others have studied the change in PEG retention of membranes before and after exposure to acidic and alkaline media [23]. Since it is identified that the structure of membranes can change reversibly as a function of pH [30], MWCO analysis during membrane filtration at high and low pH is, in our opinion, the most appropriate method for membrane characterization. To the best of our knowledge, MWCO characterization of membranes during nanofiltration of solutions with different pH has not been reported elsewhere. Such a method is complicated by the variation in the pH of the samples, leading to different ion contents. We demonstrate that GPC can be used for analysis of PEG mixtures with different pH, by neutralization of the sample and subsequent appropriate matching of the salt content with that of the eluent.

2.2 Experimental

2.2.1 Chemicals and Materials

Analytical grade sodium nitrate ($NaNO_3$), sodium azide (NaN_3) and ethylene glycol (EG) and synthesis quality of polyethylene glycol (PEG) with mean molecular weights of 200 g mol^{-1}, 600 g mol^{-1} and 1500 g mol^{-1} were acquired from Merck (Germany). Analytical grade sodium chloride (NaCl) (used for salt retention experiments) was acquired from Arcos Organics (Belgium). Analytical grade potassium chloride (KCl) for zeta potential measurements was obtained from Fluka (Germany). Standard volumetric solutions of 0.1 M nitric acid (HNO_3) and sodium hydroxide (NaOH) (used to alter the pH of the solutions) were purchased from Fluka (Germany). Ultrapure water from Synergy water purification system (Millipore, USA) was used to prepare all solutions.

The investigated NF membrane NF-270 was kindly provided by DOW FILMTEC™ (USA). The membrane has a polyamide skin layer on a polysulphone support, and is mechanically supported by a polyester non-woven backing.

2.2.2 Nanofiltration Setup and Filtration Protocol

Permeation experiments were carried out in a dead-end filtration setup equipped with three test cells, each having a hold up capacity of 350 cm^3 (Fig. 1). The effective membrane surface area in each cell was 13.86 cm^2. The membrane was supported by a relatively open filter paper (Blue Ribbon 589/3 Ashless Quantitative Filter Paper, Schleicher & Schuell, Germany) on top of a porous stainless steel disk. The cells were equipped with magnetic bars suspended from the top which provided continuous stirring on the membrane surface, in order to avoid concentration polarization. The bars were driven with external explosion proof magnetic stirrers (Variomag®, H+P Labortechnik GmbH, Germany), which were set at a constant rotation of 500 rpm for all experiments. The speed of the magnetic stirrers was limited to this value to avoid vortex formation inside the test

cells. The test cells were equipped with sampling valves to collect retentate samples from close to the membrane surface.

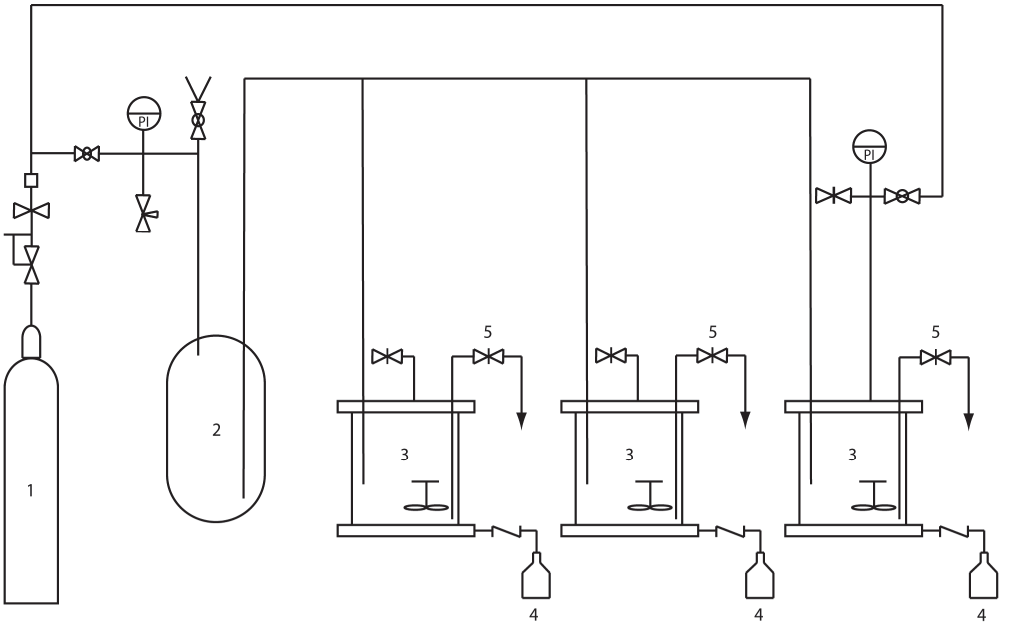

1: Gas cylinder, 2: Feed reservoir, 3: Stirred permeation cells, 4: Permeate vessels, 5: Sampling valve

Figure 1: Schematic representation of the dead-end permeation setup

All experiments were performed at room temperature (22 ± 2 °C). The following protocol was used: three membranes were clamped in the test cells with ethylene-propylene elastomer o-rings (Eriks B.V., The Netherlands). Helium gas was used to apply pressure up to 20 bar. Before each experiment, the setup was rinsed 4 to 5 times with ultrapure water. Then the feed solution, without any solutes, was supplied via the feed reservoir and the membranes were preconditioned for 1 hour, at the experimental pressure. After pre-conditioning the system was depressurized, the solution in the setup was completely removed and fresh feed solution, with solutes, was added in the feed reservoir. Filtration was performed for 1.5 hours, to reach a stable flux and concurrently avoid a significant change in the retentate concentration. Liquid permeated in the first 5 minutes was discarded. After 5 minutes a sample of the solution inside each test cell was taken. Subsequently, every 15 minutes the collected permeate weight was monitored for

each cell. After the filtration experiment, samples of the solutions inside the test cells and the collected permeates were analyzed for their compositions.

From the above analysis the flux was calculated by

$$J = \frac{V}{At} \tag{1}$$

where J is the permeate flux in [L m^{-2} hr^{-1}], V is the permeate volume [L], A is the membrane area in [m^2] and t is the permeation time [hr].

The retention R was calculated from

$$R = \frac{c - c_{\text{permeate}}}{c} \tag{2}$$

where c_{permeate} is the permeate concentration and c is the concentration inside the test cell. As the filtration was carried out in dead-end mode using a finite volume of liquid, the concentration c in the test cell will change in time and a correct analysis of the retention will require solving an in-stationary mass balance over the test cell. However, in the set-up the (change in) liquid volume in each test cell could not be accurately determined as function of time. Consequently, the average of the original feed and final retentate composition was considered in the calculations.

Salt retention

Monovalent salt retention of the membrane samples was measured using an aqueous solution of 2 g L^{-1} NaCl. Compositions of the feed, collected permeate and retentate samples were analyzed by measuring the conductivity and temperature of the samples using a 340i conductivity meter (WTW, Germany). Retention and flux were determined using the above mentioned protocol.

Molecular weight cut off

The membrane MWCO was evaluated at 10 bar, with an aqueous solution containing a mixture of PEGs with mean molar masses 200 g mol^{-1}, 600 g mol^{-1} and 1500 g mol^{-1} (each fraction 1 g L^{-1}). These PEG fractions have a broad molecular weight distribution [28], and combined form a broad distributed feed mixture. Ethylene glycol (EG) (0.2 g L^{-1}) was used as a flow marker (internal standard). During MWCO determination the pH of the feed, collected permeate, and retentate samples was measured using a 340i pH meter (WTW, Germany). Compositions of feed, permeate and retentate were analyzed by gel permeation chromatography (GPC).

GPC analyses

The GPC equipment consisted of two SUPREMA 100 Å columns from PSS Polymer Standards Service GmbH (Germany), a HPLC pump from Waters (Millipore B.V., The Netherlands) delivering the eluent at 1 ml min^{-1}, and a Shodex RI- Detector from Showa Denko GmbH (Germany). The columns were calibrated using 16 different PEG standards from the molecular weight of 62 to 42000 g mol^{-1} acquired from PSS Polymer Standards Service GmbH (Germany). During analysis 100 µL of aqueous samples containing PEGs (feed, permeate or retentate) were injected to the GPC system.

The protocol of adjusting the salt content of the mobile phase and samples at different pH is schematically illustrated in Fig. 2. Prior to GPC analyses samples were neutralized with appropriate acid or base, containing additional $NaNO_3$ to achieve a final salt concentration of 0.05 M. The $NaNO_3$ concentration of the mobile phase (eluent) was also adjusted to 0.05 M. To prevent bio fouling inside the GPC system NaN_3 (0.05 g L^{-1}) was added to both the eluent and the samples.

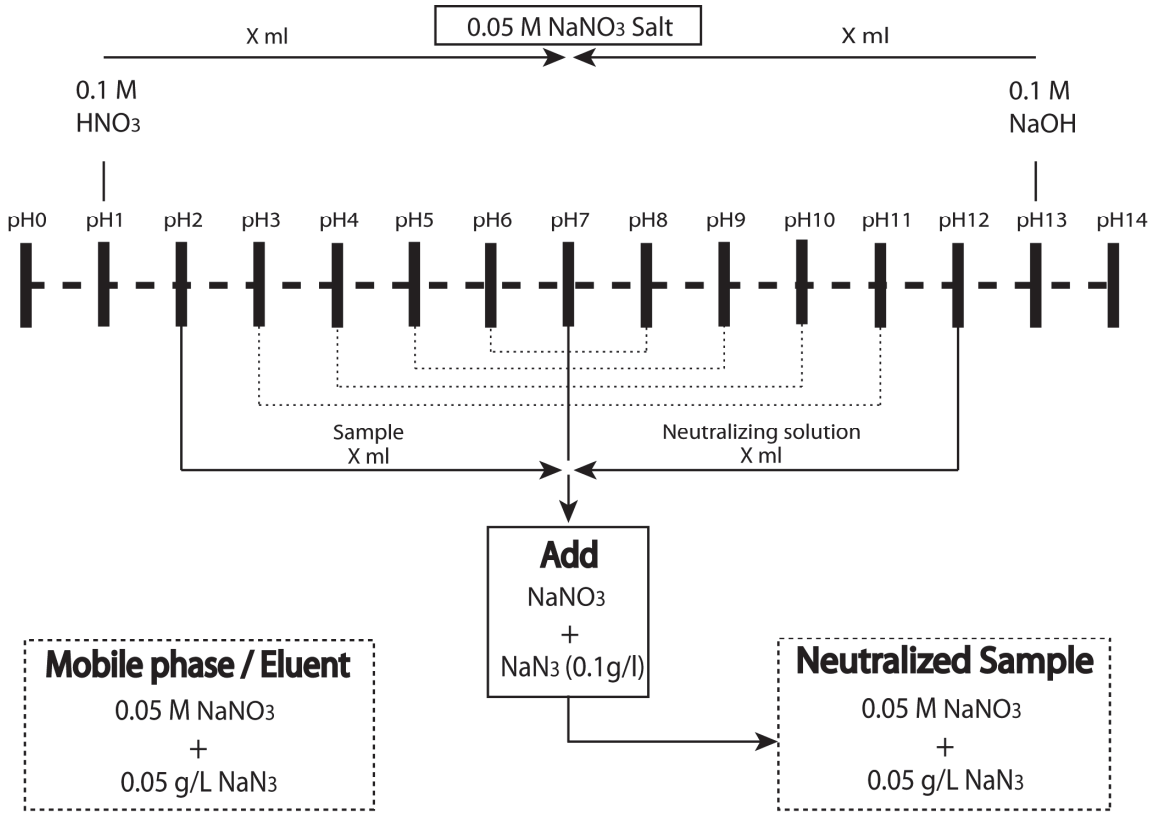

Figure 2: Protocol for modification of GPC samples obtained at different pH. A sample of *X* ml with pH = *y* is neutralized with *X* ml of liquid with pH = 14 - *y*. For samples with 1<pH<13 $NaNO_3$ is added to achieve a concentration of 0.05 M.

2.2.3 Zeta potential experiments

For NF-270 membranes the conventional Fairbrother and Mastin procedure of accounting for the surface conductance may not be sufficient [31-33]. To avoid the need of surface conductivity corrections associated with streaming potential measurements, streaming current measurements were performed yielding the true zeta potential of the membrane material [33, 34]. These measurements were performed using an electrokinetic analyzer SurPASS (Anton Paar, Graz, Austria), with an adjustable gap cell. For each experiment 2 samples of 20 mm x 10 mm were fixed on sample holders of the adjustable gap cell, with a double sided adhesive tape. The cell was sealed using a silicone block, to form a rectangular slit channel between the two membrane samples. The height of the rectangular slit

was always adjusted to constant value of ~135 μm. Streaming current was measured in 5 mM KCl solution at 25 °C with Ag/AgCl electrodes attached very close to the rectangular slit formed by the membranes. The pH of the electrolyte solution was adjusted with 0.1 M HNO_3 and 0.1 M NaOH and four measurements for each pH point were conducted alternatively in two flow directions, for continuously increasing pressure values (20 mbar to 200 mbar). After mounting the samples in the cell, the measurements were always commenced from neutral conditions. Fresh samples were used for the two ranges, and the experiments were performed in duplicates with virgin samples for each range.

The zeta potential was calculated according to the equation:

$$\zeta = \frac{dI}{dP} \times \frac{\eta}{\varepsilon \times \varepsilon_o} \times \frac{L_s}{A_s} \tag{3}$$

where ζ is the zeta potential [V], dI/dP is the slope of streaming current versus pressure [Ampere/Pa], η is the electrolyte viscosity [Pa.s], ε_0 is the vacuum permittivity [F/m], ε is the dielectric constant of the electrolyte, L_s is the length of the streaming channel [m], and A_s is the cross section of the streaming channel [m^2].

2.3 Results

2.3.1 GPC analysis of PEG solutions at pH=1-13

a)

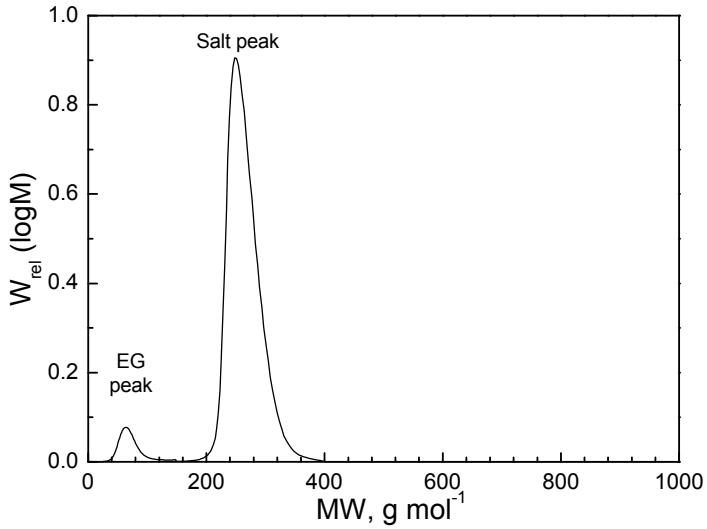

b)

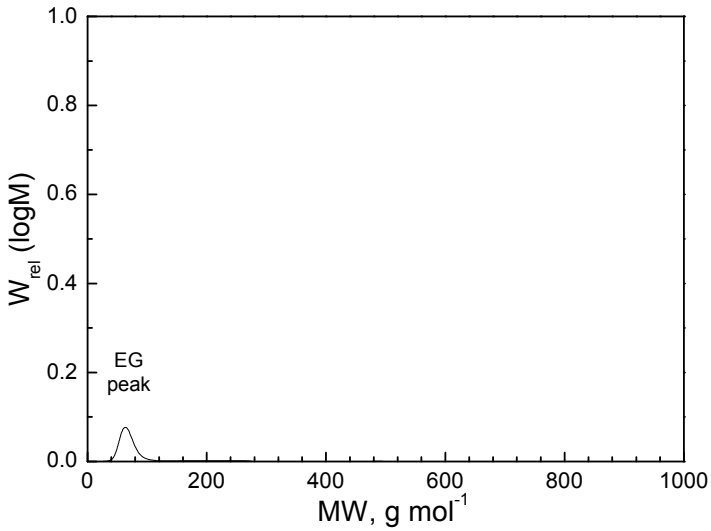

Figure 3: Effect of eluent salt content modification. a) GPC elugram after sample neutralization using a standard eluent (0.5 g L^{-1} NaN_3). b) GPC elugram after neutralization of the sample and ion content modification of the eluent (0.5 M $NaNO_3$, 0.05 g L^{-1} NaN_3).

Fig. 3 shows two GPC elugrams of an EG solution at pH=13. The elugram on the left was obtained when a neutralized EG solution was injected to the GPC with the standard eluent (0.5 g L^{-1} NaN_3) proposed by the manufacturer of the GPC.

The elugram shows two peaks, a small peak corresponding to EG and a much larger peak corresponding to the $NaNO_3$ salt generated during neutralization of the sample. The elugram on the right was obtained when the neutralized EG solution was fed to the GPC using the salt-content-adjusted-eluent prepared via the procedure described in Fig. 2. In comparison to the Figure on the left, the EG peak is similar, whereas the salt peak disappeares. Similar results were obtained for various PEG mixtures in the range pH=1-13.

2.3.2 pH stability of PEG marker molecules

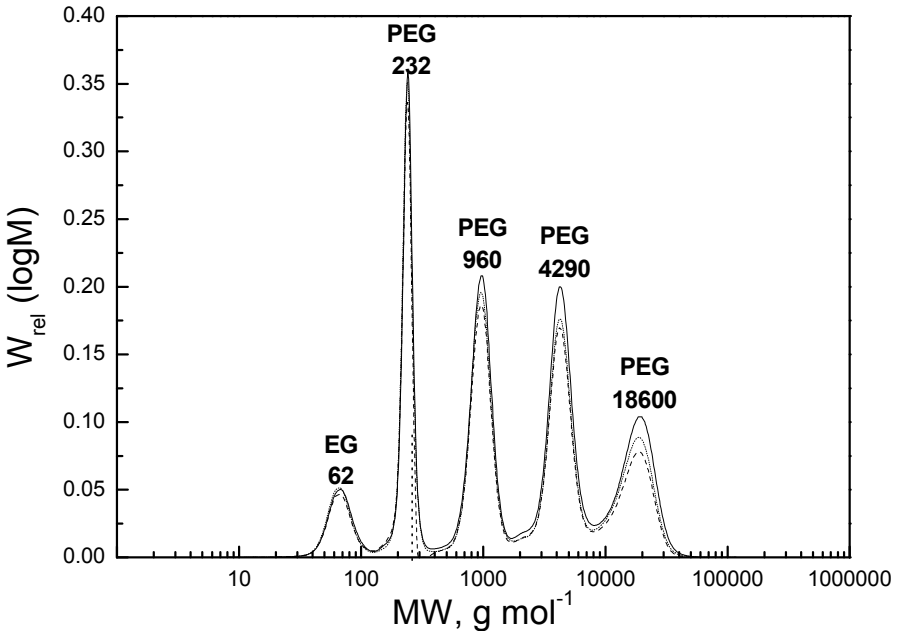

Figure 4: Stability tests on PEG standards: 3 GPC elugrams of five different PEG standards: i) At neutral conditions ii) exposed to 0.1 M NaOH iii) exposed to 0.1 M HNO_3

Fig. 4 depicts GPC elugrams of three PEG solutions (neutral, exposed for 24 hours to 0.1 M NaOH and 0.1 M HNO_3), after neutralization. To avoid the disturbance from the salt peak in the elugram, the earlier mentioned protocol was used for the GPC analysis. The elugrams show 5 peaks corresponding to the individual PEG fractions. No significant differences are evident for the three

mixtures. The 5 peaks show complete overlap and no additional peaks have appeared after exposure to NaOH and HNO_3.

2.3.3 Membrane performance at neutral pH

a)

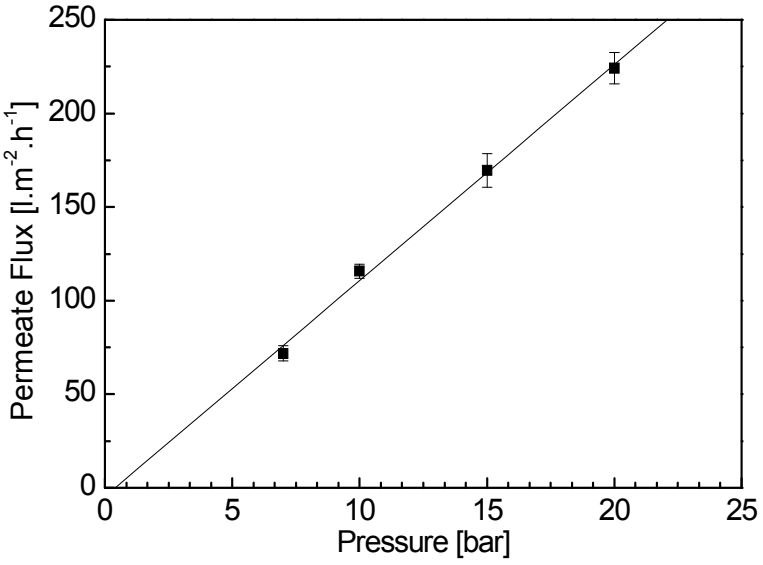

b)

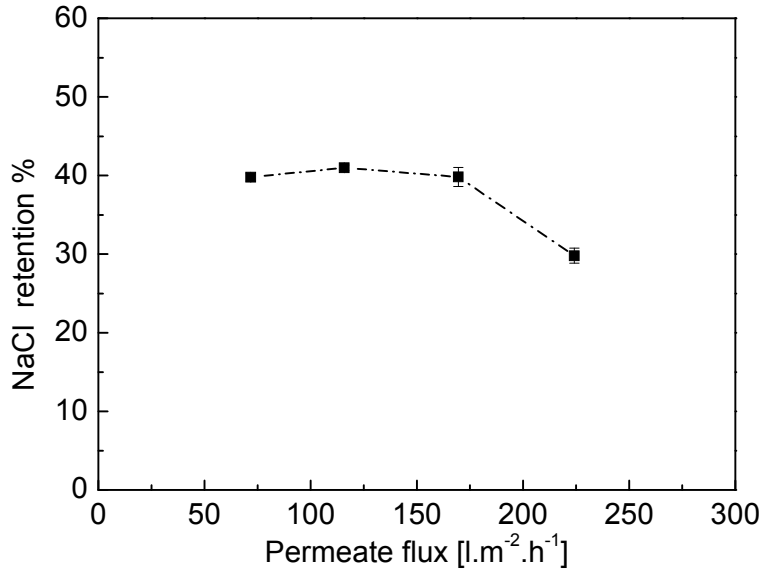

Figure 5: a) Permeate flux and b) NaCl retention of the NF-270 membrane (error bars indicate standard deviation)

Fig. 5 depicts the average flux and retention of an aqueous solution of 2 g L^{-1} NaCl for six NF-270 membrane samples. In the entire pressure range applied (7 - 20 bar) the flux increases linearly with pressure. Up to a flux of 170 L $m^{-2}hr^{-1}$ the salt retention is approximately 40% and no significant dependence on the flux is observed. At the highest flux a lower retention is observed, ~30%. The flux and retention are in the same range as previously reported data for NF-270 membranes [35, 36].

Fig. 6 presents the average PEG retention of the six different NF-270 membrane samples. The graph displays the sieve curve of the permeate, and the average sieve curve of the feed and the retentate. From the ratio of the sieve curves the retention is determined. The retention of the PEG molecules increases with molecular weight and reaches an asymptotic value of approximately 99%. The molecular weight corresponding to 90% retention (the MWCO) is around 270 g mol^{-1}, which is in excellent agreement with the MWCO reported by the manufacturer.

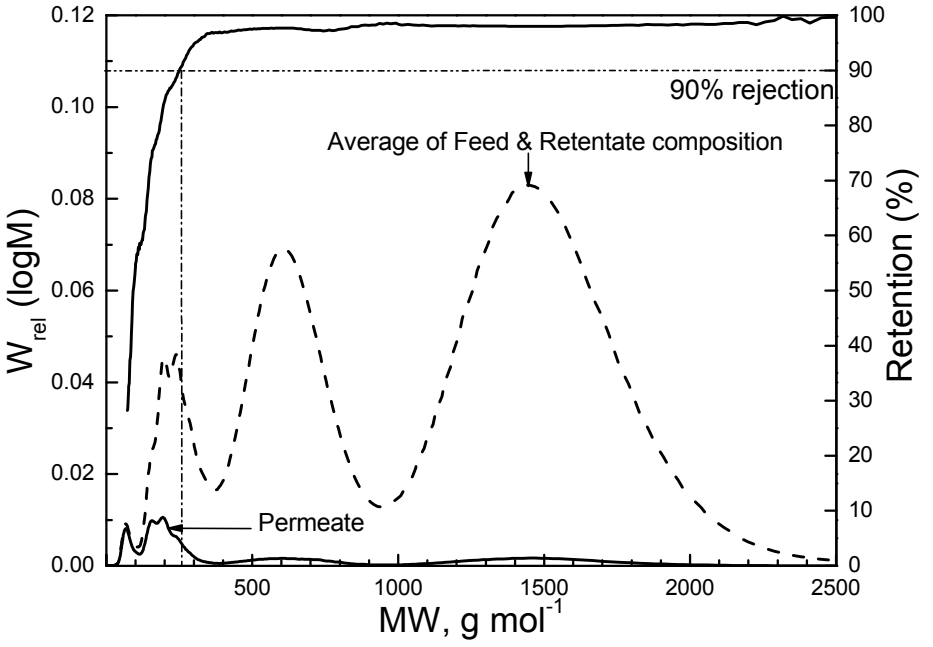

Figure 6: PEG-retention curve and MWCO of NF-270 membrane at neutral pH.

2.3.4 Membrane performance in the range pH = 2-12

a)

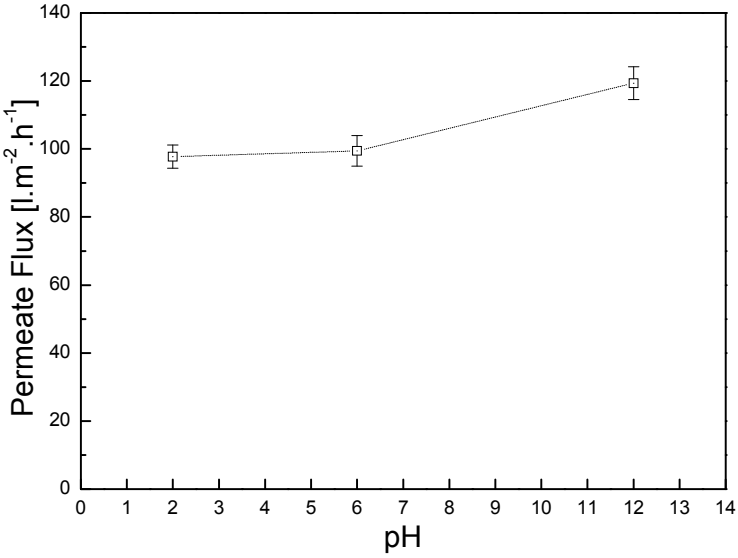

b)

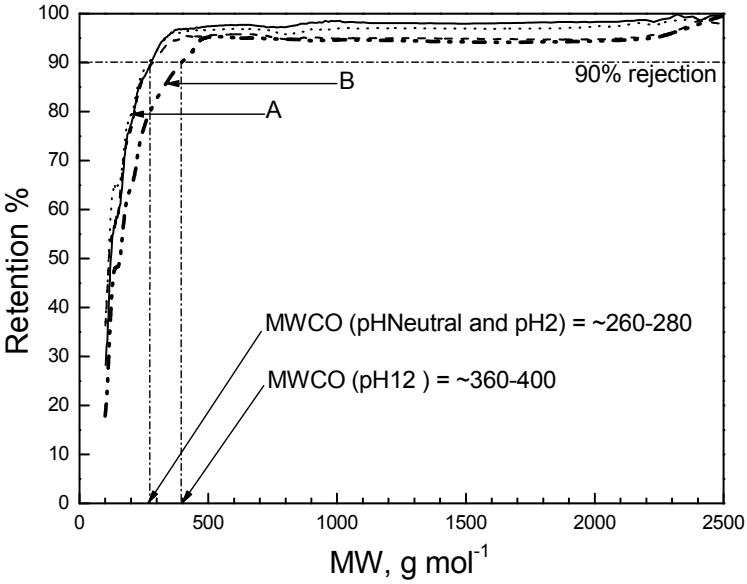

Figure 7: pH dependent a) flux and b) PEG-retention for the NF-270 membrane (error bars indicate standard deviation). A: Three retention curves : i) pH neutral ii) pH=2 iii) pH neutral, after exposure to acidic and alkaline conditions. B: Retention curve at pH=12

The flux and PEG retention of NF-270 membranes measured in the range pH = 2-12. Results are depicted in Fig. 7 and 8. No significant difference is observed for the average flux at pH=2 and neutral pH. At pH=12 the average flux is slightly higher and a *t*-test suggests that the difference between the flux values is statistically significant. PEG retention data determined at pH=2 and neutral pH are almost identical. The corresponding MWCO is around 270 g mol^{-1}. At pH=12 the MWCO shifts to around 380 g mol^{-1}. The small differences between the retention of PEG molecules with higher molecular weight appears to be within experimental error. When the conditions were reverted back to neutral conditions the changes in flux and as well as the retentions were found to be reversible.

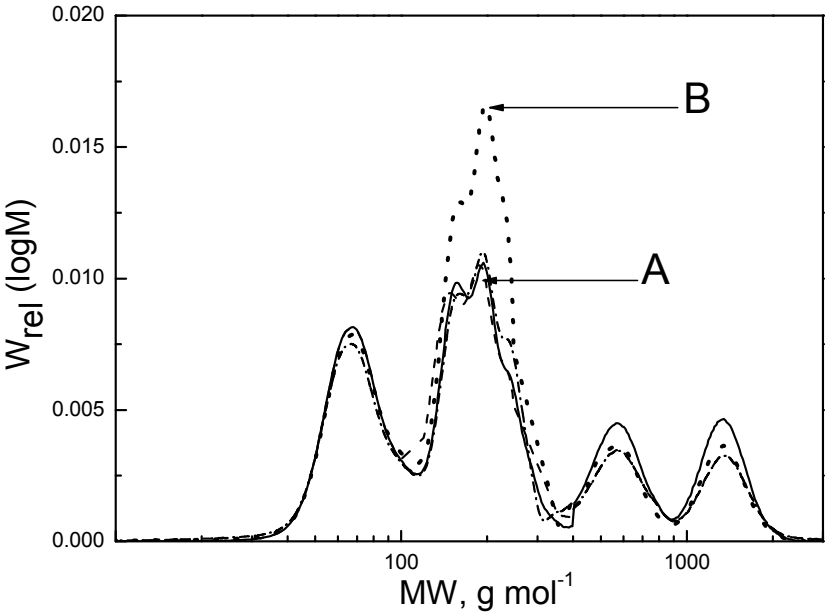

Figure 8: Permeate comparison. A: Permeate sample from: i) pH neutral ii) pH=2 iii) pH neutral after exposure to acidic and alkaline conditions. B: Permeate at pH=12

2.3.5 Zeta potential

Fig. 9 shows the zeta potential of an NF-270 membrane as function of pH. The membrane has an isoelectric point at approximately pH=3.2, which is in agreement with previously reported data [35].

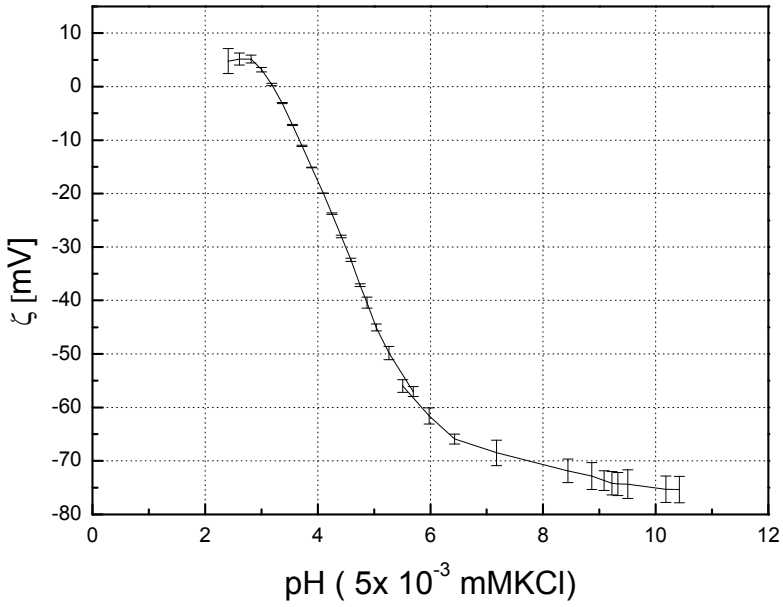

Figure 9: Zeta potential versus pH for the NF-270 membrane

2.4 Discussion

2.4.1 GPC analysis of PEG solutions at pH=1-13

MWCO study as function of pH does not allow standard GPC analysis. Samples need to be neutralized, upon which salt is generated. The amount of salt generated depends on the initial pH of the sample. For example, for a solution with pH=1 the final salt concentration after neutralization is 0.05 M.

$$\underset{(0.1M)}{HNO_3} + \underset{(0.1M)}{NaOH} \rightarrow \underset{(0.05M)}{NaNO_3} + H_2O \qquad (4)$$

In the GPC a difference in salt concentration between sample and mobile phase will be detected by the refractive index detector, resulting in an additional (salt) peak in the elugram. In Fig. 3 the location of the salt peak is in the range 200 – 400 g mol^{-1}, coinciding with typical nanofiltration MWCO values, and the magnitude of the salt peak is large as compared to the peaks of the oligomers. This problem is circumvented by adjusting the mobile phase to contain the same $NaNO_3$ content as in the sample after neutralization. The maximum $NaNO_3$ content in the mobile phase is determined by the limits of the pH range of interest, here pH=1-13. For a pH value in between these limits the salt concentration after neutralization will be less, and additional salt has to be added. For instance, for filtration at pH=2, neutralization is carried out with a pH=12 solution, thereby generating 0.005 M salt. Additional salt has to be added to achieve a concentration of 0.05 M. Neutralization for other pH conditions was achieved in a similar manner. If the limits had been chosen to be pH=0-14 the salt concentration in the samples and mobile phase would be 0.5M $NaNO_3$ (42.5 g L^{-1}). It should be noted that such high concentrations can cause problems like precipitation within the capillaries of the GPC system.

2.4.2 pH stability of PEG marker molecules

The pH stability of PEG molecules follows from a comparison of the elugrams of PEG solutions before and after exposure to harsh conditions. Fig. 4 shows that the corresponding elugrams are almost perfectly overlapping each other, suggesting no degradation of PEGs in acidic or alkaline environments. Small differences are observed at higher molecular weights. These differences are suspected to result from concentration differences of PEGs in the solutions and not due to any degradation. This is supported by the fact that degradation would result in additional peaks of lower molecular weight fractions.

2.4.3 Membrane performance at neutral pH

Fig. 5a demonstrates a linear increase of flux with applied pressure, indicating no compaction effects on the membrane up to a pressure of 20 bar. However a reduced NaCl retention at 20 bar pressure (Fig. 5b) suggests significant concentration polarization effects in the measuring cell. MWCO analyses performed under neutral conditions, at a pressure of 10 bar, reveal a cut-off around 270 g mol^{-1} (Fig. 6). The difference in the MWCO value observed with different samples is statistically insignificant.

2.4.4 Membrane performance in the range pH = 2-12

The data for flux and retention in Fig. 7 and 8 suggest that the structure of NF-270 membranes becomes more open in alkaline environments as compared to acidic and neutral conditions. The reversibility of this trend indicates that no irreversible degradation of the membrane occurs. For NF-270 Mänttäri et al. also observed a decrease in glucose retention in alkaline conditions [30]. The reversibility of the change in membrane performance as a function of pH clearly highlights the importance of MWCO analysis over the entire pH range of interest.

Several factors might have contributed to the reversible change in membrane performance in alkaline conditions. Previous studies have shown that the presence of ions can affect the retention of uncharged molecules [37]. Studies have correlated such changes in performance to the membrane charge density at different pH conditions [30, 38]. These studies [30, 37, 38] can explain the PEG retention results we have obtained with our characterization method for NF-270 qualitatively. At pH=12 and pH=7 the surface of NF-270 is strongly charged (see Fig. 9). Since the ion concentration in the solution at pH=12 is considerably higher than that at pH=7 a lower retention for PEG is expected at pH=12 on the basis of Bargeman et al. [37]. For the solution at pH=2 the ion concentration in the liquid is the same as for the solution at pH=12. However, the zeta potential for NF270 at pH=2 is close to zero, whereas that at pH=12 is strongly negative (around -70 mV). Therefore, on the basis of [30, 38] it is expected that the

presence of the ions does not affect the retention of the neutral PEG to a large extent for the solution at pH=2, whereas for the solution at pH=12 the strongly negative membrane charge in combination with the presence of ions in the solution has a significant effect on PEG retention. However, quantitative prediction of the effects cannot be made on the basis of [30, 37, 38].

A more detailed analysis of the underlying phenomena causing the changes in performance at different pH is beyond the scope of this paper. The goal of this work is to present a method that allows observation of changes in transport of neutral molecules during filtration at different pH conditions. The method we present allows capturing reversible changes, which would not have been evident from performance characterization before and after exposure to the pH conditions of interest.

2.5 Conclusion

In this work a method is presented that allows a MWCO analysis of membranes as a function of pH during nanofiltration at different pH conditions. The method is based on the retention analysis of PEG molecules at the relevant pH values, as opposed to analysis after exposure to these pH conditions. Compositions of permeate, feed and retentate are analyzed by GPC. It is shown that appropriate modification of the ion content of the samples obtained at various pH is crucial for proper GPC analysis.

For an NF-270 membrane it is shown that performance changes reversibly at alkaline conditions, as compared to acidic and neutral conditions. The flux and MWCO display an increase at pH=12, which is reversed if the conditions are reverted back to neutral conditions. Since the observed trend is reversible, the change in MWCO is not due to any degradation of the membrane material. Quantitative prediction of the change in MWCO with pH cannot be easily derived from membrane surface characteristics and various other phenomena may have attributed to the change in performance, signifying the importance of MWCO measurements during membrane filtration at these conditions.

References

[1] M. Mulder, Basic Principles of Membrane Technology, Kluver Academic publishers, 2003.

[2] R.J. Petersen, Composite reverse osmosis and nanofiltration membranes, Journal of Membrane Science, 83 (1993) 81-150.

[3] P. Vandezande, L.E.M. Gevers, I.F.J. Vankelecom, Solvent resistant nanofiltration: separating on a molecular level, Chemical Society Reviews, (2008) -.

[4] A.I. Schafer, A.G. Fane, T.D. Waite, Nanofiltration — Principles and Applications, Elsevier, 2005.

[5] Y.H. See Toh, X.X. Loh, K. Li, A. Bismarck, A.G. Livingston, In search of a standard method for the characterisation of organic solvent nanofiltration membranes, Journal of Membrane Science, 291 (2007) 120-125.

[6] F.P. Cuperus, C.A. Smolders, Characterization of UF membranes : Membrane characteristics and characterization techniques, Advances in Colloid and Interface Science, 34 (1991) 135-173.

[7] W.S.W. Ho, K.K. Sirkar, Membrane handbook, Kluwer Academic Publishers, 1992.

[8] D. Bhanushali, S. Kloos, D. Bhattacharyya, Solute transport in solvent-resistant nanofiltration membranes for non-aqueous systems: experimental results and the role of solute-solvent coupling, Journal of Membrane Science, 208 (2002) 343-359.

[9] X.J. Yang, A.G. Livingston, L. Freitas dos Santos, Experimental observations of nanofiltration with organic solvents, Journal of Membrane Science, 190 (2001) 45-55.

[10] D. Bhanushali, S. Kloos, C. Kurth, D. Bhattacharyya, Performance of solvent-resistant membranes for non-aqueous systems: solvent permeation results and modeling, Journal of Membrane Science, 189 (2001) 1-21.

[11] K. Ruohomäki, P. Väisänen, S. Metsämuuronen, M. Kulovaara, M. Nyström, Characterization and removal of humic substances in ultra- and nanofiltration, Desalination, 118 (1998) 273-283.

[12] L.S. White, Transport properties of a polyimide solvent resistant nanofiltration membrane, Journal of Membrane Science, 205 (2002) 191-202.

[13] R.S. Jeyaseelan, J.P. Wagne, Ultrafiltration of Guayule Resin, Journal of Membrane Science, 103 (1995) 45-50.

[14] H. Peng, A.Y. Tremblay, The selective removal of oil from wastewaters while minimizing concentrate production using a membrane cascade, Desalination, 229 (2008) 318-330.

[15] M. Minhalma, M.N. de Pinho, Tannic-membrane interactions on ultrafiltration of cork processing wastewaters, Separation and Purification Technology, 22-23 (2001) 479-488.

[16] N. Hilal, M. Al-Abri, H. Al-Hinai, M. Abu-Arabi, Characterization and retention of NF membranes using PEG, HS and polyelectrolytes, Desalination, 221 (2008) 284-293.

[17] N. Hilal, M. Al-Abri, H. Al-Hinai, Characterization and retention of UF membranes using PEG, HS and polyelectrolytes, Desalination, 206 (2007) 568-578.

[18] M.J. López-Muñoz, A. Sotto, J.M. Arsuaga, B. Van der Bruggen, Influence of membrane, solute and solution properties on the retention of phenolic compounds in aqueous solution by nanofiltration membranes, Separation and Purification Technology, 66 (2009) 194-201.

[19] P. Puhlfürß, A. Voigt, R. Weber, M. Morbé, Microporous TiO2 membranes with a cut off <500 Da, Journal of Membrane Science, 174 (2000) 123-133.

[20] R. Weber, H. Chmiel, V. Mavrov, Characteristics and application of new ceramic nanofiltration membranes, Desalination, 157 (2003) 113-125.

[21] S. Sarrade, G.M. Rios, M. Carlès, Dynamic characterization and transport mechanisms of two inorganic membranes for nanofiltration, Journal of Membrane Science, 97 (1994) 155-166.

[22] J. Schaep, C. Vandecasteele, B. Peeters, J. Luyten, C. Dotremont, D. Roels, Characteristics and retention properties of a mesoporous [gamma]-Al2O3 membrane for nanofiltration, Journal of Membrane Science, 163 (1999) 229-237.

[23] T. Van Gestel, C. Vandecasteele, A. Buekenhoudt, C. Dotremont, J. Luyten, B. Van der Bruggen, G. Maes, Corrosion properties of alumina and titania NF membranes, Journal of Membrane Science, 214 (2003) 21-29.

[24] T. Van Gestel, C. Vandecasteele, A. Buekenhoudt, C. Dotremont, J. Luyten, R. Leysen, B. Van der Bruggen, G. Maes, Salt retention in nanofiltration with multilayer ceramic TiO2 membranes, Journal of Membrane Science, 209 (2002) 379-389.

[25] T. Van Gestel, C. Vandecasteele, A. Buekenhoudt, C. Dotremont, J. Luyten, R. Leysen, B. Van der Bruggen, G. Maes, Alumina and titania multilayer membranes for nanofiltration: preparation, characterization and chemical stability, Journal of Membrane Science, 207 (2002) 73-89.

[26] T. Van Gestel, H. Kruidhof, D.H.A. Blank, H.J.M. Bouwmeester, ZrO2 and TiO2 membranes for nanofiltration and pervaporation: Part 1. Preparation and characterization of a corrosion-resistant ZrO2 nanofiltration membrane with a MWCO < 300, Journal of Membrane Science, 284 (2006) 128-136.

[27] G. Cornelis, K. Boussu, B. Van der Bruggen, I. Devreese, C. Vandecasteele, Nanofiltration of Nonionic Surfactants: Effect of the Molecular Weight Cutoff and Contact Angle on Flux Behavior, Industrial & Engineering Chemistry Research, 44 (2005) 7652-7658.

[28] X. Li, F. Monsuur, B. Denoulet, A. Dobrak, P. Vandezande, I.F.J. Vankelecom, Evaporative Light Scattering Detector: Toward a General Molecular Weight Cutoff Characterization of Nanofiltration Membranes, Analytical Chemistry, 81 (2009) 1801-1809.

[29] S. Bouranene, A. Szymczyk, P. Fievet, A. Vidonne, Effect of salts on the retention of polyethyleneglycol by a nanofiltration ceramic membrane, Desalination, 240 (2009) 94-98.

[30] M. Mänttäri, A. Pihlajamäki, M. Nyström, Effect of pH on hydrophilicity and charge and their effect on the filtration efficiency of NF membranes at different pH, Journal of Membrane Science, 280 (2006) 311-320.

[31] M. Sbai, A. Szymczyk, P. Fievet, A. Sorin, A. Vidonne, S. Pellet-Rostaing, A. Favre-Reguillon, M. Lemaire, Influence of the Membrane Pore Conductance on Tangential Streaming Potential, Langmuir, 19 (2003) 8867-8871.

[32] P. Fievet, M. Sbaï, A. Szymczyk, A. Vidonne, Determining the [zeta]-potential of plane membranes from tangential streaming potential measurements: effect of the membrane body conductance, Journal of Membrane Science, 226 (2003) 227-236.

[33] A. Yaroshchuk, V. Ribitsch, Role of Channel Wall Conductance in the Determination of ζ- Potential from Electrokinetic Measurements, Langmuir, 18 (2002) 2036-2038.

[34] T. Luxbacher, Electrokinetic characterization of flat sheet membranes by streaming current measurement, Desalination, 199 (2006) 376-377.

[35] J. Tanninen, M. Mänttäri, M. Nyström, Effect of salt mixture concentration on fractionation with NF membranes, Journal of Membrane Science, 283 (2006) 57-64.

[36] K. Boussu, C. Kindts, C. Vandecasteele, B. Van der Bruggen, Applicability of nanofiltration in the carwash industry, Separation and Purification Technology, 54 (2007) 139-146.

[37] G. Bargeman, J.M. Vollenbroek, J. Straatsma, C.G.P.H. Schroën, R.M. Boom, Nanofiltration of multi-component feeds. Interactions between neutral and charged components and their effect on retention, Journal of Membrane Science, 247 (2005) 11-20.

[38] A. Braghetta, F.A. DiGiano, W.P. Ball, Nanofiltration of Natural Organic Matter: pH and Ionic Strength Effects, Journal of Environmental Engineering, 123 (1997) 628-641.

Effect of pH on the performance of polyamide / polyacrylonitrile based thin film composite membranes

THIS CHAPTER HAS BEEN PUBLISHED:

M. Dalwani; N.E. Benes; G. Bargeman; D. Stamatialis; M. Wessling, Effect of pH on the performance of polyamide/polyacrylonitrile based thin film composite membranes, Journal of Membrane Science 372 (2011) 228-238.

ABSTRACT

In this study the effect of pH on the performance of thin film composite (TFC) nanofiltration (NF) membranes has been investigated at the relevant pH conditions, in the range of pH=1-13. TFC polyamide NF membranes have been fabricated on a polyacrylonitrile support via interfacial polymerization between piperazine in an aqueous phase and trimesoyl chloride in an organic phase. Membrane characterization has revealed that the produced membranes show a NaCl retention similar to NF-270 and Desal-5DK, a permeance in between those of NF-270 and Desal-5DK, and a slightly higher iso-electric point than NF-270 and Desal-5DK. The molecular weight cut-off of the membranes appeared to be practically constant in acidic and neutral conditions. At extremely alkaline conditions (pH>11) an increase in molecular weight cut-off and a reduction in membrane flux has been observed. According to the Donnan steric partitioning pore model (DSPM) the change in performance in alkaline conditions originates from a larger effective average pore size and a larger effective membrane thickness as compared to the other pH conditions.

3.1 Introduction

Thin film composite (TFC) membranes prepared via interfacial polymerization (IP) have often been used for nanofiltration (NF) due to their superior permeation performance [1]. Although most commercial TFC NF membranes are suitable for treating aqueous streams at pH levels between 2 and 10, many potential applications in the chemical industry involve much more aggressive conditions [2, 3]. Advances in development of stable membranes and their performance characterization in these harsh applications will therefore expand the application window of such membranes in commercial processes.

Several recipes to fabricate polyamide (PA) TFC membranes via IP have been published in literature [2, 4-8]. Many commercial NF membrane manufacturers seem to favor poly (piperazine-amide) based recipes [2, 3, 9], probably due to a superior chlorine resistance of these membranes [4]. Materials like polysulfone [10, 11], polyacrylonitrile [12, 13], polyethersulfone [14], polypropylene[15], poly(tetrafluoroethylene) [16] have been reported as support membranes for the IP process. Little is known about the performance of these membranes at extreme pH conditions.

In this work composite nanofiltration membranes have been fabricated using an aliphatic amine piperazine (PIP) and acyl chloride trimesoyl (TMC) chloride with a controlled fabrication technique. Ultrafiltration polyacrylonitrile (PAN) membranes (type HV3), supplied by GKSS-Forschungszentrum Geesthacht GmbH (Germany), which have been reported to encompass reasonable chemical stability [17], have been used as support membranes for the IP process. The performance of the membranes has been evaluated in a pH range from 1 – 13, using polyethylene glycol (PEG) [18] and glucose molecules, using a batch filtration setup. The performance has been compared to the performance of commercial nanofiltration membranes at neutral pH.

Changes in the performance of the membranes have been related to structural changes using the Donnan Steric Partitioning Pore Model (DSPM) developed by Bowen and coworkers [19, 20]. This model is based on the extended Nernst-Plank

equation, and has often been used to characterize commercial NF membranes [21-26]. Other researchers have also successfully characterized PA TFC membranes using the DSPM [27-29]. Ahmad et al. have used the model to analyze the effect of the fabrication parameters of PA TFC membranes prepared via the IP route [30-32]. However, the effect of feed pH on the membrane performance is rarely studied. Labbez and coworkers have studied the effect of pH on the volume charge of a ceramic titania membrane, which encompasses a fixed pore radius [33]. Mänttäri and coworkers have reported the effect of pH on the filtration performance of commercial nanofiltration membranes using a mixture of glucose and NaCl [34]. Kaya [35] and Nanda [36] have studied the change in the fouling potential of commercial membranes with a change in the feed pH. The present work analyses the retention of uncharged molecules for IP membranes on PAN support in the absence of salt in a range of feed pH. The absence of salt limits the disturbance in retention of an uncharged molecule due to the presence of charged species in the feed [37] mixture. DSPM has been used to determine the effective pore radius and the effective thickness/porosity ratio of a PA TFC membrane prepared via the IP route as function of pH.

3.2 Theoretical background: Donnan Steric Partitioning Pore Model

The Donnan Steric Partitioning Pore Model (DSPM) developed by W.R. Bowen and coworkers [19, 25] has been used to illustrate the effect of pH on the membrane characteristics. The model assumes the membrane is porous consisting of identical pores of radius r_p and there are no coupling effects between the solute and the solvent.

The model is based on the following extended Nernst-Planck equation which gives the flux of the solute *i* (j_i) resulting from transport due to diffusion, electrical and convection forces:

$$j_i = -D_{i,p}\frac{dc_i}{dx} - \frac{z_i c_i D_{i,p}}{RT} F \frac{d\psi}{dx} + K_{i,c} c_i v \qquad (1)$$

where

$$D_{i,p} = K_{i,d} D_{i,\infty} \tag{2}$$

For uncharged solutes like glucose and PEGs the transport is governed purely by diffusive and convective flows inside the membrane thereby reducing the above mentioned Nernst-Planck equation to

$$j_i = -D_{i,p} \frac{dc_i}{dx} + K_{i,c} c_i v \tag{3}$$

$K_{i,d}$ and $K_{i,c}$, which are functions of the ratio of solute to pore radius (λ), account for the hindrance due to diffusion and convection respectively. $K_{i,d}$ and $K_{i,c}$ can be related to the hydrodynamic coefficients K^{-1} (enhanced drag) and G (lag coefficient) according to the following equations [19, 30]:

$$K^{-1}(\lambda,0) = 1.0 - 2.3\lambda + 1.154\lambda^2 + 0.224\lambda^3 \tag{4}$$

$$G(\lambda,0) = 1.0 + 0.054\lambda - 0.988\lambda^2 + 0.441\lambda^3 \tag{5}$$

where

$$\lambda = \frac{r_s}{r_p} \tag{6}$$

r_s represents the solute radius in [m] and r_p the effective pore radius of the membrane in [m]. For a homogeneous solute velocity through the membrane $K_{i,d}$ and $K_{i,c}$ follow from

$$K_{i,d} = K^{-1}(\lambda,0) \tag{7}$$

$$K_{i,c} = G(\lambda,0) \tag{8}$$

When the solute velocity has a parabolic profile of the Hagen-Poiseuille type, the hindrance factors become

$$K_{i,d} = K^{-1}(\lambda,0) \tag{9}$$

$$K_{i,c} = (2 - \Phi)\, G(\lambda,0) \tag{10}$$

Equation 3 can be expressed in terms of real rejection of the solute by the membrane as:

$$R_{real} = \frac{C_{i,m} - C_{i,p}}{C_{i,m}} = 1 - \frac{K_{i,c}\Phi}{1 - \exp(-Pe_m)[1 - \Phi K_{i,c}]} \tag{11}$$

For purely steric interactions between the neutral solute and the membrane pore walls, Φ can be written in terms of λ according to:

$$\Phi = (1 - \lambda)^2 \tag{12}$$

Pe_m the Peclet number is defined as:

$$Pe_m = \frac{K_{i,c}J}{K_{i,d}D_{i,\infty}}\frac{\Delta x}{A_k} \tag{13}$$

where J is the permeate flux in [$m^3m^{-2}s^{-1}$], $D_{i,\infty}$ is the bulk diffusivity in [m^2s^{-1}] and $\Delta x/A_k$ is the ratio between the effective thickness and porosity [m].

The ratio of the pure water flux J_w and the pressure drop across the membrane (ΔP) are related to membrane and solvent characteristics by the Hagen-Poiseuille equation:

$$\frac{J_w}{\Delta P} = \frac{r_p^{\,2}}{8\mu(\Delta x / A_k)} \tag{14}$$

where $J_w/\Delta P$ is the pure water permeance in [$ms^{-1}kPa^{-1}$] and μ is dynamic viscosity of the solution in [kPas].

In the limiting case of $Pe_m \rightarrow \infty$, the limiting rejection, derived from equation 11 is expressed as:

$$R_{\lim} = 1 - K_{i,c}\Phi \tag{15}$$

r_p was determined from the full range rejection data by solving equations 4-14 to obtain the best fit to the J - R_{real} curves of permeation experiments with neutral molecules (glucose and PEGs). r_p was also determined from the limiting rejection data using equation 15. In both cases $\Delta x/A_k$ was calculated from the Hagen-Poiseuille equation (equation 14).

3.3 Experimental

3.3.1 Chemicals and materials

Piperazine (PIP, 99% purity) and trimesoyl chloride (TMC, 98% purity) acquired from Sigma Aldrich (Germany) were used as received without further purification and synthesis grade Sodium dodecyl sulfate (SDS) was acquired from Merck (Germany). Analytical grade sodium nitrate ($NaNO_3$), sodium azide (NaN_3) and ethylene glycol (EG) and synthesis quality polyethylene glycol (PEG) with mean molecular weights of 200 g mol^{-1}, 600 g mol^{-1} and 1500 g mol^{-1} were acquired from Merck (Germany). Analytical grade sodium chloride (NaCl) (used for salt retention experiments) was acquired from Arcos Organics (Belgium). Analytical grade potassium chloride (KCl) for zeta potential measurements was obtained from Fluka (Germany). Cell culture tested glucose (≥99.5) acquired from Sigma Aldrich (Germany), was used in glucose retention experiments. Standard volumetric solutions of 0.1 M nitric acid (HNO_3), hydrochloric acid (HCl) and sodium hydroxide (NaOH) (used to alter the pH of the solutions) were purchased from Fluka (Germany). Ultrapure water from a Synergy water purification system (Millipore, USA) was used to prepare all solutions.

3.3.2 Membranes

Ultrafiltration polyacrylonitrile (PAN) membranes (type HV3) were generously supplied by GKSS-Forschungszentrum Geesthacht GmbH (Germany). The PAN HV3 membranes, supported on a polyester nonwoven encompass a molecular weight cut-off (MWCO) of 30 kg mol^{-1} and were used as support membranes for interfacial polymerization (IP).

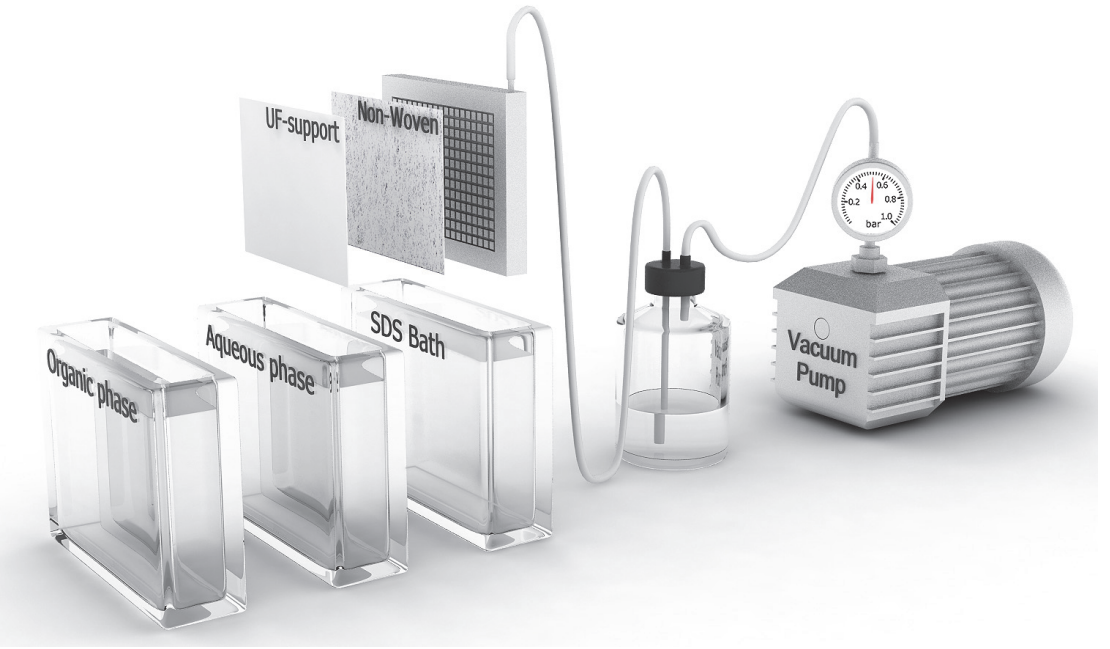

Figure 1: Schematic of composite membrane fabtication setup

Thin film composite (TFC) polyamide membranes were prepared by the IP technique using the setup illustrated in Fig. 1. The PAN HV3 membrane supported by an additional nonwoven was first glued on the perforated aluminum plate by means of a double sided tape Tesa 4965 (Tesa BV, The Netherlands). The plate was then connected to a vacuum pump immersed in an aqueous SDS solution (0.05 wt %) for 10 minutes. The trans-membrane pressure was kept constant to 0.5 bar during the entire process. This pretreatment step is to increase the wettability properties of the support membrane. The membrane (with the plate) was then removed from the SDS bath and allowed to drain for 2 minutes. Subsequently, the membrane was impregnated with an aqueous solution of 1 wt% PIP. The aqueous phase was sucked through the membrane for around 10 minutes. The vacuum across the membrane was then released and the excess aqueous phase was allowed to drain out. In the final step the membrane was immersed in an organic solution of 0.05 wt% TMC in hexane for a certain time. Almost immediately the amine reacted with the acyl halide and a thin polyamide film was formed on top of the support according to the well known reaction shown in Fig. 2.

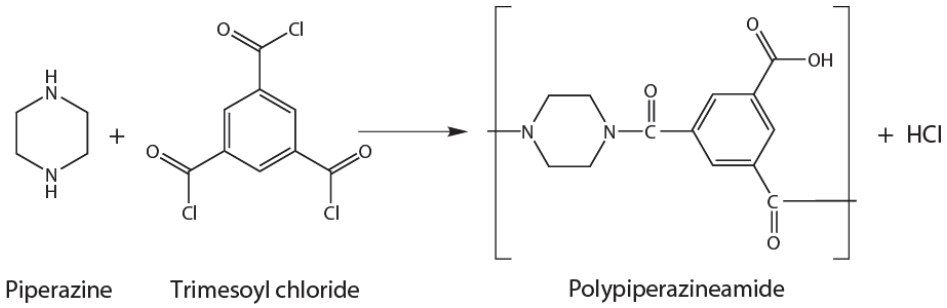

Figure 2: Schematic showing Interfacial polymerization reaction between piperazine and trimesoylchloride

In the last step the membrane was cut from the perforated plate and dried in a nitrogen box at room temperature for at least 24 hours. Defect free TFC membrane sheets up to A4 size could be prepared reproducibly via this technique. The concentration of the monomer solutions were fixed to 1 wt% PIP in water and 0.05 wt% TMC in hexane according to a previous study [13]. Other parameters of the fabrication protocol (reaction time, drying time, vacuum etc…) were optimized to achieve a very thin IP layer in the range of those found for commercial IP membranes. The developed membranes are coded TFC IP-UT.

The performance of the fabricated membranes was compared with commercial nanofiltration membranes: NF-270 (Dow-Film Tech, USA), Desal-5 DK (GE Osmonics-Desalogics Membrane Supplies GmbH, Germany) and MPF-34 (Koch Membrane Systems, United Kingdom). Desal-5 DK is believed to be a poly (piperazine-amide) based interfacial polymerization membrane on a polysulfone support layer and two proprietary layers backed by a polyester support [2]. NF-270 is a semi aromatic piperazine based polyamide composite membrane on a poly-sulfone support, mechanically supported by a polyester non-woven backing [9].

3.3.3 Surface Characterization

Scanning electron microscopy

Scanning electron microscopy (SEM) images were taken using LEO-1550 Schottky field emission scanning electron microscope (Carl–Zeiss, Germany). Virgin membrane samples were examined for their top surface and cross section morphology, without any sputtering.

Zeta potential

To avoid the need of surface conductivity corrections associated with streaming potential measurements, streaming current measurements were performed yielding the true zeta potential of the membrane material [38]. These measurements were performed using an electrokinetic analyzer SurPASS (Anton Paar, Graz, Austria), using an adjustable gap cell with a procedure described elsewhere [18]. For each experiment 2 samples of 20 mm x 10 mm were used and streaming current was measured in a 5 mM KCl solution at 25 °C with Ag/AgCl electrodes attached very close to the rectangular slit formed by the membranes. The pH of the electrolyte solution was adjusted through addition of a 0.1 M HNO_3 or 0.1 M NaOH solution and all measurements were performed in duplicate.

The zeta potential was calculated according to the equation:

$$\zeta = \frac{dI}{dP} \times \frac{\eta}{\varepsilon \times \varepsilon_o} \times \frac{L_s}{A_s} \tag{16}$$

where ζ is the zeta potential [V], dI/dP is the slope of streaming current versus pressure [Ampere Pa^{-1}], η is the electrolyte dynamic viscosity [Pa s], ε_0 is the vacuum permittivity [F m^{-1}], ε is the dielectric constant of the electrolyte, L_s is the length of the streaming channel [m], and A_s is the cross section area of the streaming channel [m^2]. The zeta potentials of the PAN support and NF-270 were measured on virgin samples without any pretreatment steps. Desal 5-DK was

delivered with a preservative which was removed by clean water permeation at 15-20 bars for around 2 hours, after which the zeta potential curve of the native membranes was determined. The developed membranes and MPF-34 were soaked in ultrapure water for 2 to 3 hours before measuring its zeta potential to rinse left over monomers off the membrane surface.

Fourier Transform Infrared Spectroscopy

The chemical structures of the membranes were analyzed by Fourier Transform Infrared Spectroscopy (FTIR) using an ALPHA FT-IR Spectrometer (Bruker Optics Inc, Germany). The measurements were performed using an Attenuated Total Reflectance (ATR) attachment. Dry and clean membrane samples were pressed on the crystal, without any further sample preparation.

3.3.4 Permeation experiments

Permeation experiments at different trans-membrane pressures (ranging from 7 to 30 bar) were performed at room temperature in a dead-end filtration setup with a protocol described in our previous work [18]. In brief, the setup was equipped with magnetic stirrers of radius 18.5 mm, which were set at constant rotation of 500 rpm and the effective membrane surface area was 13.86 cm^2. Before every experiment the membranes were pre-conditioned with the feed solution for 1 hour and all measurements were performed on at least three different membrane samples to ensure reproducibility (all error bars represent standard deviation from the mean).

The permeate flux was calculated by:

$$J = \frac{V}{At} \tag{17}$$

where J is the permeate flux in [$m^3\ m^{-2}\ s^{-1}$], V is the permeate volume [m^3], A is the membrane area in [m^2] and t is the permeation time [s].

The observed retention R_{obs} was calculated from

$$R_{obs} = \frac{c_b - c_{permeate}}{c_b} \tag{18}$$

where $c_{permeate}$ is the average permeate concentration and c_b is the average bulk concentration inside the test cell over the total permeation time t, measured as described in our previous work [18].

For a stirred cell configuration R_{real} can be calculated from R_{obs} by variation of the stirrer speed at different applied pressures using the following relation [19, 20].

$$\ln\left(\frac{1-R_{obs}}{R_{obs}}\right) = \ln\left(\frac{1-R_{real}}{R_{real}}\right) + \frac{J}{k'\omega^{0.567}} \tag{19}$$

k' can be determined by the slope of the plot of $\ln[(1-R_{obs})/ R_{obs}]$ v/s $J/\omega^{0.567}$ where ω is the stirring speed. Another empirical equation has been often used for calculating the k' for a stirred cell configuration [19, 21, 28, 30]

$$k' = 0.23\left(\frac{r^2}{\upsilon}\right)^{0.567}\left(\frac{\upsilon}{D_\infty}\right)^{0.33}\frac{D_\infty}{r} \tag{20}$$

where r is stirrer radius in [m], D_∞ is the diffusivity of the solute in [$m^2\ s^{-1}$] and υ is the kinematic viscosity of the solution in [$m^2\ s^{-1}$]. Table 1 lists the properties of neutral solutes used in this study.

Table 1: Diffusivity and stokes radius of neutral molecules

	Glucose [19]	PEG 200 [39]	PEG 600 [39]	PEG 1500 [39]
D_∞ [$m^2\ s^{-1}$]	0.69×10^{-9}	0.653×10^{-9}	0.475×10^{-9}	0.283×10^{-9}
r_s [nm]	0.365	0.43	0.58	0.98

Salt retention

Mono-valent salt retention of the membranes was measured using an aqueous solution of 2 g L^{-1} NaCl. Compositions of the feed, collected permeate and

retentate samples were analyzed by measuring the conductivity and temperature of the samples using a 340i conductivity meter (WTW, Germany).

Glucose retention

During retention experiments using glucose the compositions of the feed, permeate and retentate was analyzed by the Johnson & Johnson Vitros DT60 II Chemistry System. 10 µL of the samples are pipetted on fresh GLU DT slides which contain a certain enzyme. The enzyme oxidizes the glucose in the chemistry system and its concentration in the samples is determined by reflectance photometry.

Molecular weight cut-off

The MWCO of the membranes was evaluated with an aqueous solution containing a mixture of PEGs with mean molar masses 200 g mol^{-1}, 600 g mol^{-1} and 1500 g mol^{-1} (each fraction 1 g L^{-1}). 0.2 g L^{-1} Ethylene glycol (EG) was used as a flow marker (internal standard). During MWCO determination the pH of the feed, collected permeate, and retentate samples was measured using a 340i pH meter (WTW, Germany). Compositions of feed, permeate and retentate were analyzed by gel permeation chromatography (GPC) and the MWCO was determined using the protocol developed in our previous work [18]. The $NaNO_3$ concentration of the mobile phase (eluent) of the GPC and the samples was adjusted to 0.05 M. To prevent bio fouling inside the GPC system NaN_3 (0.05 g L-1) was added to both the eluent and the samples.

3.4 Results and Discussions

3.4.1 Membrane characterization

a)

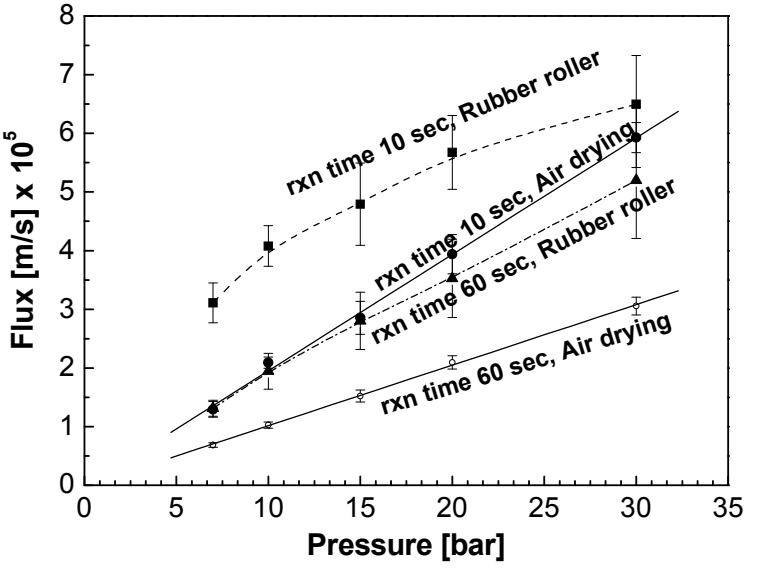

b)

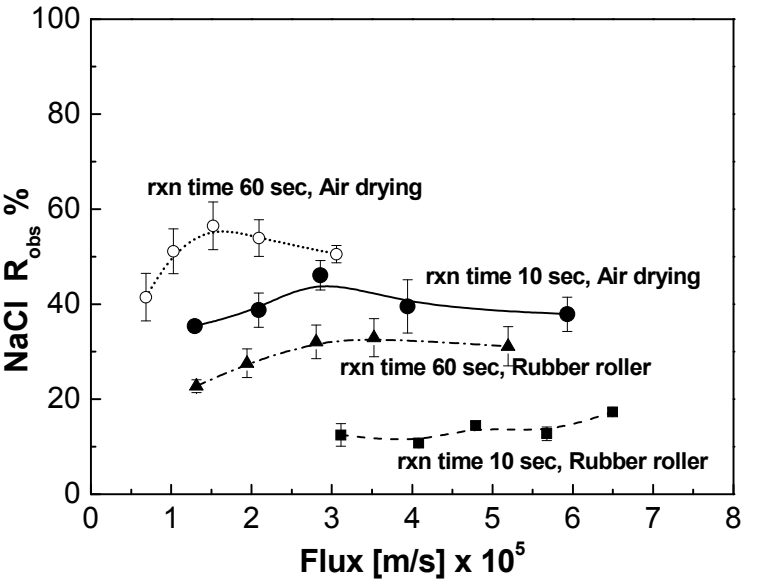

Figure 3: Effect of fabrication parameters on a) Membrane flux and b) NaCl retention of TFC IP-UT membranes

Fig. 3 shows the effect of two parameters of membrane fabrication that were found to have a crucial effect on membrane performance: the reaction time and

removal procedure of the excess aqueous phase solution. A higher reaction time generally leads to a thicker IP layer and consequently a reduced flux [31, 40, 41], as is indeed observed from Fig. 3a. The procedure for removal of excess aqueous phase after impregnation of the support, affects the magnitude and reproducibility of the flux. When a rubber roller is used for removal of excess water [12, 42-45] the flux shows a non-linear dependence on the transmembrane pressure, with a significant standard deviation from the mean value. The decreasing slope of the curve is indicative of an inhomogeneous membrane structure or membrane compaction. When the excess aqueous phase is removed via drying in air for 1 hour, instead of using a rubber roller, a linear relation between flux and pressure is observed, with smaller standard deviation from the mean. This indicates that air drying allows for a more reproducible fabrication method, yielding membranes that do not show significant compaction effects in the applied pressure range. The corresponding mono-valent salt (NaCl) retention as a function of membrane flux and fabrication parameters is illustrated Fig. 3b. When the flux exceeds 3 x 10^{-5} m s^{-1} the retention is not significantly dependent on the value of the flux. This indicates that the dominant transport mechanism is convective flow, and concentration polarization effects are not pronounced. Membranes prepared via the air drying technique show a higher retention as compared to membranes prepared with the use of a rubber roller. Consequently, all subsequent membranes samples were prepared using a 10 seconds reaction time and air drying to remove excess aqueous phase, and are coded as TFC IP-UT.

Fig. 4 shows the SEM image of the ultra-filtration PAN support (pore size 13-18 nm) and the developed IP membrane (TFC IP-UT) with a uniform top layer thickness of around 80-100 nm.

The polyamide layer thickness of the developed membranes is comparable to NF-270 (~90 nm) and Desal-5-DK (~120 nm) (SEM images not shown).

a)

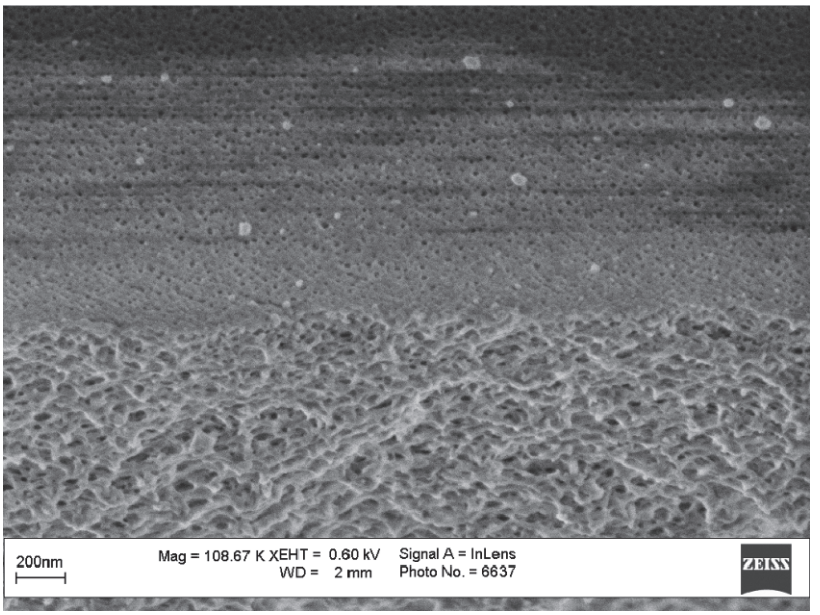

b)

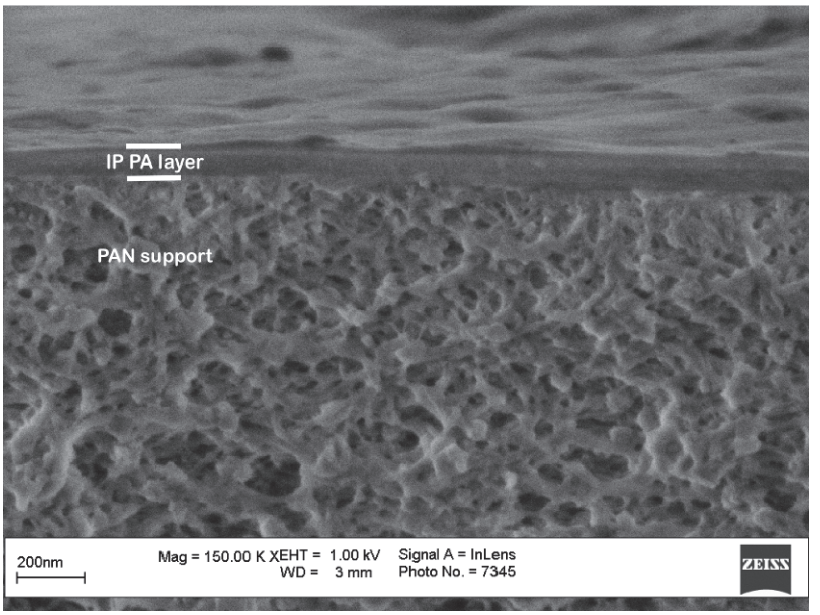

Figure 4: Scanning electron microscopy images of a) PAN support b) TFC IP-UT membrane

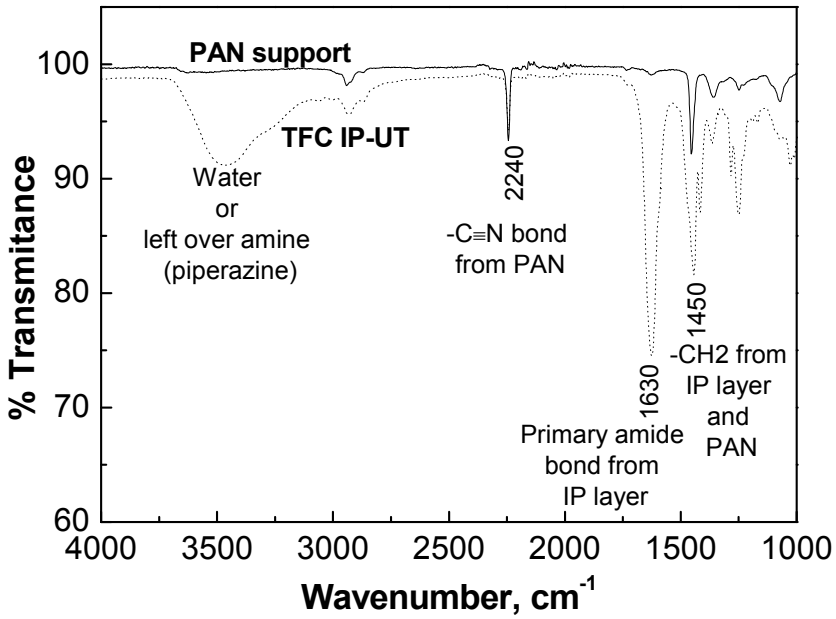

Figure 5: Fourier transform infrared spectrocopy (FTIR) of PAN support and TFC IP-UT membranes

The presence of the polyamide IP layer is evident from the FTIR bands (Fig. 5). The solid line represents the virgin support and the dotted line represents the TFC IP-UT membrane. An intense peak at 2240 cm^{-1}, representing the nitrile group (-C≡N) of the PAN support, can be seen for both the support and the TFC IP membrane. The band at 1450 cm^{-1} represents CH_2 peaks from the PAN as well as the polyamide layer. The TFC membranes have a distinct peak at 1630 cm^{-1} which represents the primary amide bond formed by the IP process.

TFC IP-UT membranes up to A4 size sheets were prepared successfully via the aforementioned protocol. Similar IP layer thickness and permeation performance was observed for all membranes sizes, illustrating the robustness of our fabrication technique.

a)

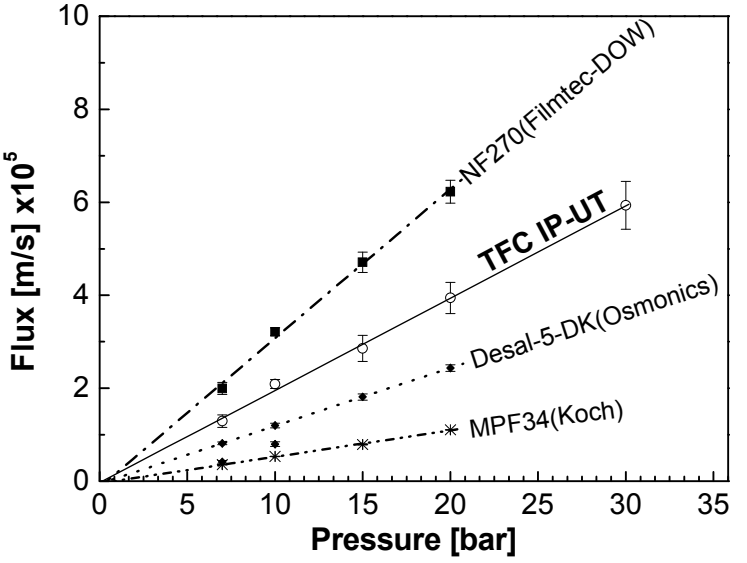

b)

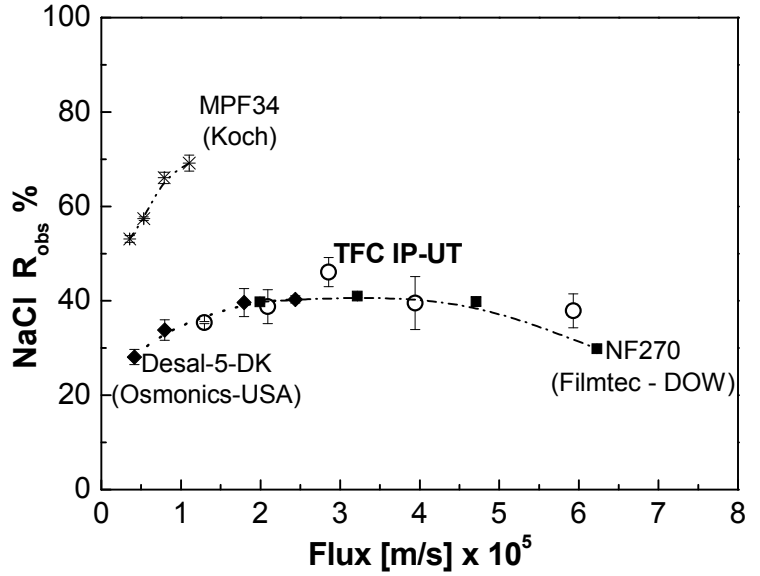

Figure 6: Permeation performance of TFC IP-UT in relation to commercial membranes

Fig. 6 compares the permeation performance of the developed TFC membranes (TFC IP-UT) and commercial nanofiltration membranes for permeation of a 2g L^{-1} NaCl solution at different trans-membrane pressures. The permeance and NaCl retention for commercial membranes are in close agreement with previously reported data on these membranes [46, 47]. The permeance of the TFC IP-UT membrane is in the range of commercial nanofiltration membranes. The developed membranes show similar NaCl retention as compared to commercial

poly (piperazine amide) based nanofiltration membranes (NF-270 and Desal 5-DK). Furthermore, for all membranes, at relatively low flux the NaCl retention increases with increasing flux since the transport of NaCl and water are most likely dominated by diffusion at these low flux values. When the flux increases (as a consequence of increasing operating pressure) the contribution of convective transport increases. Thus, the water transport is increased while NaCl transport is hindered by the size exclusion and Donnan exclusion effect, leading to higher NaCl retention. For the highest fluxes obtained concentration polarization is likely to occur resulting in a drop in NaCl retention at very high flux. MPF-34, which is composed of unknown proprietary polymeric layers, shows much higher NaCl retention, but much lower flux than the other commercially available membranes. Corresponding to the low flux values observed in the applied pressure range, the transport in MPF-34 is most likely diffusion dominated.

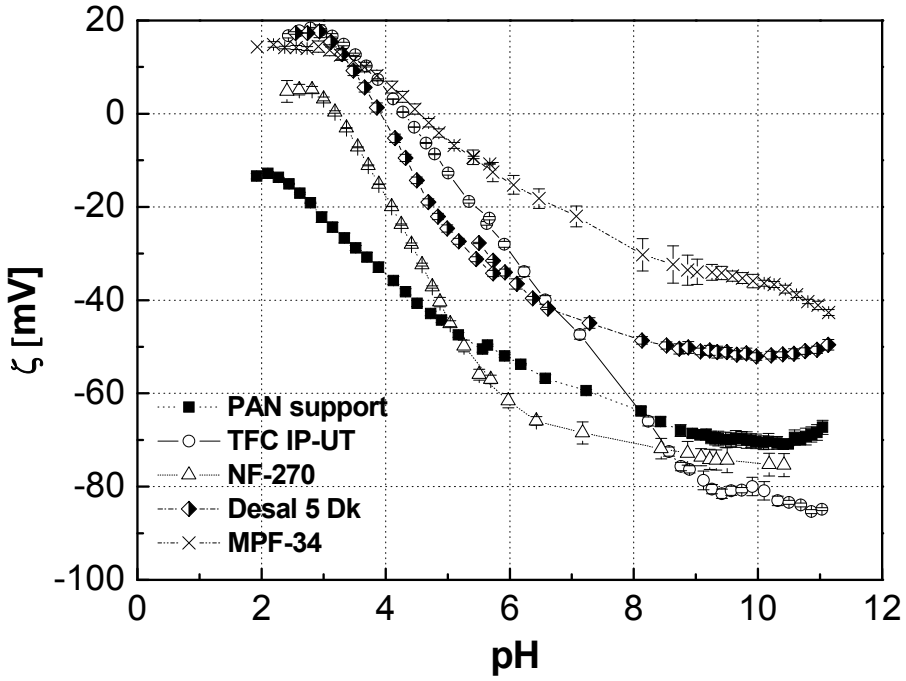

Figure 7: Zeta potential curves via streaming current measurements of the PAN support, TFC IP-UT and commercial membranes

Fig. 7 illustrates the charge characteristics of the unmodified PAN support, the developed and commercial membranes. PAN support has a negative zeta potential in the entire pH range although the membrane has no charged groups. This is a typical phenomenon observed for PAN membranes attributed to the specific adsorption of electrolyte anions onto the surface [48-51]. The TFC IP-UT membranes have an iso-electric point (IEP) of around 4.2 and have a surface charge which is characteristic for a PIP-TMC membrane [45]. It has been reported that the outer surface of the thin polyamide layer is richer in carboxylic groups as compared to the rest of the layer, which is richer in amine groups [52, 53]. Since in zeta-potential measurements predominantly the carboxylic rich outer surface is probed, the membranes exhibit a much smaller positive charge at lower pH than a negative charge at higher pH (due to de-protonation of the carboxylic acid groups at high pH). Although the membrane charge characteristics have been determined by streaming current measurements, the IEPs of the commercial membranes (IEP=3.2 for NF-270, IEP=3.9 for Desal-5DK and IEP=4.5 for MPF-34) compare well with previously reported data via conventional streaming potential techniques [9, 54].

3.4.2 Permeation experiments using glucose

Fig. 8 shows the effect of pH on flux and glucose retention for the TFC IP-UT membranes. The pH of the feed was adjusted using HCl or NaOH solutions for the acidic and alkaline ranges respectively. The flux through the membranes measured at different trans-membrane pressures is independent of pH (within the limits of experimental error) in the acidic to neutral range (Figure 8a). However, in the alkaline region membrane flux appears to decrease with increasing pH. A similar trend is observed for glucose retention, which at pH=11 was lower than at pH=3 or neutral pH (Figure 8b). Retention measurements with glucose were not performed at further pH extremes (pH < 3 or pH > 11), since glucose degradation is expected [55] and in fact was observed at these extreme conditions.

a)

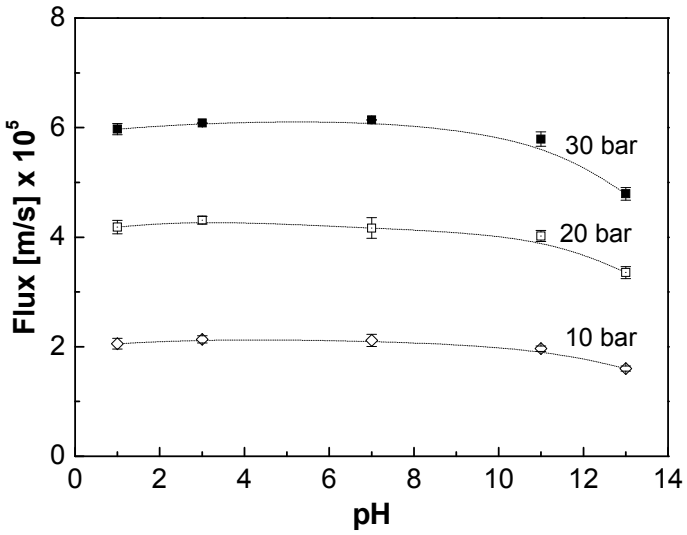

b)

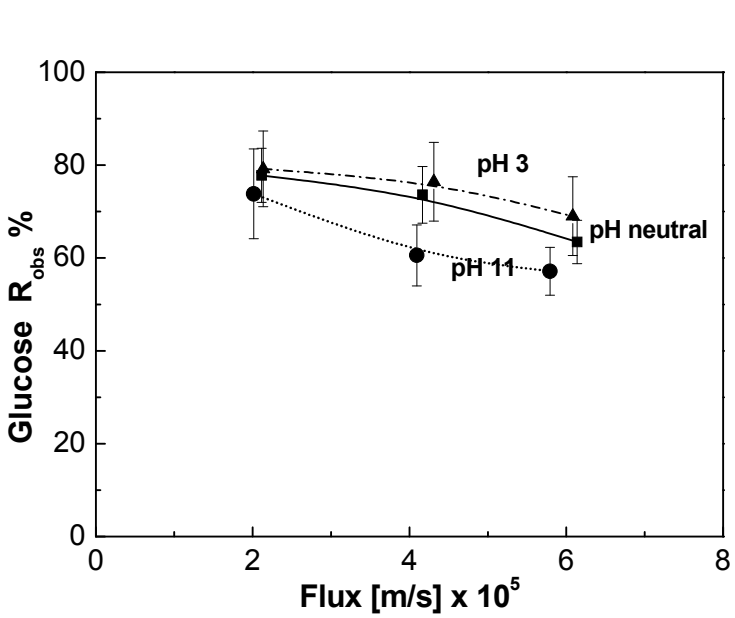

Figure 8: Permeate flux and glucose retention as a function of pH for TFC IP-UT

3.4.3 Molecular weight cut-off measurements

Figure 9a shows a sample cut-off analysis performed at neutral pH conditions, at a pressure of 10 bar, on a fresh TFC IP-UT membrane sample. MWCO determined at 90% rejection for different membrane samples is in the range of 220-240 g mol^{-1}. Figure 9a shows that synthesis grades of PEGs used in the feed solution comprise a broad molecular weight distribution which helps to construct a high resolution retention curve. For example PEG 200 encompasses oligomers ranging

from ~100 to ~400 g mol^{-1} with a significant peak at ~192 g mol^{-1} and ~238 g mol^{-1}. Such polydispersed nature of PEGs has also been reported in a previous study [56].

a)

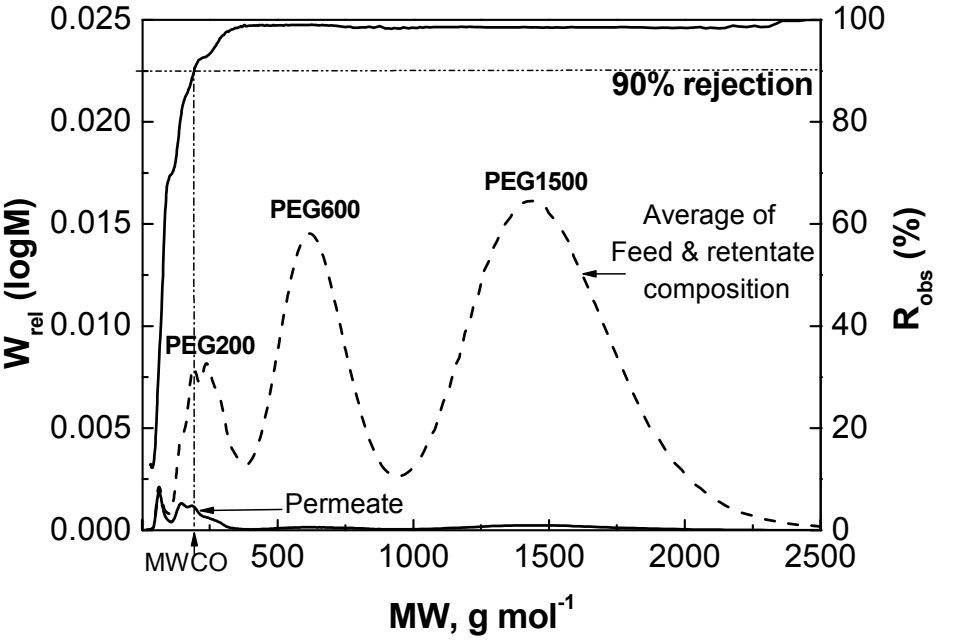

b)

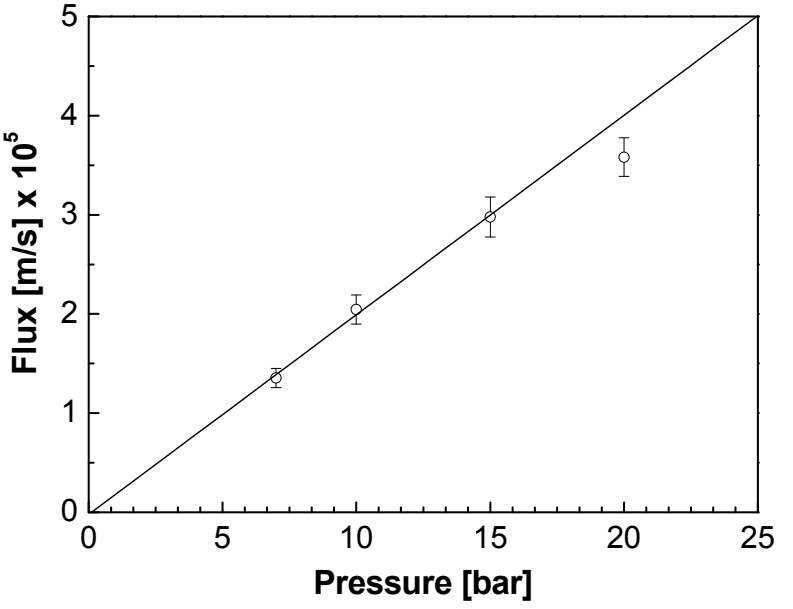

c)

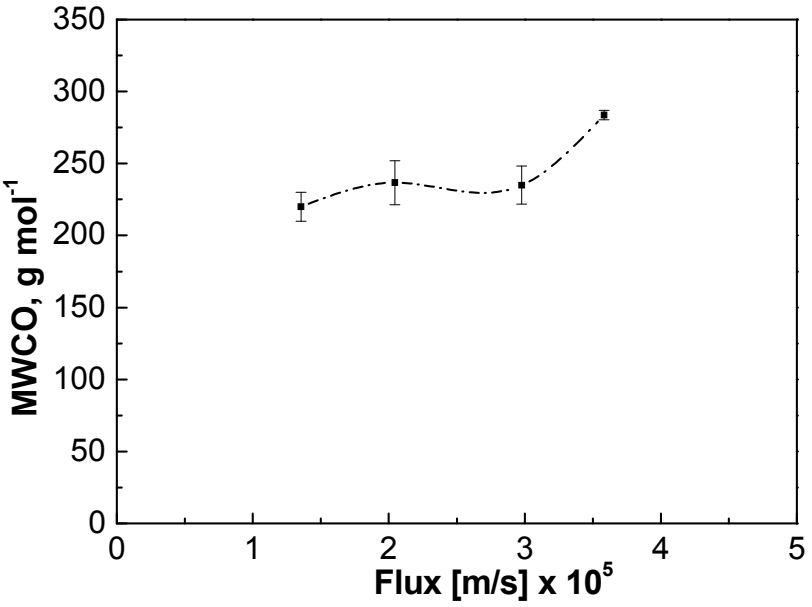

Figure 9: Neutral pH experiments for TFC IP-UT a) Sample MWCO calculation at 10 bar b) Effect of pressure on flux c) Effect of flux on molecular weight cut-off on based on PEG rejection

Fig. 9b and 9c illustrate the effect of applied pressure on the flux and MWCO of the membranes. Up to a pressure of 15 bar a linear increase in flux with the applied pressure is observed (Fig. 9b). Within the limits of experimental error the MWCO also remains constant for these conditions (Fig. 9c). However, at a pressure of 20 bar a drop in flux and an increase in MWCO is observed. These trends were found to be completely reversible when the applied pressure was lowered again. Since no compaction effects were observed on these membranes during pure water flux measurements and NaCl retention experiments (Fig. 6a), this trend could be attributed to concentration polarization effects in the measuring cell due to an increased flux at higher trans-membrane pressures. To minimize concentration polarization, MWCO measurements with feed solutions of varying pH were performed at 10 bar with a stirrer speed of 500 rpm.

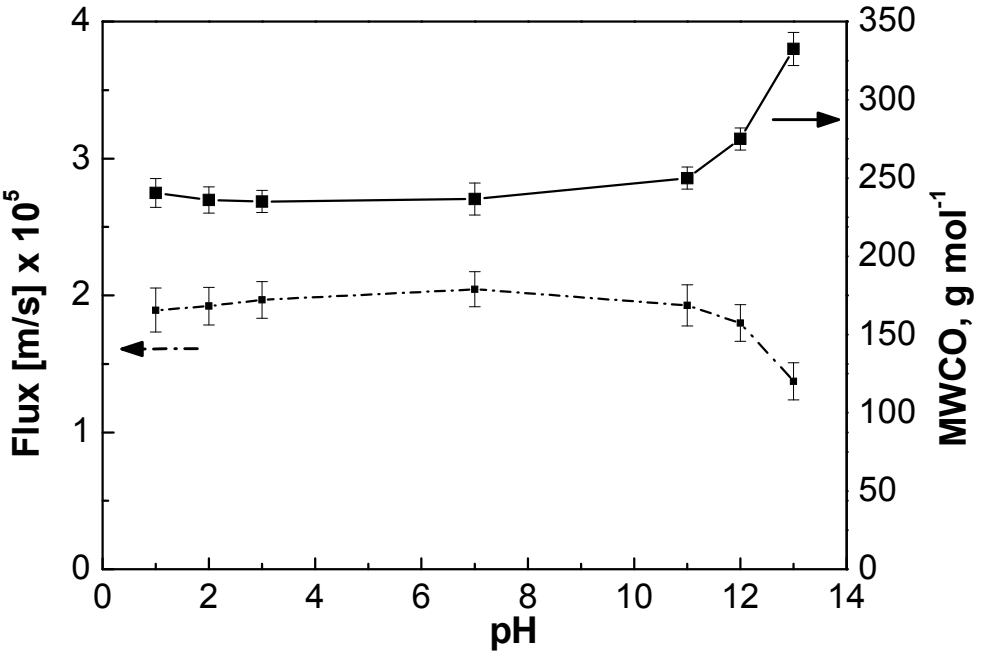

Figure 10: Permeate flux and MWCO (based on PEG molecules) as a function of pH at a constant transmembrane pressure of 10 bar

Fig. 10 illustrates the effect of pH on the flux and MWCO of the membrane samples at a constant trans-membrane pressure of 10 bars. During these experiments the pH of the feed was adjusted using HNO_3 for measurements in the acidic region and NaOH in the alkaline region. Similar to glucose retention results a higher MWCO (reduced retention) and reduced flux are observed in the alkaline region. The higher MWCO at high pH is not caused by defects in the membrane, since subsequent nanofiltration at neutral pH showed the same MWCO and flux as found at the same conditions prior to nanofiltration at high pH. The protocol developed in our previous work [18] enables us to evaluate the effect of pH on the membrane performance in a broader pH range than possible from glucose retention experiments.

3.4.4 Donnan Steric Partitioning Pore Model

a)

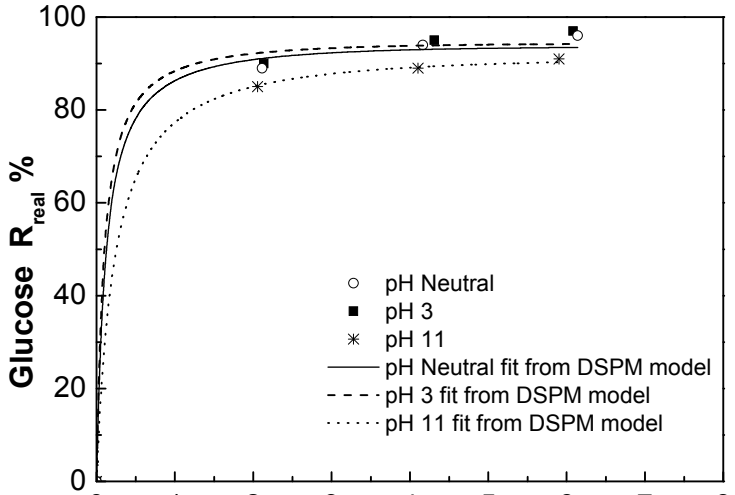

b)

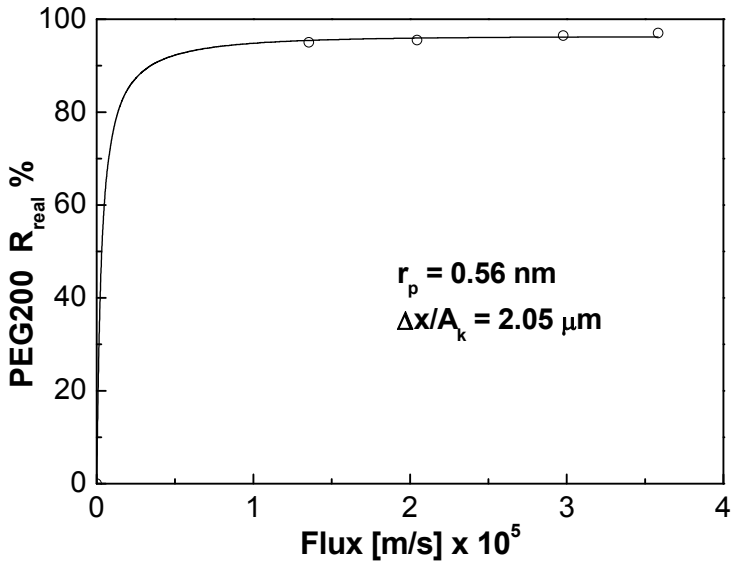

Figure 11: Effect of pH on permeation performance a) Real Glucose rejection v/s flux (lines represent fit from DSPM model) b) Real PEG 200 rejection v/s Flux at neutral pH at ΔP=10 bar (solid line represents fit from the DSPM model)

In order to relate the changes in performance to changes in the structural properties of the membranes, the Donnan Steric Partitioning Pore Model has been used. The validity of equation 20 was checked via NaCl retention

experiments at different stirrer speeds between 100 and 500 rpm. The experimentally determined k' obtained on the basis of the slope of the plot of $\ln[(1-R_{obs})/ R_{obs}]$ as function of $J/\omega^{0.567}$ of $4.4\text{x}10^{-6}$ m $\text{rad}^{-0.567}\text{s}^{-0.433}$ (±3%) is practically the same as k' obtained from equation 21 ($4.5\text{x}10^{-6}$ m $\text{rad}^{-0.567}\text{s}^{-0.433}$ ±3%). This justifies the use of equation 21 for the calculation of k' for our permeation setup. To account for concentration polarization effects in the measuring cell, the observed rejection was converted to the real rejection using equation 20. Resulting real rejection values as a function of permeate flux, at the three pH conditions are shown in Fig. 11a. The continuous lines in Fig. 11a are fitted curves using DSPM and the resulting r_p and $\Delta x/A_k$ are obtained in neutral, acidic and alkaline environments, as illustrated in Fig. 12a. It should be noted that all the DSPM calculations presented in this work are based on the assumption of a homogenous solute velocity, i.e., using equations 7 and 8 [19, 30]. All calculations were also repeated assuming a parabolic solute velocity, i.e. using equations 9 and 10 [19]. Both approaches revealed similar trends of r_p versus pH for both glucose as well as PEG molecules, with slightly lower values for r_p when a parabolic velocity profile was assumed. For example, for glucose retention at neutral conditions the value of r_p determined assuming the parabolic velocity model is 0.48 nm as compared to 0.52 nm when assuming a homogeneous solute velocity. The values of pore radius and the ratio of effective thickness and porosity are in the range of commercial nanofiltration membranes [24, 57] (e.g. For Desal-5DK r_p = 0.42nm and $\Delta x/A_k$ = 1.53µm [22]). Higher values of r_p and $\Delta x/A_k$ are observed in the alkaline region as compared to the neutral or acidic region (Fig. 12a), which is synchronous with the lower rejection observed under alkaline conditions.

a)

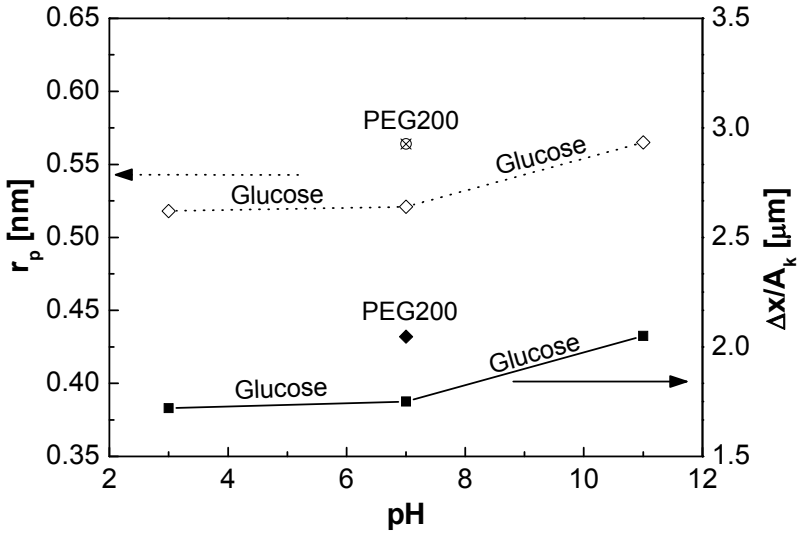

b)

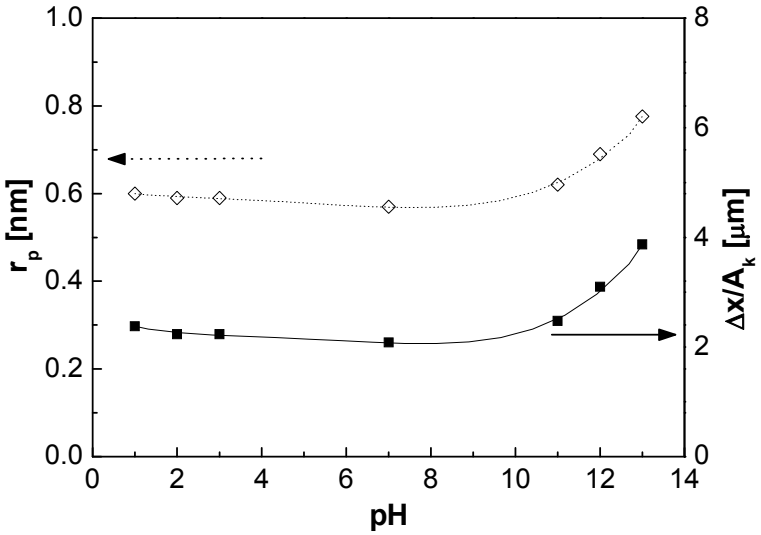

Figure 12: Effect of pH on the pore size & thickness/porosity ratio a) rp and Δx/Ak (determined from full rejection data) as a function pH of the feed b) rp and Δx/Ak (determined using the limiting rejection approach) as a function pH of the feed

Figure 11b shows the fit of the DSPM model on the real rejection of PEG 200 under neutral conditions. The rejection of PEG 200 at varying flux values (different trans-membrane pressures) was derived from the corresponding peaks of the GPC chromatogram in the permeate, retentate and feed streams. Although the average molecular weight of PEG200 is quite close to glucose (MW~180 g/mol), the DSPM fit of PEG200 reveals a slightly higher pore radius (~0.56 nm) as compared to glucose measurements (~0.52 nm) (Figure 12a). This might be

explained due to the presence of higher molecular weight solutes (PEG 600 and PEG 1500) in the feed solution that limit the diffusion of PEG 200 from the membrane surface to the bulk feed, which may have caused a small drop in the retention thus leading to a slightly increased effective pore radius r_p. Another reason may be the relatively big difference in the Stokes radius for glucose and PEG 200 molecules used in the calculations (Figure 13). DSPM fits were not produced for PEG 600 and PEG 1500 molecules since the observed retentions for these molecules reach an asymptotic value of ~99% (Figure 9a). Figure 12b shows the r_p and $\Delta x/A_k$ trends as a function of pH calculated using the limiting rejection approach from the PEG 200 rejection data. At neutral pH the pore radius estimated using the limiting rejection approach (~0.57 nm) is very close to the full rejection approach (~0.56 nm) determined from rejection data obtained at a range of trans-membrane pressures. Similar to Figure 12a higher values of r_p and $\Delta x/A_k$ are observed in the alkaline region as compared to the neutral or acidic region (Figure 12b).

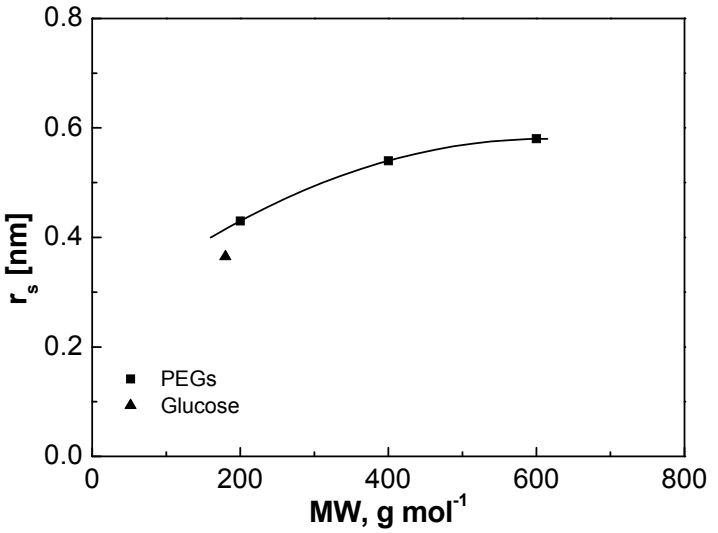

Figure 13: Stokes radius used in DSPM for PEGs [37] and glucose [19] as a function of the molecular weight

Analysis of flux through the PAN support at neutral conditions revealed a permeance of 6.3×10^{-5} m s^{-1} bar $^{-1}$ (±5%), which is ~30 times higher as compared

to the permeance of TFC IP-UT membrane (0.2 x10^{-5} m s^{-1} bar $^{-1}$). Thus the resistance of the support can be considered negligible as compared to the resistance caused by the polyamide layer. Upon exposure of the PAN support with solutions of varying pH a small irreversible decrease in permeance to 5x10^{-5} m s^{-1} bar $^{-1}$ (±5%), was observed at pH 13. This reduction will only cause an insignificant change in the overall resistance provided by the TFC membrane. The decrease in permeance of the PAN support is irreversible, whereas reversible changes have been observed in the performance of the TFC IP-UT membranes as a function of pH. Consequently, it seems reasonable to assume that the changes in performance with varying pH originate predominantly from the polyamide layer.

A probable explanation could be attributed to a change in the effective pore size of the membrane (because of the presence of a pore size distribution in the membrane) due to presence of ions in the feed solution [37, 58]. It has been shown for charged membrane surfaces that addition of certain ions in the feed reduces the membrane flux through the smaller pores to a greater extent than that through the larger pores [37]. A more pronounced zeta potential of the developed TFC IP-UT membranes in alkaline region (Figure 7) as compared to the neutral and acidic region implies that the membrane has a higher surface charge under alkaline conditions. It can be thus reasoned that in alkaline conditions the presence of Na^+ and OH^- ions reduces the overall flux through the membrane pores, causing a decrease in the effective membrane porosity (and thus increasing $\Delta x/A_k$ in Figure 12a). Since the flux in the smaller pores is reduced to a larger extent than in the larger pores, the larger pores have a larger contribution to the overall permeate flux, thereby increasing the effective pore radius r_p (Figure 12a). Since these larger pores have lower solute retention than the smaller pores a reduced retention (increased MWCO) is observed.

3.5 Conclusion

TFC polyamide nanofiltration membranes have been fabricated on a polyacrylonitrile support via interfacial polymerization between piperazine in an aqueous phase and trimesoyl chloride in an organic phase. FTIR spectroscopy and SEM images confirmed the formation of a ~ 80-100 nm thin IP layer on the PAN support. Membrane characterization has revealed that the produced membranes show a NaCl retention similar to NF-270 and Desal-5DK, a permeance in between those of NF-270 and Desal-5DK and a slightly higher iso-electric point than NF-270 and Desal-5DK. The molecular weight cut-off of the membranes appeared to be practically constant in acidic and neutral conditions. At extremely alkaline conditions (pH>11) an increase in molecular weight cut-off and a reduction in membrane flux was found. The Donnan steric partitioning pore model (DSPM) suggests that the membrane has a higher effective average pore size and a greater effective thickness v/s porosity ratio in alkaline conditions as compared to the other pH conditions. A plausible explanation for this phenomenon can be attributed to an increase in the effective average pore size and a decrease in the membrane porosity under alkaline conditions. These changes in the membrane morphology and thus the performance could be crucial, and therefore must be taken into account while using the membranes in applications involving operation at extreme pH conditions.

Nomenclature

A	membrane surface area	[m^2]
A_k	porosity of the membrane	
A_s	cross section area of the streaming channel	[m^2]
c_b	average bulk retentate concentration	[mol m^{-3}]
c_i	concentration of component i in the membrane	[mol m^{-3}]
$C_{i,m}$	concentration of component i on the feed side of the membrane	[mol m^{-3}]
$C_{i,p}$	concentration of component i on the permeate side of the membrane	[mol m^{-3}]
$c_{permeate}$	average permeate concentration	[mol m^{-3}]
D_∞	diffusivity of the solute	[m^2 s^{-1}]
$D_{i,\infty}$	bulk diffusivity of solute i	[m^2 s^{-1}]
$D_{i,p}$	hindered diffusivity	[m^2 s^{-1}]
dI/dP	slope of streaming current versus pressure	[Ampere Pa^{-1}]
F	Faraday constant	[C mol^{-1}]
G	hydrodynamic enhanced lag coefficient	
J	volume flux	[m^3 m^{-2} s^{-1}]
j_i	flux of component i	[mol m^{-2} s^{-1}]
$J_w/\Delta P$	pure water permeance	[m s^{-1} kPa^{-1}]
k'	mass transfer constant	[m $rad^{-0.567}s^{-0.433}$]
K^{-1}	hydrodynamic enhanced drag coefficient	
$K_{i,c}$	hindrance factor for convection	
$K_{i,d}$	hindrance factor for diffusion	
L_s	length of the streaming channel	[m]
Pe_m	Peclet number	
R	universal gas constant	[J mol^{-1} K^{-1}]
r	stirrer radius	[m]
R_{lim}	limiting rejection	
R_{obs}	observed rejection	

r_p	effective pore radius	[m]
R_{real}	real rejection	
r_s	solute Stokes radius	[m]
T	absolute temperature	[K]
t	the permeation time	[s]
V	permeate volume	[m^3]
x	distance normal to membrane	[m]
z_i	valence of component i	
Δx	effective membrane thickness	[m]
ε	dielectric constant of the electrolyte	
ε_0	vacuum permittivity	[F m^{-1}]
ζ	zeta potential	[V]
η	electrolyte dynamic viscosity	[Pa s]
λ	ratio of solute to pore radius	
μ	dynamic viscosity of solution	[kPa s]
v	solute velocity	[m s^{-1}]
υ	kinematic viscosity of the solution	[m^2 s^{-1}].
ψ	electric potential in axial direction	[V]
ω	stirring speed	[rad s^{-1}]
Φ	steric partition term	

References

[1] S.P. Nunes, K.V. Peinemann, Membrane Technology in the Chemical Industry, Wiley-VCH, Weinhim, 2001.

[2] P. Vandezande, L.E.M. Gevers, I.F.J. Vankelecom, Solvent resistant nanofiltration: separating on a molecular level, Chemical Society Reviews, (2008) -.

[3] A.I. Schafer, A.G. Fane, T.D. Waite, Nanofiltration — Principles and Applications, Elsevier, 2005.

[4] R.J. Petersen, Composite reverse osmosis and nanofiltration membranes, Journal of Membrane Science, 83 (1993) 81-150.

[5] L. Li, B. Wang, H. Tan, T. Chen, J. Xu, A novel nanofiltration membrane prepared with PAMAM and TMC by in situ interfacial polymerization on PEK-C ultrafiltration membrane, Journal of Membrane Science, 269 (2006) 84-93.

[6] H. Wang, L. Li, X. Zhang, S. Zhang, Polyamide thin film composite membranes prepared from a novel triamine 3,5-diamino-N-(4-aminophenyl)-benzamide monomer and m-phenylenediamine, Journal of Membrane Science, In Press, Accepted Manuscript.

[7] X.-Z. Wei, L.-P. Zhu, H.-Y. Deng, Y.-Y. Xu, B.-K. Zhu, Z.-M. Huang, New type of nanofiltration membrane based on crosslinked hyperbranched polymers, Journal of Membrane Science, 323 (2008) 278-287.

[8] F.L.B.S. Yujun Song, Preparation, characterization, and application of thin film composite nanofiltration membranes, Journal of Applied Polymer Science, 95 (2005) 1251-1261.

[9] J. Tanninen, M. Mänttäri, M. Nyström, Effect of electrolyte strength on acid separation with NF membranes, Journal of Membrane Science, 294 (2007) 207-212.

[10] M.M. Jayarani, S.S. Kulkarni, Thin-film composite poly(esteramide)-based membranes, Desalination, 130 (2000) 17-30.

[11] M. Liu, S. Yu, Y. Zhou, C. Gao, Study on the thin-film composite nanofiltration membrane for the removal of sulfate from concentrated salt aqueous: Preparation and performance, Journal of Membrane Science, 310 (2008) 289-295.

[12] I.-C. Kim, J. Jegal, K.-H. Lee, Effect of aqueous and organic solutions on the performance of polyamide thin-film-composite nanofiltration membranes, Journal of Polymer Science Part B: Polymer Physics, 40 (2002) 2151-2163.

[13] N.-W. Oh, J. Jegal, K.-H. Lee, Preparation and characterization of nanofiltration composite membranes using polyacrylonitrile (PAN). II. Preparation and characterization of polyamide composite membranes, Journal of Applied Polymer Science, 80 (2001) 2729-2736.

[14] M.N.A. Seman, M. Khayet, N. Hilal, Nanofiltration thin-film composite polyester polyethersulfone-based membranes prepared by interfacial polymerization, Journal of Membrane Science, 348 (2010) 109-116.

[15] P.B. Kosaraju, K.K. Sirkar, Interfacially polymerized thin film composite membranes on microporous polypropylene supports for solvent-resistant nanofiltration, Journal of Membrane Science, 321 (2008) 155-161.

[16] Y.-L. Liu, C.-H. Yu, J.-Y. Lai, Poly(tetrafluoroethylene)/polyamide thin-film composite membranes via interfacial polymerization for pervaporation dehydration on an isopropanol aqueous solution, Journal of Membrane Science, 315 (2008) 106-115.

[17] N. Scharnagl, H. Buschatz, Polyacrylonitrile (PAN) membranes for ultra- and microfiltration, Desalination, 139 (2001) 191-198.

[18] M. Dalwani, N.E. Benes, G. Bargeman, D. Stamatialis, M. Wessling, A method for characterizing membranes during nanofiltration at extreme pH, Journal of Membrane Science, 363 (2010) 188-194.

[19] W.R. Bowen, A.W. Mohammad, N. Hilal, Characterisation of nanofiltration membranes for predictive purposes -- use of salts, uncharged solutes and atomic force microscopy, Journal of Membrane Science, 126 (1997) 91-105.

[20] W.R. Bowen, H. Mukhtar, Characterisation and prediction of separation performance of nanofiltration membranes, Journal of Membrane Science, 112 (1996) 263-274.

[21] W.R. Bowen, A.W. Mohammad, Diafiltration by nanofiltration: Prediction and optimization, AIChE Journal, 44 (1998) 1799-1812.

[22] W.R. Bowen, J.S. Welfoot, Modelling the performance of membrane nanofiltration--critical assessment and model development, Chemical Engineering Science, 57 (2002) 1121-1137.

[23] A.W. Mohammad, A modified Donnan steric-pore model for predicting flux and rejection of dye/NaCl mixture in nanofiltration membranes, Separation Science and Technology, 37 (2002) 1009 - 1029.

[24] W.R. Bowen, A.W. Mohammad, Characterization and Prediction of Nanofiltration Membrane Performance--A General Assessment, Chemical Engineering Research and Design, 76 (1998) 885-893.

[25] J. Schaep, C. Vandecasteele, A.W. Mohammad, W.R. Bowen, Analysis of the Salt Retention of Nanofiltration Membranes Using the Donnanâ€“Steric Partitioning Pore Model, Separation Science and Technology, 34 (1999) 3009 - 3030.

[26] C. Labbez, P. Fievet, F. Thomas, A. Szymczyk, A. Vidonne, A. Foissy, P. Pagetti, Evaluation of the "DSPM" model on a titania membrane: measurements of charged and uncharged solute retention, electrokinetic charge, pore size, and water permeability, Journal of Colloid and Interface Science, 262 (2003) 200-211.

[27] C. Labbez, P. Fievet, A. Szymczyk, A. Vidonne, A. Foissy, J. Pagetti, Retention of mineral salts by a polyamide nanofiltration membrane, Separation and Purification Technology, 30 (2003) 47-55.

[28] A.W. Mohammad, N.a. Ali, N. Hilal, Investigating Characteristics of Increasing Molecular Weight Cutoff Polyamide Nanofiltration Membranes Using Solutes Rejection and Atomic Force Microscopy, Separation Science and Technology, 38 (2003) 1307 - 1327.

[29] A.W. Mohammad, N. Ali, Understanding the steric and charge contributions in NF membranes using increasing MWCO polyamide membranes, Desalination, 147 (2002) 205-212.

[30] A.L. Ahmad, B.S. Ooi, A.W. Mohammad, J.P. Choudhury, Composite Nanofiltration Polyamide Membrane: A Study on the Diamine Ratio and Its Performance Evaluation, Industrial & Engineering Chemistry Research, 43 (2004) 8074-8082.

[31] A.L. Ahmad, B.S. Ooi, Properties-performance of thin film composites membrane: study on trimesoyl chloride content and polymerization time, Journal of Membrane Science, 255 (2005) 67-77.

[32] A.L. Ahmad, B.S. Ooi, Optimization of composite nanofiltration membrane through pH control: Application in CuSO4 removal, Separation and Purification Technology, 47 (2006) 162-172.

[33] C. Labbez, P. Fievet, A. Szymczyk, A. Vidonne, A. Foissy, J. Pagetti, Analysis of the salt retention of a titania membrane using the "DSPM" model: effect of pH, salt concentration and nature, Journal of Membrane Science, 208 (2002) 315-329.

[34] M. Mänttäri, A. Pihlajamäki, M. Nyström, Effect of pH on hydrophilicity and charge and their effect on the filtration efficiency of NF membranes at different pH, Journal of Membrane Science, 280 (2006) 311-320.

[35] Y. Kaya, Z.B. Gönder, I. Vergili, H. Barlas, The effect of transmembrane pressure and pH on treatment of paper machine process waters by using a two-step nanofiltration process: Flux decline analysis, Desalination, 250 (2010) 150-157.

[36] D. Nanda, K.-L. Tung, Y.-L. Li, N.-J. Lin, C.-J. Chuang, Effect of pH on membrane morphology, fouling potential, and filtration performance of nanofiltration membrane for water softening, Journal of Membrane Science, 349 (2010) 411-420.

[37] G. Bargeman, J.M. Vollenbroek, J. Straatsma, C.G.P.H. Schroën, R.M. Boom, Nanofiltration of multi-component feeds. Interactions between neutral and charged components and their effect on retention, Journal of Membrane Science, 247 (2005) 11-20.

[38] T. Luxbacher, Electrokinetic characterization of flat sheet membranes by streaming current measurement, Desalination, 199 (2006) 376-377.

[39] S. Sarrade, G.M. Rios, M. Carlès, Dynamic characterization and transport mechanisms of two inorganic membranes for nanofiltration, Journal of Membrane Science, 97 (1994) 155-166.

[40] F. Yang, S. Zhang, D. Yang, X. Jian, Preparation and characterization of polypiperazine amide/PPESK hollow fiber composite nanofiltration membrane, Journal of Membrane Science, 301 (2007) 85-92.

[41] S.-H. Chen, D.-J. Chang, R.-M. Liou, C.-S. Hsu, S.-S. Lin, Preparation and separation properties of polyamide nanofiltration membrane, Journal of Applied Polymer Science, 83 (2002) 1112-1118.

[42] B. Tang, Z. Huo, P. Wu, Study on a novel polyester composite nanofiltration membrane by interfacial polymerization of triethanolamine (TEOA) and trimesoyl chloride (TMC): I. Preparation, characterization and nanofiltration properties test of membrane, Journal of Membrane Science, 320 (2008) 198-205.

[43] H.I. Kim, S.S. Kim, Plasma treatment of polypropylene and polysulfone supports for thin film composite reverse osmosis membrane, Journal of Membrane Science, 286 (2006) 193-201.

[44] B.-H. Jeong, E.M.V. Hoek, Y. Yan, A. Subramani, X. Huang, G. Hurwitz, A.K. Ghosh, A. Jawor, Interfacial polymerization of thin film nanocomposites: A new concept for reverse osmosis membranes, Journal of Membrane Science, 294 (2007) 1-7.

[45] S. Verissimo, K.V. Peinemann, J. Bordado, Influence of the diamine structure on the nanofiltration performance, surface morphology and surface charge of the composite polyamide membranes, Journal of Membrane Science, 279 (2006) 266-275.

[46] J. Tanninen, M. Mänttäri, M. Nyström, Effect of salt mixture concentration on fractionation with NF membranes, Journal of Membrane Science, 283 (2006) 57-64.

[47] A. Sungpet, R. Jiraratananon, P. Luangsowan, Treatment of effluents from textile-rinsing operations by thermally stable nanofiltration membranes, Desalination, 160 (2004) 75-81.

[48] S. Zhang, K. Saito, H. Matsumoto, M. Minagawa, A. Tanioka, Characterization of Insulin Adsorption Behavior on Amphoteric Charged Membranes, Polym. J, 40 (2008) 837-841.

[49] T. Jimbo, A. Tanioka, N. Minoura, Pore-surface characterization of poly(acrylonitrile) membrane having amphoteric charge groups by means of zeta potential measurement, Colloids and Surfaces A: Physicochemical and Engineering Aspects, 159 (1999) 459-466.

[50] M. Ulbricht, K. Richau, H. Kamusewitz, Chemically and morphologically defined ultrafiltration membrane surfaces prepared by heterogeneous photo-initiated graft polymerization, Colloids and Surfaces A: Physicochemical and Engineering Aspects, 138 (1998) 353-366.

[51] D.A. Musale, A. Kumar, G. Pleizier, Formation and characterization of poly(acrylonitrile)/Chitosan composite ultrafiltration membranes, Journal of Membrane Science, 154 (1999) 163-173.

[52] V. Freger, J. Gilron, S. Belfer, TFC polyamide membranes modified by grafting of hydrophilic polymers: an FT-IR/AFM/TEM study, Journal of Membrane Science, 209 (2002) 283-292.

[53] V. Freger, Nanoscale Heterogeneity of Polyamide Membranes Formed by Interfacial Polymerization, Langmuir, 19 (2003) 4791-4797.

[54] J. Warczok, M. Ferrando, F. López, A. Pihlajamäki, C. Güell, Reconcentration of spent solutions from osmotic dehydration using direct osmosis in two configurations, Journal of Food Engineering, 80 (2007) 317-326.

[55] A. Lehninger, Biochemistry, the molecular basis of cell structure and function, Second Edition (1976).

[56] X. Li, F. Monsuur, B. Denoulet, A. Dobrak, P. Vandezande, I.F.J. Vankelecom, Evaporative Light Scattering Detector: Toward a General Molecular Weight Cutoff Characterization of Nanofiltration Membranes, Analytical Chemistry, 81 (2009) 1801-1809.

[57] J. Straatsma, G. Bargeman, H.C. van der Horst, J.A. Wesselingh, Can nanofiltration be fully predicted by a model?, Journal of Membrane Science, 198 (2002) 273-284.

[58] W.R. Bowen, J.S. Welfoot, Modelling of membrane nanofiltration--pore size distribution effects, Chemical Engineering Science, 57 (2002) 1393-1407.

Sulfonated poly(ether ether ketone) based composite membranes for nanofiltration of acidic and alkaline media

THIS CHAPTER HAS BEEN PUBLISHED:

M. Dalwani; G. Bargeman; S. Hosseiny; M. Boerrigter; M. Wessling; N.E. Benes, Sulfonated poly (ether ether ketone) based composite membranes for nanofiltration of acidic and alkaline media, Journal of Membrane 381 (2011) 81-89

ABSTRACT

Several thin film composite nanofiltration membranes have been prepared by spin coating a sulfonated poly (ether ether ketone) solution on a polyethersulfone support, followed by thermal treatment. The most optimal developed nanofiltration membrane shows a clean water permeance of ~ 4.5 L m^{-2} h^{-1} bar^{-1} and a molecular weight cut off (MWCO) of ~500 g mol^{-1}. No irreversible changes in membrane performance have been observed after prolonged exposure (up to several weeks) of this membrane to solutions with a pH in the range 0-14. Compared to Desal-5-DK, the developed membrane displays a similar water permeance and a higher NaCl retention. In comparison to commercially available pH stable membranes, MPF-34 and NP030P, it reveals a higher water permeance. Permeance and MWCO analysis at varying pH indicates that charge effects induce reversible changes in the membrane materials properties. Especially at strongly alkaline conditions the developed membrane appears to be more open.

4.1 Introduction

Currently nanofiltration (NF) is a topic of principal industrial interest [1], due to the attainable high retention of divalent salts and neutral molecules of low molecular weight (200 to 1000 g mol^{-1}). The moderate stability of standard commercially available polymeric membranes limits their use to aqueous streams with a pH between 2 and 11 [2], thus excluding many potential industrial applications that involve more aggressive conditions [1]. Examples of applications that would benefit from nanofiltration operation at high pH conditions include the filtration and reuse of Cleaning In Place solutions in the dairy industry [3-5], the production of sodium sulfate crystals from mother liquor obtained from salt production [6], the treatment of effluents from the pulp and paper [7] and the textile industry [1], and the separation of hemicellulose from concentrated alkaline process liquors [2]. Applications involving very low pH conditions include the purification of acids [8, 9], the recovery of phosphorous from sewage sludge [10], the removal of metals like copper and gold from process streams with a high sulfuric acid concentration [11], and the removal of sulfate ions from effluents in the mining industry [12]. These lists are not exhaustive, implying a broad potential application landscape for pH-stable membranes.

Sulfonated aromatic polymers, like sulfonated polysulfones [13, 14] and sulfonated poly (arylene ether sulfone)s [15], have excellent chlorine resistance and are reported as superior alternatives to standard reverse osmosis polyamide membranes. Various commercial pH stable membranes comprise top layers based on hydrophilized/sulfonated polyethersulfone (PES). Examples include NP010 / NP030 / NF-PES-10 from Microdyn-Nadir [16-18] (stable in pH 0-14) and NTR 7450 from Hydranautics, Nitto Denko [18, 19] (stable in pH 2-14). However, most of these membranes suffer from a relatively low flux or fall in the nanofiltration membrane category with a relatively high MWCO.

Sulfonated poly (ether ether ketone) (SPEEK) is also a sulfonated aromatic polymer and has been widely investigated for application as ion exchange membranes [20-33]. With the exception of a few cases [34-36], SPEEK is usually prepared by sulfonation of poly (ether ether ketone) (PEEK) in concentrated

sulfuric acid [20-33]. The sulfonation introduces many charged groups on the PEEK polymer, thus making the material more hydrophilic. Although a higher degree of sulfonation is desired for creating a higher charge density in SPEEK, the corresponding excessive swelling propensity results in a polymer with poorer mechanical, dimensional and morphological properties. Several studies have aimed at overcoming these drawbacks by crosslinking [37], either covalently [30-33] or physically via ionic bonding [24, 25]. Blending the acidic SPEEK with basic polymers such as polybenzimidazole [26, 29] and polysulfone bearing benzimidazole groups [27, 28], or incorporation of inorganic particles [22, 23] have also been reported to reduce the extent of swelling. All these approaches involve a small loss in functionality. Most of these techniques include thermal curing, which is known to increase the mechanical integrity of the SPEEK polymer network due to crosslinking by SO_2 bridges [20].

In the nanofiltration field researchers have blended polymers such as polysulfone [38-41], PES [42-44] and polyimides [45, 46] with SPEEK. The aim of such an approach is to enhance the charge density in the original polymer matrix, leading to improved separation performance. Studies have demonstrated the applicability of SPEEK as a polyanion for the fabrication of high performance composite NF membranes via the layer-by-layer technique, which involves alternate deposition of oppositely charged polyelectrolytes [47, 48]. Ba et al. developed a neutrally charged NF membrane by coating SPEEK on a positively charged polyimide-polyethyleneimine membrane with fouling resistant properties [49]. He et al. coated highly sulfonated SPEEK on PES hollow fibers without post curing or crosslinking for application in neutral conditions [50]. The MWCO of all these membranes were at least ~ 5000 g mol^{-1}. These membranes consequently showed ultrafiltration (UF) instead of NF characteristics.

In this work thin film composite (TFC) membranes for application in extreme pH conditions have been prepared by coating SPEEK on PES supports. The performance of these membranes has been compared to commercial nanofiltration membranes and their stability has been evaluated during long-term exposure to extreme pH conditions. Optimal fabrication parameters have been

searched for, with the upper limit of the curing temperature constrained by the polymeric UF supports. The benefits of using a known crosslinker, 1,4-Benzenedimethanol [33, 51], have been evaluated. Variations in the membrane performance as a function of pH have been qualitatively correlated with changes in the membrane charge density.

4.2 Experimental

4.2.1 Chemicals and materials

Poly (ether ether ketone) (PEEK) powder of the grade 450 PF was purchased from Vitrex plc. (United Kingdom). Concentrated sulfuric acid (95-98%, extra pure) and methanol were obtained from Merck (Germany). Anhydrous zinc chloride ($ZnCl_2$) was acquired from Alfa Aesar (Germany). Analytical grade sodium nitrate ($NaNO_3$), sodium azide (NaN_3) and ethylene glycol (EG) and synthesis quality polyethylene glycol (PEG) with mean molecular weights of 200 g mol^{-1}, 600 g mol^{-1} and 1500 g mol^{-1} were acquired from Merck (Germany). Analytical grade sodium chloride (NaCl) (used for salt retention experiments) was acquired from Arcos Organics (Belgium). Analytical grade potassium chloride (KCl) for zeta potential measurements and 1,4 Benzenedimethanol (≥97%) were obtained from Fluka (Germany). Standard volumetric solutions of 1 M hydrochloric acid (HCl), 0.1 M nitric acid (HNO_3) and sodium hydroxide (NaOH) were purchased from Fluka (Germany). Ultrapure water from a Synergy water purification system (Millipore, USA) was used to prepare all solutions and for clean water flux experiments.

4.2.2 Membrane preparation

Sulfonated poly (ether ether ketone) (SPEEK) was prepared from its precursor PEEK 450 PF. Poly (ether ether ketone) polymer was first dried in a 30˚C vacuum oven for more than 24 hours. Sixty grams of PEEK was dissolved in 1 liter concentrated sulfuric acid and stirred at 25˚C for 185 hours to obtain the desired

sulfonation degree (*SD*) (Fig. 1). The polymer was then precipitated in ice water and washed until a pH 6-7 was obtained. After drying at room temperature the obtained SPEEK was dried in a 30°C vacuum oven for at least 48 hours, to remove the residual water.

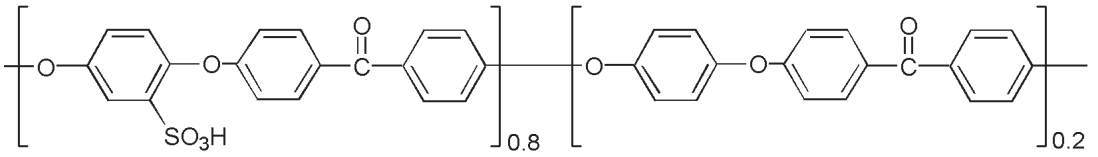

Figure 1: Repeat unit of SPEEK with a SD=80%

Dense SPEEK membranes were prepared via the solvent-evaporation method, and were used to determine the ion exchange capacity (IEC) of the prepared polymer via back titration [21]. SPEEK was dissolved in a concentration of 5 wt% in methanol and casted on a glass plate with a 0.5mm casting knife. The films were dried in a nitrogen atmosphere for 24 hours, and then placed overnight in a 30°C vacuum oven to evaporate the residual methanol. Around 0.7 g membrane was immersed in 150 mL 1 M HCl for 24 hours to bring the membrane in the H^+ form. The sample was then rinsed and soaked in ultrapure water in order to remove the sorbed HCl. Subsequently, the membrane was converted to the Na^+ form by immersion in 150 ml 2M NaCl solution, followed by drying in a vacuum oven at 30°C. The released amount of H^+ ions in the NaCl solution was determined by titrating the solution with 0.1M NaOH. The IEC capacity [meq g^{-1}] was calculated using equation 1

$$IEC = \frac{v}{w} \times c \qquad (1)$$

where v is the volume of NaOH [mL] needed to reach the equivalency point during titration. w is the weight of the dry membrane [g] and c is the molar concentration of NaOH solution [mmol mL^{-1}] . The sulfonation degree *SD* was calculated using:

$$SD = \frac{M_{w,\,p} IEC}{1 - M_{w,\,f} IEC} \tag{2}$$

where $M_{w,p}$ is the molecular weight [g mmol^{-1}] of the non-functional polymer (PEEK) repeat unit and $M_{w,f}$ is the molecular weight [g mmol^{-1}] of the functional group (-SO_3H).

Composite membranes were prepared by spin-coating a SPEEK polymer dope on a support. A 5 wt% solution of SPEEK in methanol was prepared and filtered through a 0.45 μm filter. Crosslinker 1,4 benzenedimethanol was added to the solution in the molar ratio 3:1 (mol SPEEK repeat unit: mol benzenedimethanol). As a catalyst to the Friedel-Crafts reaction 1 wt % of $ZnCl_2$ with respect to the dry weight of SPEEK was added to the solution.

PES membranes UP020, having a nominal MWCO ~20 kg mol^{-1}, acquired from Microdyn-Nadir GmbH (Germany) were used as supports. Preliminary investigations revealed that this support was more suitable for coating the SPEEK than UH030 (Microdyn-Nadir, Germany), PAN HV3 (GKSS, Germany), Polyethylene (PE Solsep, The Netherlands), and Polypropylene (PP IE R/P, Membrana GmbH, Germany). The polymer solution was spin-coated at 1000 rpm onto the support (7 cm x 7 cm) under nitrogen atmosphere and left spinning for ~ 4 minutes. The TFC was then kept in a nitrogen flushed box to ensure complete solvent evaporation. After drying, the membranes were subjected to a curing (heat treatment) procedure using temperatures up to 150°C in a nitrogen flushed oven, for 30 minutes up to 24 hours. Membranes were denoted UT-*TT*-*tt* with *TT* the curing temperature [°C] and *tt* the curing time [hr] and uncured membranes were denoted UT-RT. For samples which were prepared without adding a crosslinker to the SPEEK dope (S) was added to the aforementioned nomenclature.

4.2.3 Surface Characterization

Scanning electron microscopy

Samples were prepared for Scanning electron microscopy (SEM) by freezing the TFCs in liquid nitrogen and subsequently breaking them. After drying under vacuum, samples were coated with platinum. Images were taken using JEOL JSM-6000F scanning electron microscope.

Zeta potential

To avoid the need for surface conductivity corrections associated with streaming potential measurements, streaming current measurements were performed yielding the true zeta potential of the membrane material [52]. These measurements were performed using an electrokinetic analyzer SurPASS (Anton Paar, Graz, Austria), with an adjustable gap cell with a procedure described elsewhere [53, 54]. The zeta potential was calculated according to the equation:

$$\zeta = \frac{dI}{dP} \times \frac{\eta}{\varepsilon \times \varepsilon_o} \times \frac{L_s}{A_s} \tag{3}$$

where ζ is the zeta potential [V], dI/dP is the slope of streaming current versus pressure [Ampere Pa^{-1}], η is the electrolyte dynamic viscosity [Pa s], ε_0 is the vacuum permittivity [F m^{-1}], ε is the dielectric constant of the electrolyte, L_s is the length of the streaming channel [m], and A_s is the cross section area of the streaming channel [m^2].

Fourier Transform Infrared Spectroscopy

The chemical structures of the membranes were analyzed by Attenuated Total Reflection Fourier Transform Infrared Spectroscopy (ATR FT-IR) using an

ALPHA FT-IR Spectrometer (Bruker Optics Inc, Germany) which is equipped with an ATR diamond crystal.

4.2.4 Permeation experiments

Permeation experiments at different trans-membrane pressure (going from 7 to 30 bar) were performed at room temperature in a dead-end filtration setup described in detail elsewhere [53, 54]. In brief, the setup was equipped with magnetic stirrers of radius 18.5 mm, which were set at constant rotation of 500 rpm and the effective membrane surface area was 13.86 cm^2. For each experiment around 3 liters of solution was used as feed. Care was taken that the solution concentration in the setup during permeation does not change by more than 15% of the original feed. All measurements were performed on at least three different membrane samples to ensure reproducibility (all error bars represent standard deviation from the mean). The pH of the feed solutions was adjusted using NaOH and HNO_3 for respective conditions in the alkaline and acidic region.

The permeance was calculated as the ratio of the flux over the trans-membrane pressure difference (Δp in [bar]):

$$\text{permeance} = \frac{J}{\Delta p} = \frac{V}{At\Delta p} \tag{4}$$

where J is the permeate flux in [L m^{-2} hr^{-1}], V is the permeate volume [L], A is the membrane area in [m^2] and t is the permeation time [hr].

The observed retention R was calculated from

$$R = \frac{c_b - c_{permeate}}{c_b} \tag{5}$$

where $c_{permeate}$ is the average permeate concentration and c_b is the average bulk concentration inside the test cell over the total permeation time t, measured as in our previous work [53, 54] .

Salt retention

Salt retention of the membranes was measured using an aqueous solution of 2 g L^{-1} NaCl and 2 g L^{-1} Na_2SO_4. Compositions of the feed, collected permeate and retentate samples were analyzed by measuring the conductivity and temperature of the samples using a 340i conductivity meter (WTW, Germany).

Molecular weight cut-off

The MWCO of the membranes was evaluated with an aqueous solution containing a mixture of PEGs with mean molar masses 200 g mol^{-1}, 600 g mol^{-1} and 1500 g mol^{-1} (each fraction 1 g L^{-1}). 0.2 g L^{-1} Ethylene glycol (EG) was used as a flow marker (internal standard). During MWCO determination the pH of the feed, collected permeate, and retentate samples was measured using a 340i pH meter (WTW, Germany). Compositions of feed, permeate and retentate were analyzed by gel permeation chromatography (GPC) and the MWCO was determined using the protocol developed in our previous work [18]. The $NaNO_3$ concentration of the mobile phase (eluent) of the GPC and the samples was adjusted to 0.05 M. To prevent bio fouling inside the GPC system NaN_3 (0.05 g L-1) was added to both the eluent and the samples.

Long term stability test

The membranes were pre-swelled with ultrapure water in-situ in the permeation setup for around a week in order to achieve a steady state performance. The samples were exposed ex-situ to acidic and alkaline solutions at the respective pH. After exposure, the performance of the membrane samples was evaluated at neutral pH a pressure of 10 bar, via MWCO and NaCl retention experiments.

4.3 Results and Discussions

The IEC of the dense SPEEK films, determined using equation 1, is between 2.28 - 2.29 meq g^{-1}, corresponding to a sulfonation degree of SD ~ 0.8 (80 %) based on equation 2.

All TFC membranes prepared in this work showed considerable swelling and required approximately 6 days to reach a constant flux, implying that a steady state (Fig. 2) was reached. Hence all TFCs were pre-swelled under pressure at the appropriate pH until a steady state was recorded.

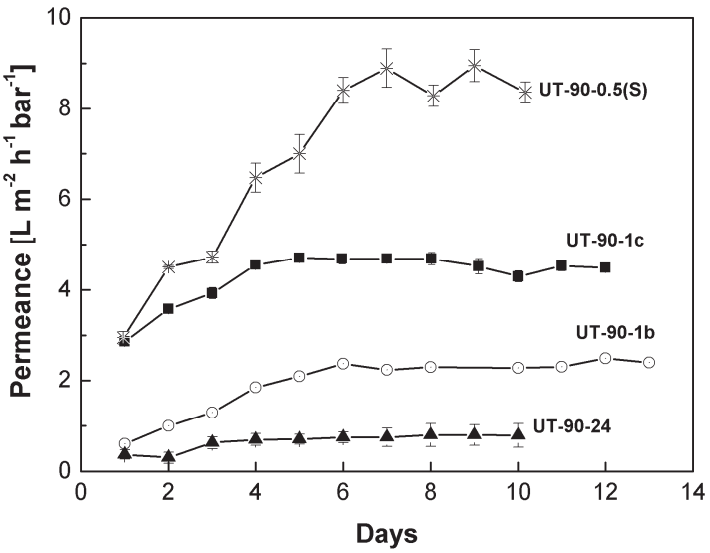

Figure 2: Effect of membrane swelling during clean water flux experments on a few TFC samples

4.3.1 Effect of post treatment on permeance and MWCO at neutral pH

a)

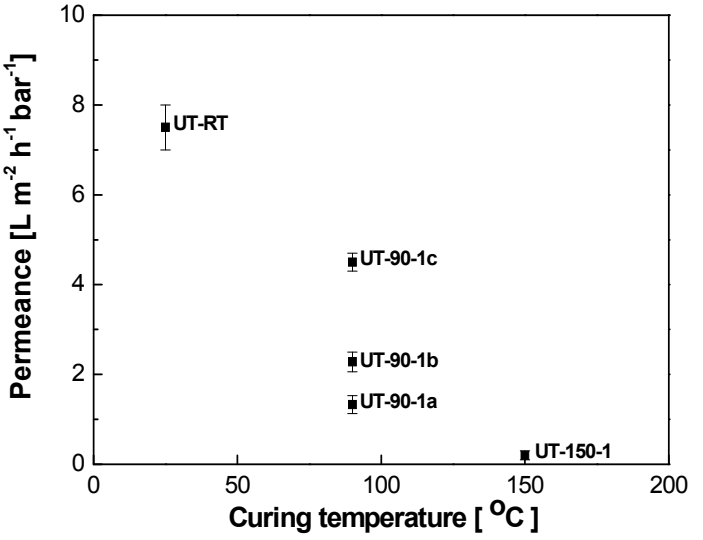

b)

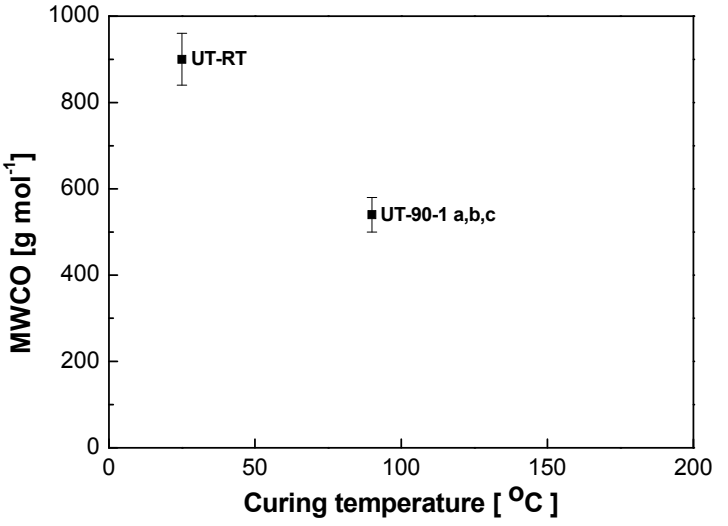

Figure 3: Membane performance as a funtion of curing temperature (1 hour curing time). Effect of curing temperature on a) Permeance b) MWCO at 10 bar trans-membrane pressure

a)

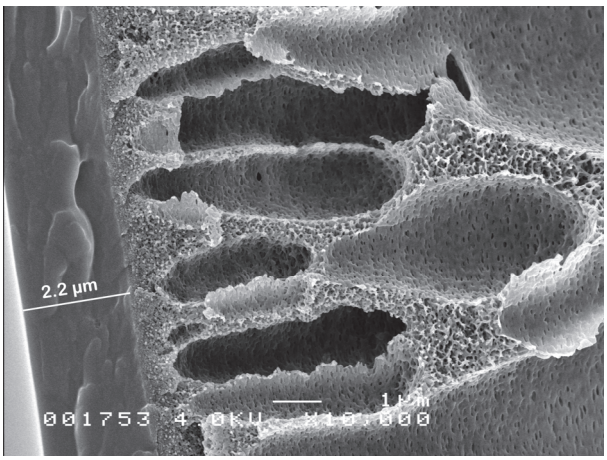

b)

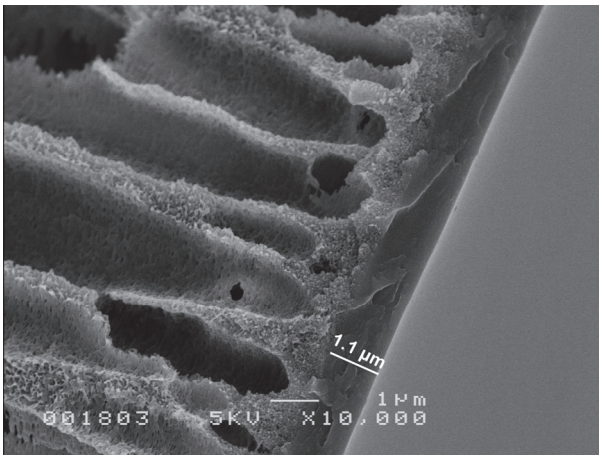

c)

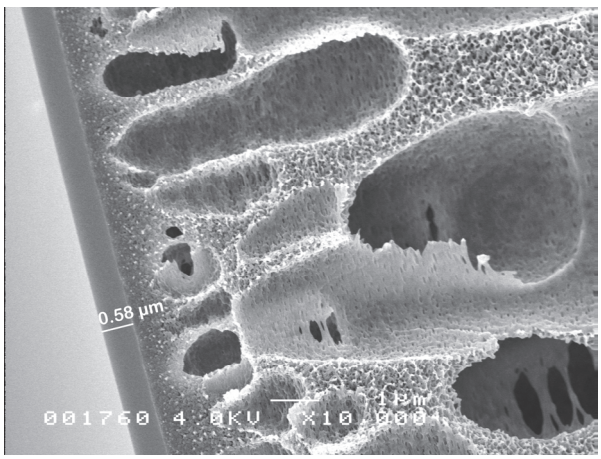

Figure 4: Scanning eletron micrograph showing top layer thickness of a) UT-90-1a (2.2 µm) b) UT-90-1b (1.1 µm) and c) UT-90-1c (0.58 µm)

Table 1 : Effect of heat treatment on PES support membrane

	Permeance L m^{-2} h^{-1} bar^{-1}	MWCO	NaCl ret.
PES UP020 (original membrane)	130 (±15%)	~ 20 kDa	-
PES UP020 cured at 90˚C for 1 hr	124 (±5%)	~ 20 kDa	-
PES UP020 cured at 90˚C for 24 hrs	1.1 (±5%)	450 Da (±6%)	43 % (±3%)
PES UP020 cured at150˚C for 1 hr	0.2 (±20%)	-	-
SPEEK TFC cured at 90˚C for 24 hrs	0.8 (±20%)	400 Da (±5%)	63 % (±3%)
SPEEK TFC cured 150˚C for 1 hr	0.2 (±15%)	-	-

The effect of curing temperature (during membrane fabrication) on permeance and retention during MWCO experiments at neutral conditions is illustrated in Fig. 3. The trends in Fig. 3 indicate that post treatment via thermal curing leads to a reduced permeance and MWCO. As compared to thermally cured membranes, TFC membranes fabricated without thermal curing reveal a higher permeance (~ 7.5 L m^{-2} h^{-1} bar^{-1}), a higher MWCO of ~ 900 g mol^{-1} and a comparatively lower NaCl retention (~ 45%, not shown). Post-curing at 150˚C for one hour results in an extremely low permeance of 0.2 L m^{-2} h^{-1} bar^{-1}. This is due to significant pore collapse in the ultrafiltration support membrane, as also observed for uncoated virgin support membranes exposed to these conditions (Table 1). Curing at 90˚C for 1 hour results in a MWCO of ~500 g mol^{-1} (at Δp =10 bar), comparable to for instance the commercial pH stable membranes NP010 / NP030 from Microdyn-Nadir (MWCO 400-1000 g mol^{-1}) [16, 55]. The variations in the permeance are due to differences in top layer thickness (UT-90-1a: 2.2 μm, UT-90-1b: 1.1 μm, and UT-90-1c: 0.58 μm, see Fig. 4), inherent to the capricious spin coating procedure. As expected, the permeance of UT-90-1a, b and c of 1.3 L m^{-2} h^{-1} bar^{-1}, 2.3 L m^{-2} h^{-1} bar^{-1} and 4.5 L m^{-2} h^{-1} bar^{-1} respectively, is approximately proportional to the thickness of the SPEEK top layer derived from SEM images. The small

deviation in the permeance versus thickness correlation may be caused by pore intrusion, which cannot be accurately quantified from the SEM images. All membranes reveal a similar MWCO (±15%), irrespective of the layer thickness of the dense layer, thereby suggesting a similar morphology for the different samples.

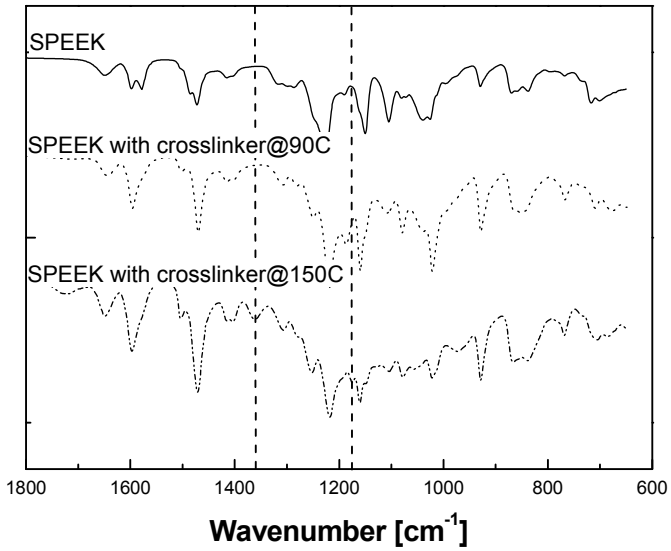

Figure 5: Fourier Transform Infrared Spectroscopy of TFC membranes

Fig. 5 displays the infrared spectra of uncured SPEEK without crosslinker, and SPEEK with crosslinker subjected to 90˚C and 150˚C. The spectrum of the sample cured at 150˚C displays asymmetric vibrations from the sulfonate ester group (1360 cm^{-1} and 1165 cm^{-1}) indicating crosslinking on at least a part of the sulfonated PEEK (Fig. 6). In the spectrum for the samples cured at 90˚C (either with or without crosslinker) the peaks associated with the sulfonate ester stretches are not visible, thereby explaining similar performance of these sets of membranes (see next paragraph).

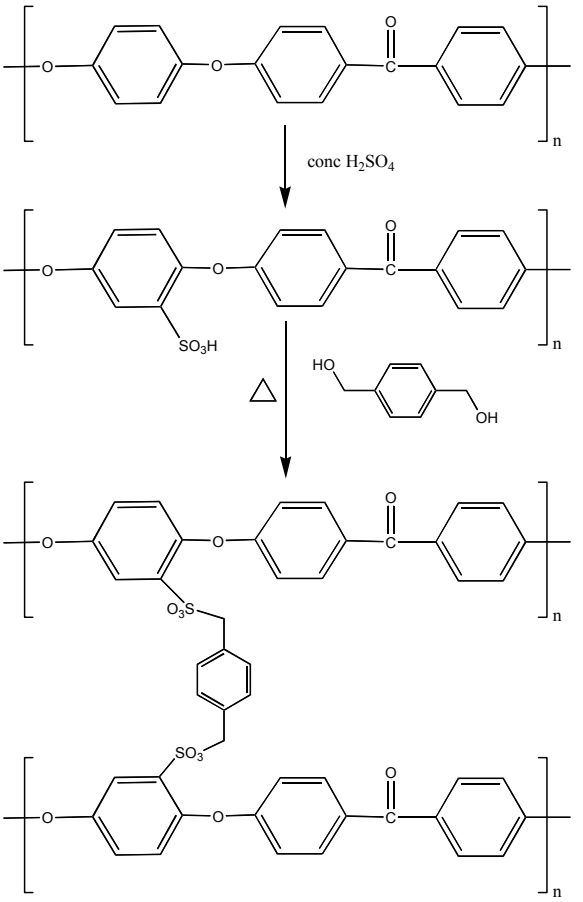

Figure 6: Crosslinking reaction on a part of the sulfonated PEEK

Fig. 7 shows the permeance and MWCO for membranes cured at 90 °C, for different curing times. The data show that longer curing times lead to lower permeance and MWCO. Although a very long post-curing time of 24 hours generates tighter TFC membranes (MWCO ~ 400 g mol^{-1}), a significant pore collapse is observed in the UF supports at these conditions (Table 1), resulting in a significantly lower permeance. No striking differences are observed between the performance of TFC membranes cured at 90°C with crosslinker (Fig. 7) and without crosslinker (Fig. 8). Also for membranes that are not thermally cured, addition or ommision of the crosslinker does not have a signigificant impact on performance (compare Fig. 7 and Fig. 8).

a)

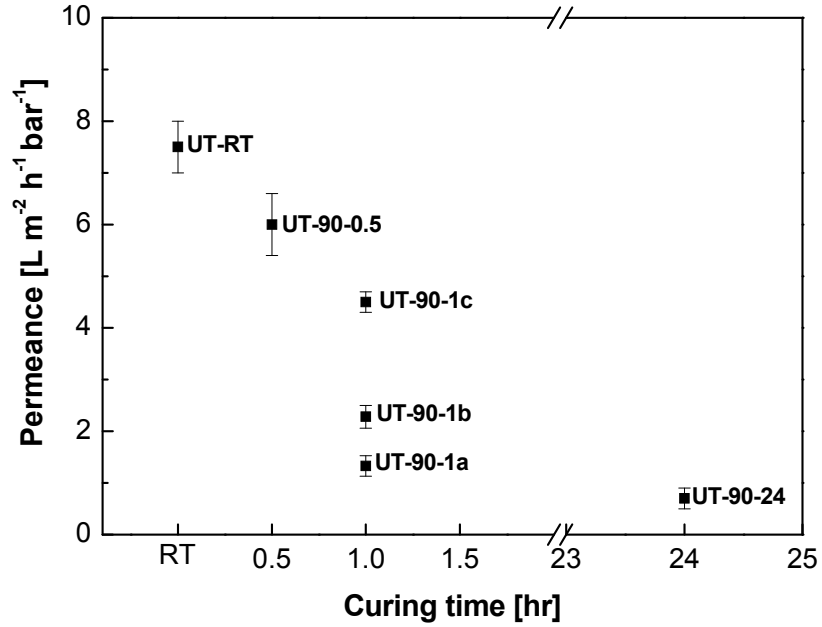

b)

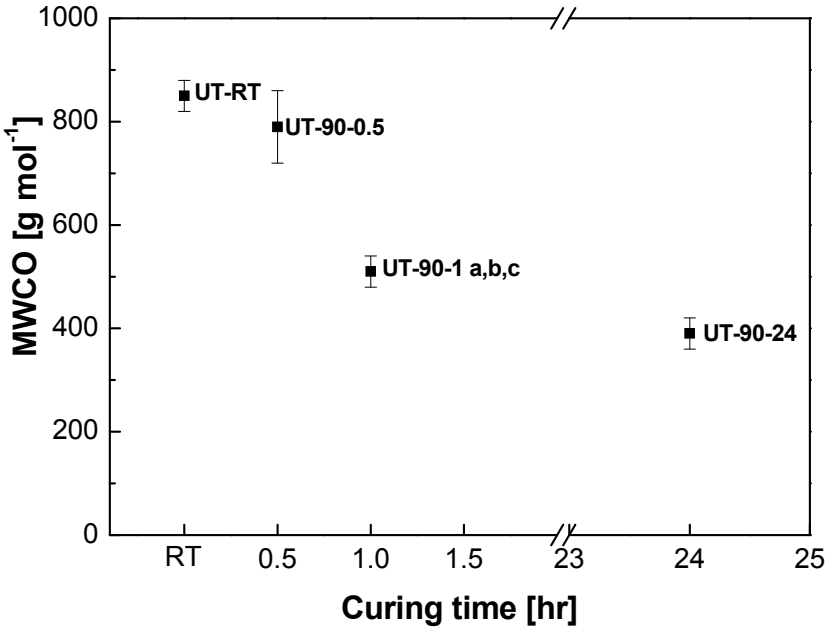

Figure 7: Membrane performance as a function of curing time. Effect of curing time at 90˚C on a) Permeance b) MWCO at 10 bar trans-membrane pressure

a)

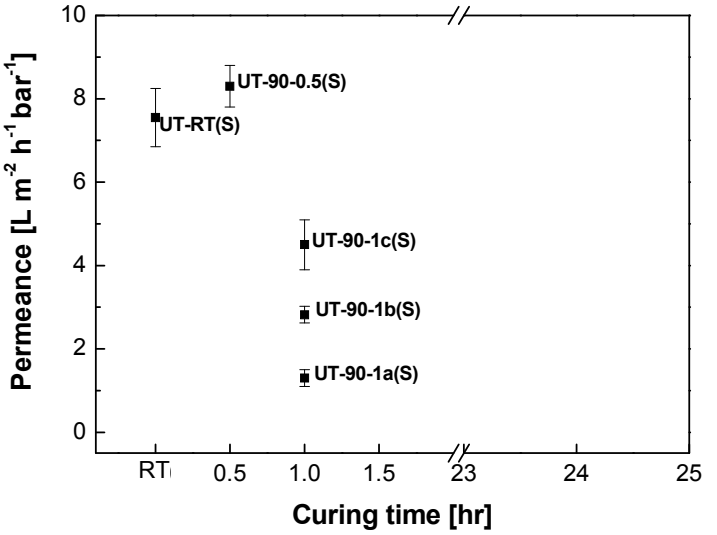

b)

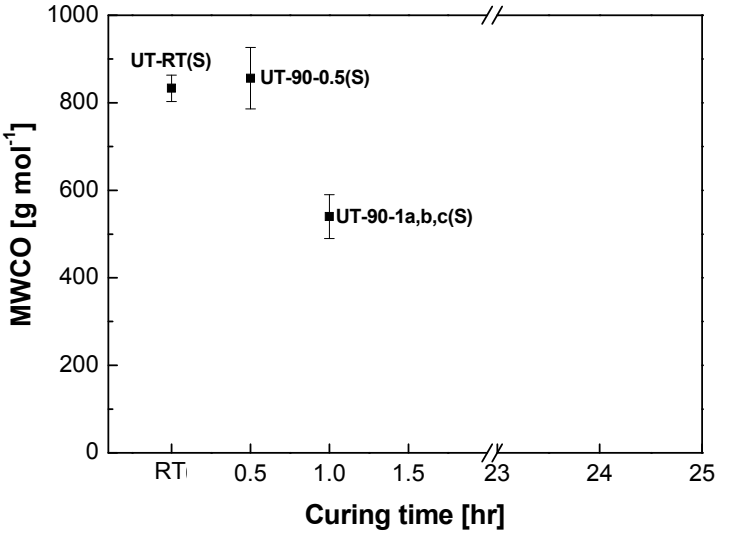

Figure 8: TFC SPEEK membranes without crosslinker post-cured at 90˚C a) Effect of curing time on permeance b) Effect of curing time on MWCO at 10 bar trans-membrane pressure

These observations indicate that performance of the SPEEK based TFC NF membranes can be tuned in particular by the curing temperature and curing time, which are constrained by the UF support. Favorable performance is observed for membranes cured at 90˚C for one hour, conditions at which the addition of the crosslinker has no apparent effect. A study on the effects of covalent crosslinking

at higher temperatures on NF performance would require the use of UF supports with high thermal stability, and is beyond the scope of this paper.

4.3.2 Salt retention during membrane characterization

a)

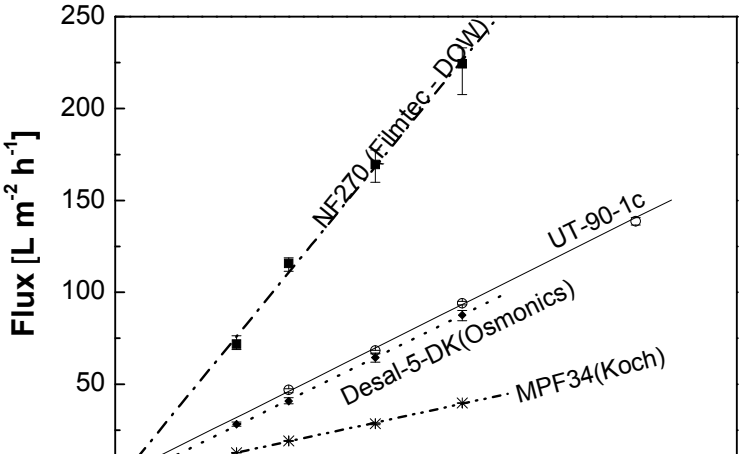

b)

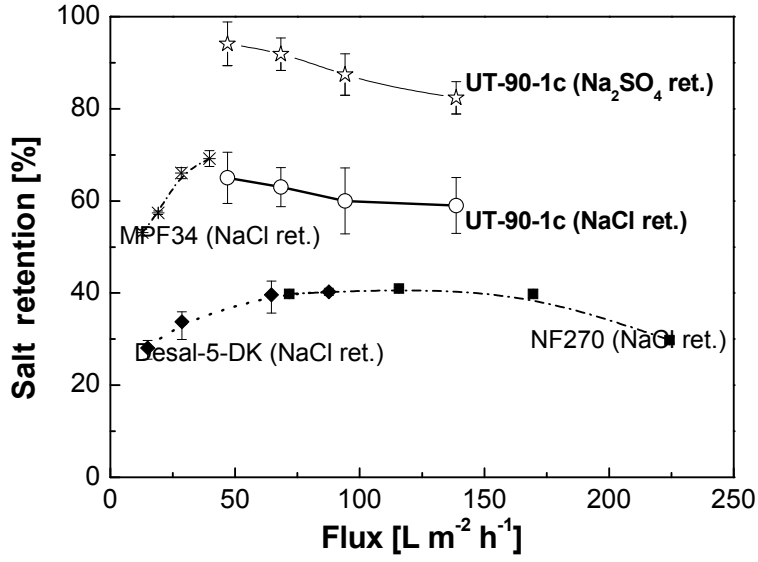

Figure 9: Flux and Salt retention of SPEEK based TFC membrane compared to commercial membranes

Fig. 9 compares the flux and salt retention of developed UT-90-1c membranes (top layer thickness ~ 0.58 μ m) during nanofiltration of 2 g L^{-1} salt solutions with

commercial nanofiltration membranes [53]. The flux of UT-90-1c is comparable to polyamide based Desal-5-DK membrane, but is significantly higher than commercial pH stable tight NF membranes like MPF-34 (Koch). The developed membrane demonstrates a NaCl retention higher than polyamide based NF membranes (NF-270 and Desal-5-DK) and similar to MPF-34 (Fig. 9b). The divalent salt (Na_2SO_4) retention of the UT-90-1c is between 85-95% at 10 to 30 bars transmembrane pressure difference. The highest salt retentions are recorded at the lowest applied pressure of 10 bar, at least for nanofiltration of the sodium sulfate solution. At higher pressures, the corresponding high fluxes may have to led to concentration polarization in the measuring cell, thereby causing a drop in the salt retention.

4.3.3 Long term pH stability

At neutral conditions the performance of these uncured membranes is stable for about 1 week of operation. Exposure to alkaline conditions results in an immediate extreme decline in the performance (permeance above 40 L m^{-2} h^{-1} bar^{-1}), indicating either exessive swelling or detoriation of the top layer. Fig. 10 illustrates the pH stability of the three different sets of membranes cured at 90 °C for 1 hour (UT-90-1a, UT-90-1b & UT-90-1c), at extended exposure to solutions of different pH. From Fig. 10 it can be reasonably concluded that the membranes show no deterioration due to chemical attack during long-term exposure in the entire pH range from 0 - 14. The difference in permeance in the different membrane samples can be correlated to the SPEEK top layer thickness (Fig. 4). Fig. 10b illustrates the retention performance of the membranes at neutral pH, before and after exposure to acidic and alkaline solutions. The MWCO and NaCl retention ranges between 420-580 g mol^{-1} and 60 to 70% respectively for all three different sets of membranes (UT-90-1a, UT-90-1b & UT-90-1c). The exposure to acid and alkaline conditions appears to lead to small but significant deviations in performance. Performance evaluation after exposure to alkaline media indicates the membranes to be relatively open compared to measurements done after acid

exposure. Interestingly, the permeance during clean water flux experiments was ~10-15 % lower than the permeance measured using 2 g L^{-1} NaCl solution (not shown). Thus the more open morphology may be due to the addition of Na^+ to the membrane matrix and subsequent charge effects caused by the same. However these changes are completely reversible, suggesting no deterioration occurs via chemical attack.

a)

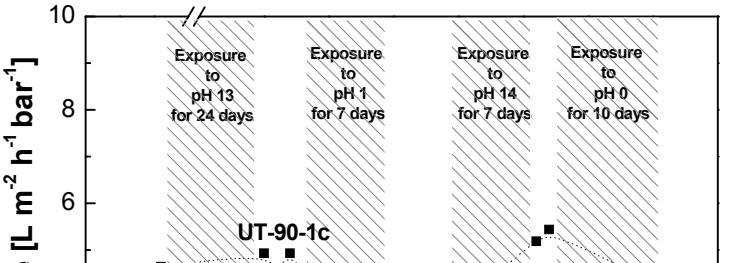

b)

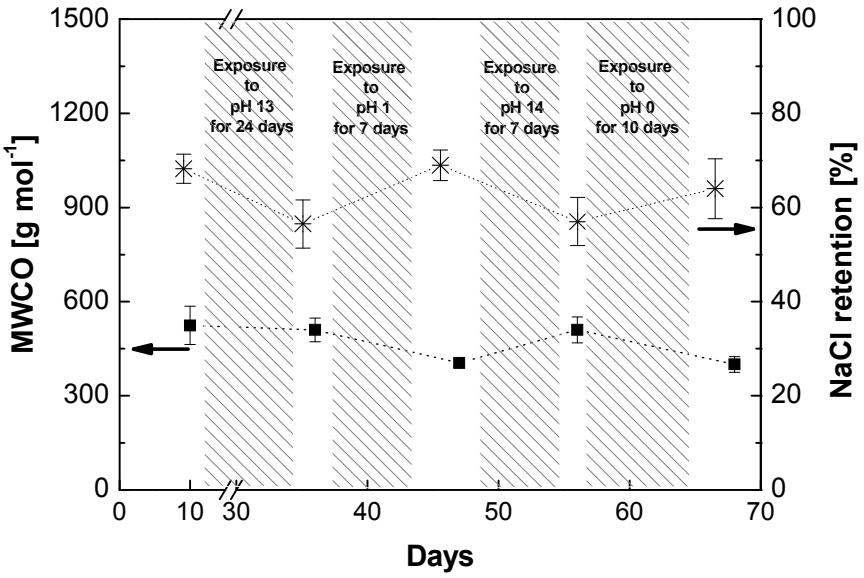

Figure 10: Long term stability tests on membranes cured at 90˚C for 1 hour (UT-90-1). Effect of exposure on a) Clean water Permeance and b) MWCO at 10 bar trans-membrane pressure

4.3.4 Molecular weight cut-off measurements as a function of pH

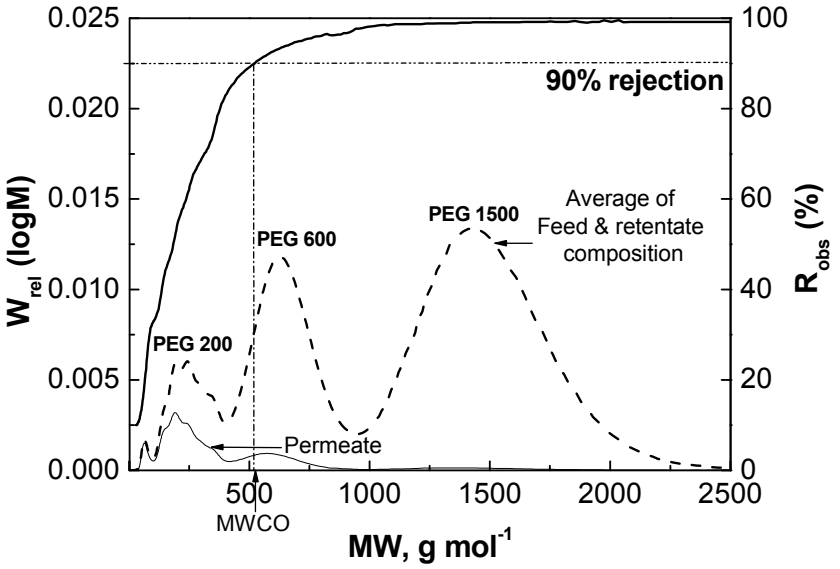

Figure 11: Sample MWCO of UT-90-1c at neutral pH at 10 bars

Fig. 11 depicts the sieving curve of UT-90-1c at neutral pH conditions, revealing a MWCO a cut-off of around 500 g mol^{-1} (±15%). Fig. 12 and Fig. 13 illustrate the effect of pH on the flux and MWCO of UT-90-1c and UT-90-1c(S) membranes respectively. At alkaline conditions the membrane morphology for these membranes appears to be more open than at neutral and acid conditions, as reflected by the relatively high MWCO and flux at alkaline conditions. This is synchronous to performance behavior of membrane samples after ex-situ long term exposure (Fig. 10). The performance change under alkaline conditions recedes completely after the membrane is exposed to neutral or acidic feed solutions for 1 - 2 weeks. The more open morphology for the developed membranes in alkaline conditions has been observed for other membranes composed of a sulfonated polymer skin layer, for instance the NTR 7450 (Hydranautics / Nitto Denko), as well [56].

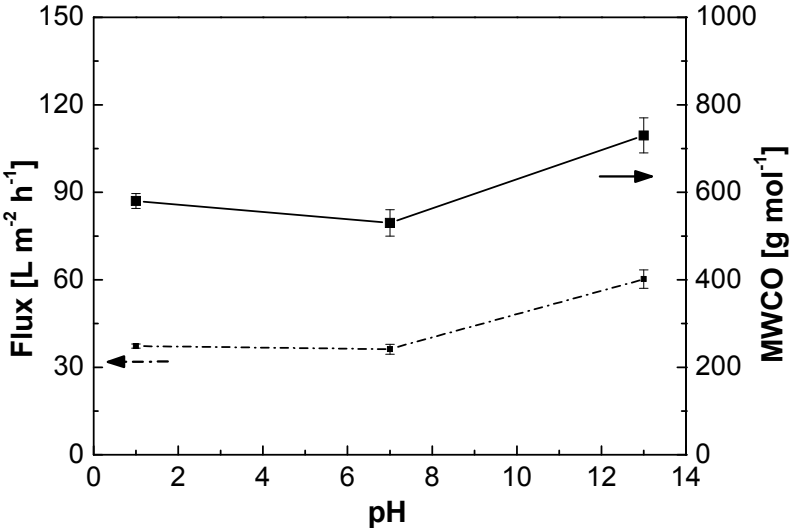

Figure 12: Flux and MWCO of UT-90-1c as a function of pH at 10 bar trans-membrane pressure

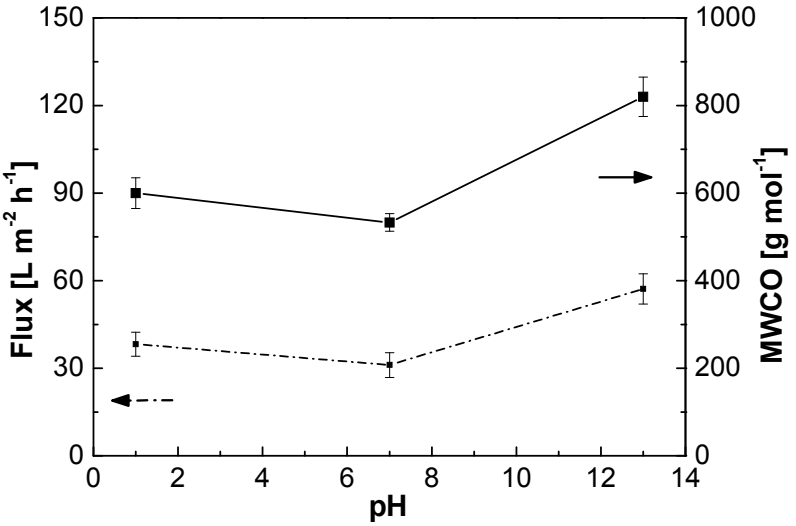

Figure 13: Permeation performance v/s pH of SPEEK membranes without crosslinker at 10 bars

Earlier studies have shown that a change in the membrane charge density, such as caused by differences in pH of the solution subjected to nanofiltration and/or the presence of even small amounts of salt ions, can lead to a significant change in the membrane morphology and consequently retention characteristics for neutral components [53, 54, 56, 57]. These changes seem to be more pronounced when

both the membrane charge density and the ion concentration in the nanofiltration permeate are high [53, 54, 58], leading to reduced retentions for especially small neutral molecules. One of the explanations given for this phenomenon is that the high charge density and a high ion concentration results in a relatively more swollen membrane matrix [56-58].

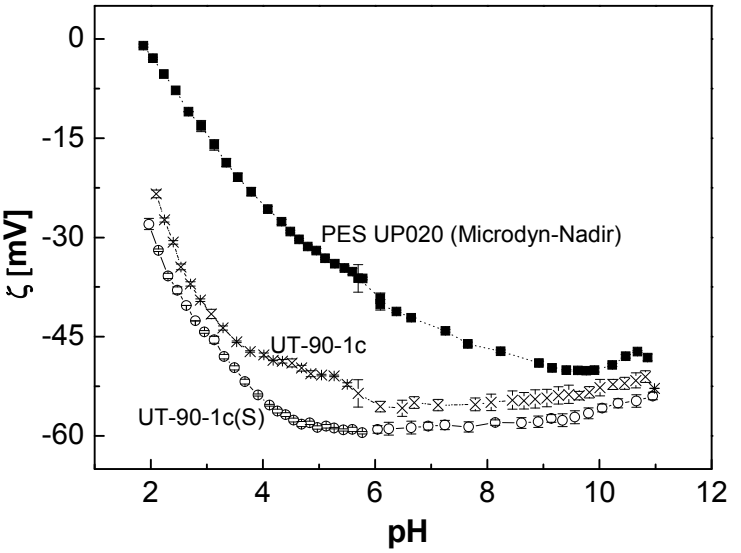

Figure. 14: Zeta potential curves of the UF support and SPEEK TFC membranes

This explanation can be used to understand the effects observed in the current study as well. Fig. 14 shows that the zeta-potentials of the TFC membranes prepared in this work are strongly negative at neutral and alkaline conditions, and less negative at acidic conditions. The more negative zeta-potential at neutral and alkaline conditions indicates that for these conditions the charge effects will affect the separation characteristics of the membrane more than at acid conditions. Although the ion concentrations are similar at acidic and alkaline conditions, the membrane charge density is higher at alkaline conditions. Thus, a more swollen membrane matrix is expected at high pH [56, 58] explaining the higher MWCO and flux at alkaline conditions as compared to acid conditions. For neutral and alkaline conditions the zeta-potential is similar. The observed differences in MWCO and flux for neutral and alkaline conditions can be explained from the very low concentration of charges at neutral pH conditions, moderating the

effects of charges on the flux of water and the retention of the neutral PEGs. In summary, at alkaline conditions the combination of the strongly negative zeta potential and high Na^+ ion concentration seems to have resulted in a relatively more swollen matrix [56, 57] than at neutral and acidic conditions, resulting in a higher MWCO and flux.

4.4 Conclusions

Thin Film Composite nanofiltration membranes prepared by coating SPEEK on PES supports reveal good stability against chemical attack in the entire pH range from 0-14. One of the most promising membranes developed demonstrates at neutral pH a molecular weight cut-off of ~ 500 g mol^{-1}, characteristic of tight nanofiltration membranes, and a permeance similar to the commercial Desal-5-DK membranes. An evaluation of the membrane fabrication parameters shows that post treatment via thermal curing is vital. Favorable nanofiltration performance is observed after curing at 90 °C for one hour, but membranes with different molecular weight cut-off and flux combinations can be obtained by changing curing conditions. Significant covalent crosslinking by 1,4 benzenedimethanol at higher temperatures is prohibited by the limited thermal stability of the polymeric UF supports used in this work. Performance characterization at various pH reveals that developed membranes show a relatively open morphology at alkaline conditions as compared to neutral and acidic conditions. These changes in performance as a consequence of pH changes are reversible. The effects of pH are explained by changes in membrane matrix swelling caused by different interactions between the ions in the solution provided to the nanofiltration membrane and the resulting membrane charge density at different pH.

References

[1] A.I. Schafer, A.G. Fane, T.D. Waite, Nanofiltration — Principles and Applications, Elsevier, 2005.

[2] R. Schlesinger, G. Gotzinger, H. Sixta, A. Friedl, M. Harasek, Evaluation of alkali resistant nanofiltration membranes for the separation of hemicellulose from concentrated alkaline process liquors, Desalination, 192 (2006) 303-314.

[3] Eacute, G. San-Guiziou, Egrave, Ve, E. Boyaval, G. Daufin, Nanofiltration for the recovery of caustic cleaning-in-place solutions: robustness towards large variations of composition, Journal of Dairy Research, 69 (2002) 633-643.

[4] G. Trägårdh, D. Johansson, Purification of alkaline cleaning solutions from the dairy industry using membrane separation technology, Desalination, 119 (1998) 21-29.

[5] J. Yacubowicz, AlkaSave process for recovery of caustic and acids in diaries, Membrane Technology, 1995 (1995) 7-9.

[6] G. Bargeman, M. Steensma, A. ten Kate, J.B. Westerink, R.L.M. Demmer, H. Bakkenes, C.F.H. Manuhutu, Nanofiltration as energy-efficient solution for sulfate waste in vacuum salt production, Desalination, 245 (2009) 460-468.

[7] M. Nyström, L. Kaipia, S. Luque, Fouling and retention of nanofiltration membranes, Journal of Membrane Science, 98 (1995) 249-262.

[8] M.P. González, R. Navarro, I. Saucedo, M. Avila, J. Revilla, C. Bouchard, Purification of phosphoric acid solutions by reverse osmosis and nanofiltration, Desalination, 147 (2002) 315-320.

[9] D. Jakobs, G. Baumgarten, Nanofiltration of nitric acidic solutions from picture tube production, Desalination, 145 (2002) 65-68.

[10] C. Niewersch, C.N. Koh, T. Wintgens, T. Melin, C. Schaum, P. Cornel, Potentials of using nanofiltration to recover phosphorus from sewage sludge, Water science and technology, 57 (2008) 704-714.

[11] S. Platt, M. Nyström, A. Bottino, G. Capannelli, Stability of NF membranes under extreme acidic conditions, Journal of Membrane Science, 239 (2004) 91-103.

[12] T.J.K. Visser, S.J. Modise, H.M. Krieg, K. Keizer, The removal of acid sulphate pollution by nanofiltration, Desalination, 140 (2001) 79-86.

[13] H.B. Park, B.D. Freeman, Z.-B. Zhang, M. Sankir, J.E. McGrath, Highly Chlorine-Tolerant Polymers for Desalination, Angewandte Chemie International Edition, 47 (2008) 6019-6024.

[14] A.E. Allegrezza, B.S. Parekh, P.L. Parise, E.J. Swiniarski, J.L. White, Chlorine resistant polysulfone reverse osmosis modules, Desalination, 64 (1987) 285-304.

[15] M. Paul, H.B. Park, B.D. Freeman, A. Roy, J.E. McGrath, J.S. Riffle, Synthesis and crosslinking of partially disulfonated poly(arylene ether sulfone) random copolymers as candidates for chlorine resistant reverse osmosis membranes, Polymer, 49 (2008) 2243-2252.

[16] Y. Kaya, H. Barlas, S. Arayici, Nanofiltration of Cleaning-in-Place (CIP) wastewater in a detergent plant: Effects of pH, temperature and transmembrane pressure on flux behavior, Separation and Purification Technology, 65 (2009) 117-129.

[17] M. Ince, E. Senturk, G. Onkal Engin, B. Keskinler, Further treatment of landfill leachate by nanofiltration and microfiltration-PAC hybrid process, Desalination, 255 (2010) 52-60.

[18] K. Boussu, B. Van der Bruggen, A. Volodin, C. Van Haesendonck, J.A. Delcour, P. Van der Meeren, C. Vandecasteele, Characterization of commercial nanofiltration membranes and comparison with self-made polyethersulfone membranes, Desalination, 191 (2006) 245-253.

[19] K. Good, I. Escobar, X. Xu, M. Coleman, M. Ponting, Modification of commercial water treatment membranes by ion beam irradiation, Desalination, 146 (2002) 259-264.

[20] M.L. Di Vona, E. Sgreccia, S. Licoccia, G. Alberti, L. Tortet, P. Knauth, Analysis of Temperature-Promoted and Solvent-Assisted Cross-Linking in

Sulfonated Poly(ether ether ketone) (SPEEK) Proton-Conducting Membranes, The Journal of Physical Chemistry B, 113 (2009) 7505-7512.

[21] J. Balster, O. Krupenko, I. Pünt, D.F. Stamatialis, M. Wessling, Preparation and characterisation of monovalent ion selective cation exchange membranes based on sulphonated poly(ether ether ketone), Journal of Membrane Science, 263 (2005) 137-145.

[22] M.L. Di Vona, E. Sgreccia, A. Donnadio, M. Casciola, J.F. Chailan, G. Auer, P. Knauth, Composite polymer electrolytes of sulfonated poly-ether-ether-ketone (SPEEK) with organically functionalized TiO2, Journal of Membrane Science, 369 (2010) 536-544.

[23] S. Feng, Y. Shang, G. Liu, W. Dong, X. Xie, J. Xu, V.K. Mathur, Novel modification method to prepare crosslinked sulfonated poly(ether ether ketone)/silica hybrid membranes for fuel cells, Journal of Power Sources, 195 (2010) 6450-6458.

[24] N.T.Q. Chi, D.X. Luu, D. Kim, Sulfonated poly(ether ether ketone) electrolyte membranes cross-linked with 4,4'-diaminodiphenyl ether, Solid State Ionics, 187 (2011) 78-84.

[25] D.X. Luu, D. Kim, Strontium cross-linked sPEEK proton exchange membranes for fuel cell, Solid State Ionics, In Press, Corrected Proof (2010).

[26] O.D. Thomas, T.J. Peckham, U. Thanganathan, Y. Yang, S. Holdcroft, Sulfonated polybenzimidazoles: Proton conduction and acid–base crosslinking, Journal of Polymer Science Part A: Polymer Chemistry, 48 (2010) 3640-3650.

[27] Y. Fu, A. Manthiram, M.D. Guiver, Blend membranes based on sulfonated poly(ether ether ketone) and polysulfone bearing benzimidazole side groups for proton exchange membrane fuel cells, Electrochemistry Communications, 8 (2006) 1386-1390.

[28] Y.Z. Fu, A. Manthiram, M.D. Guiver, Blend Membranes Based on Sulfonated Poly(ether ether ketone) and Polysulfone Bearing Benzimidazole Side Groups for DMFCs, Electrochemical and Solid-State Letters, 10 (2007) B70-B73.

[29] H. Zhang, X. Li, C. Zhao, T. Fu, Y. Shi, H. Na, Composite membranes based on highly sulfonated PEEK and PBI: Morphology characteristics and performance, Journal of Membrane Science, 308 (2008) 66-74.

[30] Y.-S. Ye, Y.-C. Yen, C.-C. Cheng, W.-Y. Chen, L.-T. Tsai, F.-C. Chang, Sulfonated poly(ether ether ketone) membranes crosslinked with sulfonic acid containing benzoxazine monomer as proton exchange membranes, Polymer, 50 (2009) 3196-3203.

[31] S.D. Mikhailenko, G.P. Robertson, M.D. Guiver, S. Kaliaguine, Properties of PEMs based on cross-linked sulfonated poly(ether ether ketone), Journal of Membrane Science, 285 (2006) 306-316.

[32] S.D. Mikhailenko, K. Wang, S. Kaliaguine, P. Xing, G.P. Robertson, M.D. Guiver, Proton conducting membranes based on cross-linked sulfonated poly(ether ether ketone) (SPEEK), Journal of Membrane Science, 233 (2004) 93-99.

[33] V.R. Hande, S. Rao, S.K. Rath, A. Thakur, M. Patri, Crosslinking of sulphonated poly (ether ether ketone) using aromatic bis(hydroxymethyl) compound, Journal of Membrane Science, 322 (2008) 67-73.

[34] C. Zhao, X. Li, Z. Wang, Z. Dou, S. Zhong, H. Na, Synthesis of the block sulfonated poly(ether ether ketone)s (S-PEEKs) materials for proton exchange membrane, Journal of Membrane Science, 280 (2006) 643-650.

[35] S. Zhong, T. Fu, Z. Dou, C. Zhao, H. Na, Preparation and evaluation of a proton exchange membrane based on crosslinkable sulfonated poly(ether ether ketone)s, Journal of Power Sources, 162 (2006) 51-57.

[36] M. Gil, X. Ji, X. Li, H. Na, J. Eric Hampsey, Y. Lu, Direct synthesis of sulfonated aromatic poly(ether ether ketone) proton exchange membranes for fuel cell applications, Journal of Membrane Science, 234 (2004) 75-81.

[37] J.A. Kerres, Development of ionomer membranes for fuel cells, Journal of Membrane Science, 185 (2001) 3-27.

[38] X. Li, S. De Feyter, I.F.J. Vankelecom, Poly(sulfone)/sulfonated poly(ether ether ketone) blend membranes: Morphology study and application in the filtration of alcohol based feeds, Journal of Membrane Science, 324 (2008) 67-75.

[39] W.R. Bowen, T.A. Doneva, H.-B. Yin, Separation of humic acid from a model surface water with PSU/SPEEK blend UF/NF membranes, Journal of Membrane Science, 206 (2002) 417-429.

[40] W.R. Bowen, T.A. Doneva, H.B. Yin, Polysulfone -- sulfonated poly(ether ether) ketone blend membranes: systematic synthesis and characterisation, Journal of Membrane Science, 181 (2001) 253-263.

[41] W.R. Bowen, T.A. Doneva, H. Yin, The effect of sulfonated poly(ether ether ketone) additives on membrane formation and performance, Desalination, 145 (2002) 39-45.

[42] A.F. Ismail, W.J. Lau, Theoretical studies on structural and electrical properties of PES/SPEEK blend nanofiltration membrane, AIChE Journal, 55 (2009) 2081-2093.

[43] W.-J. Lau, A.F. Ismail, Effect of SPEEK content on the morphological and electrical properties of PES/SPEEK blend nanofiltration membranes, Desalination, 249 (2009) 996-1005.

[44] W.J. Lau, A.F. Ismail, Theoretical studies on the morphological and electrical properties of blended PES/SPEEK nanofiltration membranes using different sulfonation degree of SPEEK, Journal of Membrane Science, 334 (2009) 30-42.

[45] W.R. Bowen, S.Y. Cheng, T.A. Doneva, D.L. Oatley, Manufacture and characterisation of polyetherimide/sulfonated poly(ether ether ketone) blend membranes, Journal of Membrane Science, 250 (2005) 1-10.

[46] K.K. Kopec, S.M. Dutczak, M. Wessling, D.F. Stamatialis, Tailoring the surface charge of an ultrafiltration hollow fiber by addition of a polyanion to the coagulation bore liquid, Journal of Membrane Science, 369 (2011) 59-67.

[47] P. Ahmadiannamini, X. Li, W. Goyens, B. Meesschaert, I.F.J. Vankelecom, Multilayered PEC nanofiltration membranes based on SPEEK/PDDA for anion separation, Journal of Membrane Science, 360 (2010) 250-258.

[48] J. Wang, Y. Yao, Z. Yue, J. Economy, Preparation of polyelectrolyte multilayer films consisting of sulfonated poly (ether ether ketone) alternating with selected anionic layers, Journal of Membrane Science, 337 (2009) 200-207.

[49] C. Ba, J. Economy, Preparation and characterization of a neutrally charged antifouling nanofiltration membrane by coating a layer of sulfonated poly(ether ether ketone) on a positively charged nanofiltration membrane, Journal of Membrane Science, 362 (2010) 192-201.

[50] T. He, M. Frank, M.H.V. Mulder, M. Wessling, Preparation and characterization of nanofiltration membranes by coating polyethersulfone hollow fibers with sulfonated poly(ether ether ketone) (SPEEK), Journal of Membrane Science, 307 (2008) 62-72.

[51] S.L.N.H. Rhoden, C.A. Linkous, N. Mohajeri, D.J. Díaz, P. Brooker, D.K. Slattery, J.M. Fenton, Low equivalent weight Friedel-Crafts cross-linkedsulfonatedpoly(etheretherketone), Journal of Membrane Science, In Press, Accepted Manuscript (2011).

[52] T. Luxbacher, Electrokinetic characterization of flat sheet membranes by streaming current measurement, Desalination, 199 (2006) 376-377.

[53] M. Dalwani, N.E. Benes, G. Bargeman, D. Stamatialis, M. Wessling, Effect of pH on the performance of polyamide/polyacrylonitrile based thin film composite membranes, Journal of Membrane Science, 372 (2011) 228-238.

[54] M. Dalwani, N.E. Benes, G. Bargeman, D. Stamatialis, M. Wessling, A method for characterizing membranes during nanofiltration at extreme pH, Journal of Membrane Science, 363 (2010) 188-194.

[55] A. Carvalho, F. Maugeri, V. Silva, A. Hernández, L. Palacio, P. Pradanos, AFM analysis of the surface of nanoporous membranes: application to the nanofiltration of potassium clavulanate, Journal of Materials Science, 46 (2010) 3356-3369.

[56] M. Mänttäri, A. Pihlajamäki, M. Nyström, Effect of pH on hydrophilicity and charge and their effect on the filtration efficiency of NF membranes at different pH, Journal of Membrane Science, 280 (2006) 311-320.

[57] A. Braghetta, F.A. DiGiano, W.P. Ball, Nanofiltration of Natural Organic Matter: pH and Ionic Strength Effects, Journal of Environmental Engineering, 123 (1997) 628-641.

[58] G. Bargeman, J.M. Vollenbroek, J. Straatsma, C.G.P.H. Schroën, R.M. Boom, Nanofiltration of multi-component feeds. Interactions between neutral and

charged components and their effect on retention, Journal of Membrane Science, 247 (2005) 11-20.

Ultra-thin hybrid polyhedral silsesquioxanes - polyamide films with potentially unlimited dimensions

THIS CHAPTER HAS BEEN SUBMITTED:

Mayur Dalwani; Jumeng Zheng; Mark A. Hempenius; Matthias Wessling; Nieck E. Benes, Ultra-thin hybrid polyhedral silsesquioxanes-polyamide films with potentially unlimited dimensions

GRAPHICAL ABSTRACT

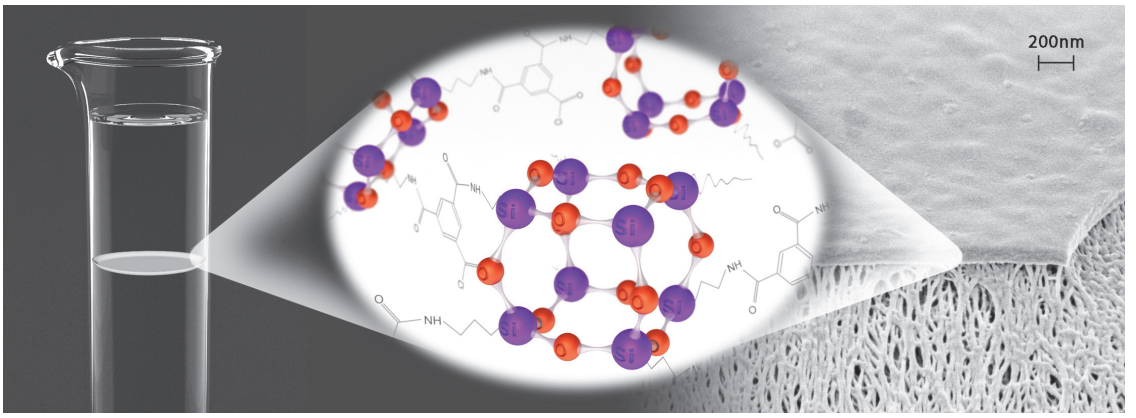

Hybrid nanocomposite materials combine the versatility of organic polymers with the superior thermo-mechanical properties of inorganic materials. Due to their unprecedented properties, hybrid materials have great potential in a variety of fields, in particular when the geometry of the material is, in one dimension, confined to the nanometer range. The application landscape of such ultra-thin films includes integrated optics for telecommunications,[1] hard coats or automotive finishes,[2] sensors,[3], light emitting diodes (LEDS),[4] membranes,[5, 6] coatings,[7] and a range of electronic or photonic devices.[8] Accordingly, there is a high demand for techniques allowing fabrication of ultra-thin (<100 nm) hybrid nanocomposite films, combining easy production of defect free large surface areas with homogeneous distribution of the inorganic and organic components on the sub-nanometer scale. Here, we report a method for the room temperature formation of hybrid polyhedral silsesquioxane-polyamide, in the form of self-supporting or supported ultra-thin films. Our approach is based on interfacial polymerization of an amine-functional polyhedral oligomeric silsesquioxane with a trifunctional acid chloride. This method combines intrinsic local ordering of inorganic and organic constituents on the molecular scale with potentially infinite macroscopic dimensions of the film.

Polyhedral oligomeric silsesquioxanes (POSS) are three-dimensional molecular structures with the basic formula $R_nSi_nO_{1.5n}$, n=6,8,12, and represent the smallest available building blocks of silica (1 – 3 nm).[9] They consist of an inorganic cage of silicon atoms linked with oxygen atoms, externally decorated with a wide variety functional groups.[10] The functional groups include hydrogen, alkyl, alkene, alcohol, acid, amine, epoxy, and sulfonate. Each POSS molecule offers 6 - 12 of these external groups, providing an excellent platform for interactions with a polymeric host in the synthesis of advanced hybrid inorganic – organic composites.[11-13] Strong covalent interactions between POSS molecules and a polymer matrix enable one to form hybrid composites with superior properties, as compared to composites in which traditional inorganic fillers are simply dispersed in the polymer host matrix. [14-16]. Traditional fillers are generally poorly soluble and have to be dispersed carefully and homogenously in a polymer dope before

processing.[17] In contrast, POSS molecules dissolve readily in a variety of solvents containing the polymer, thereby allowing hybrid composites with substantially higher particle loading. Techniques for POSS based thin film fabrication include hot pressing,[18] solution casting,[19] dip-coating,[20] spin-coating,[21] electrostatic self assembly,[22] and the Langmuir-Blodgett technique.[23] We propose a distinct method based on the principle of interfacial polymerization. This approach allows fabrication of ultrathin (~100 nm) self-supporting or supported films with high loading of covalently linked POSS molecules, distributed homogeneously on a molecular level. Thin film formation and polymerization are combined in a single step by dissolving two monomers in two different non-miscible solvents.[24] Film formation occurs at the interface between these two solvents where the monomers react. Formation of the interfacial thin film separates the two reactants causing the reaction to be self-terminating, innately avoiding formation of thicker films. The process can be performed at near ambient temperature, boosting practical feasibility and avoiding possible side reactions or thermal degradation. The technique is well established for organic polymers for industrial and academic applications; a non-exhaustive list includes micro-encapsulation for a wide range of applications like controlled drug release,[25] biosensors and actuators[26], flame retardant systems,[27] catalyst isolation [28], composite membranes for nanofiltration and reverse osmosis,[29] nanofibers for sensors,[30, 31] nanoparticles,[32] superparamagnetic microspheres,[33] and electronically conductive polymers for fabrication of metal/conductive polymer junctions.[34] The advantages of adding an inorganic function to the organic layers has been demonstrated by incorporating various inorganic particles in the thin layer, e.g., zeolites,[5, 35, 36], titanium dioxide,[37] silver,[38] gold,[39] and silica[40]. In all these cases the inorganic nanoparticles are primarily physically dispersed fillers that do not participate in the polycondensation reaction [35, 36].

In contrast, the functional groups on POSS molecules allow them to participate in the polycondensation reaction as one of the reactants. Sufficiently high POSS solubility is required to permit fabrication of a thin hybrid film, containing POSS molecules as primary building blocks. For a typical amine - acid chloride

polycondensation reaction, POSS molecules decorated with amine functional groups are insufficiently soluble to allow thin film formation. To resolve this, we propose a concept illustrated using a water soluble quaternary ammonium chloride salt functionalized POSS (POSS-$NH_3^+Cl^-$) as the aqueous phase monomer, and trimesoyl chloride (TMC) as the organic phase (hexane) monomer. The chloride functionalized POSS is highly soluble in water, but does not react with an acid chloride. Via addition of sodium hydroxide (NaOH) or triethyl amine (TEA), the ammonium chloride groups are converted to primary amines, see scheme 1. The alkaline aqueous POSS solution is brought in contact with the TMC containing hexane phase. At the water / hexane interface the amine end groups of the POSS react with TMC via a polycondensation reaction, to form a POSS-polyamide hybrid network.

Film formation occurs at a liquid-liquid interface, inherently avoiding the complications associated with film detachment from a substrate, typical for coating techniques. The polycondensation reaction progresses when the film is removed from the inter-phase boundary, in principle allowing for continuous removal of a thin film with ever-growing lateral dimensions. The formed self-supporting films are robust and flexible and have sufficient mechanical strength to be transferred onto a silicon wafer. The thickness of transferred films is typically ~100 nm, as determined with spectroscopic ellipsometry. The thickness depends on the composition of the reactive formulations, in particular the pH, as will be discussed in more detail later. Flexible films removed from the liquid-liquid system have a propensity to fold. Prompt unfolding is observed upon re-submerging a folded film in water. The process of folding and unfolding can be repeated several times without causing apparent damage to the film, contrary to what can be expected for thin films of an entirely inorganic composition. Similar to the interpenetrating network based films of Vendamme et al.[41], flexibility of the films is sufficient to allow their repeated aspiration through a small orifice, without apparent damage to the film.

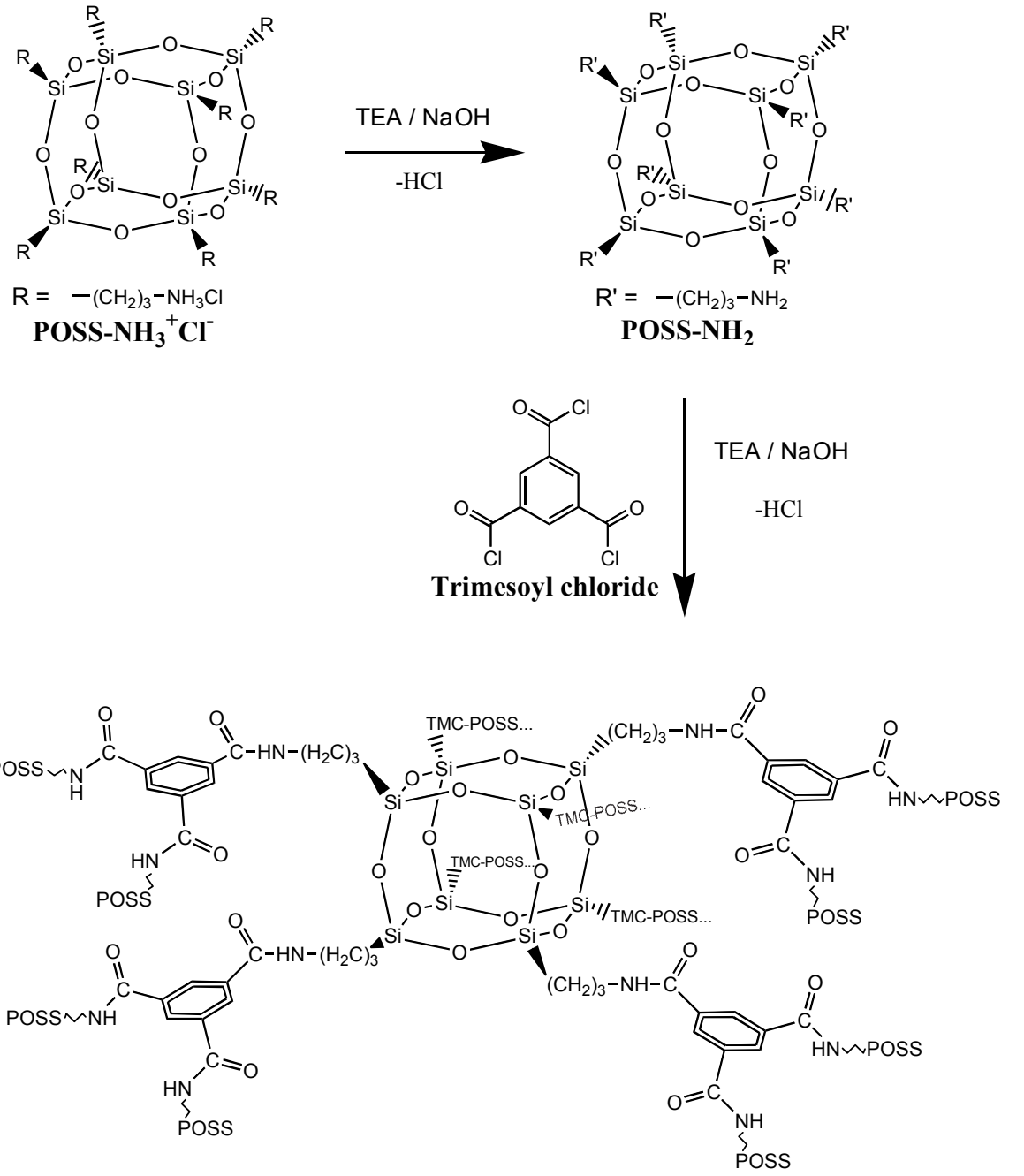

Scheme 1: Reaction mechanism showing formation of POSS-polyamide hybrid film

The above concept can be extended to fabricate supported thin film nanocomposites. For this, a hydrophilic porous material is impregnated with the aqueous alkaline POSS solution. Subsequently, the soaked porous material is brought into contact with the TMC containing hexane, allowing for interfacial polymerization to occur. The result is a thin film formed on the porous support.

For illustration, in figure 1 a SEM image is displayed of a ~100 nm thin POSS derived film on top of an ultra-porous polyacrylonitrile (PAN) support.

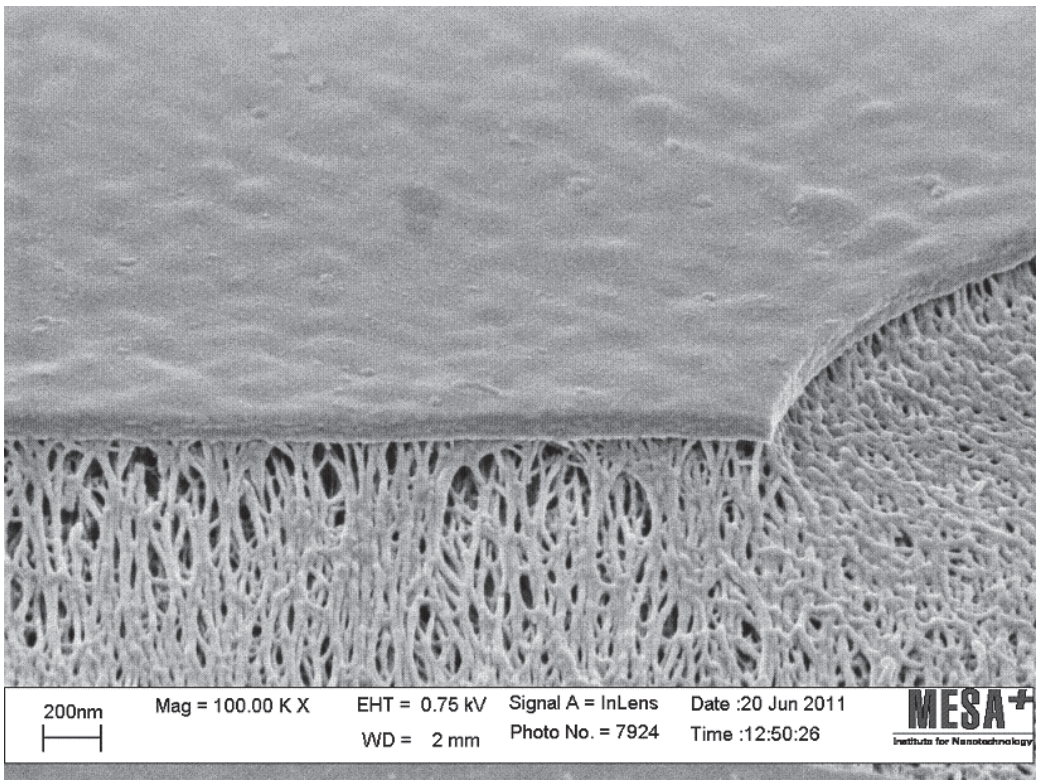

Figure 1: Scanning electron microscopy image of POSS-polyamide-PAN composite.

Incorporation of the POSS-$NH_3^+Cl^-$ into the hybrid polyamide network can be confirmed by X-ray photoelectron spectroscopy (XPS). Analysis of the fresh POSS-$NH_3^+Cl^-$ powder verifies the cage like structure of this molecule (see Table S.1 in supporting information). For the POSS-polyamide hybrid film, the C1s binding energy peak at 287.9 eV, N1s peak at 399.6 eV and O1s peak at 531.3 eV can be attributed to, respectively, C=O, NH-C=O, and O=C of the amide group (Figure 2). The slight shift of the NH_3Cl peak in the N1s spectra of the POSS-polyamide from 401 eV to 401.3 eV is probably due to conversion of NH_3Cl to NH_2 (step 1 of Scheme 1). The absence of any shift or additional binding energies in the Si2p peaks of the hybrid film suggests a similar Si-O-Si structure in the POSS monomer and the polymerized product. The ratio of the intensities of the

two O1s peaks, corresponding to Si-O-Si in POSS and O=C in TMC, indicates that 6 to 7 of the 8 functional groups of the POSS-$NH_3^+Cl^-$ contribute to polyamide linkages with TMC molecules. A similar analysis, based on the N1s spectra, reveals a comparable indication, within the limits of experimental error.

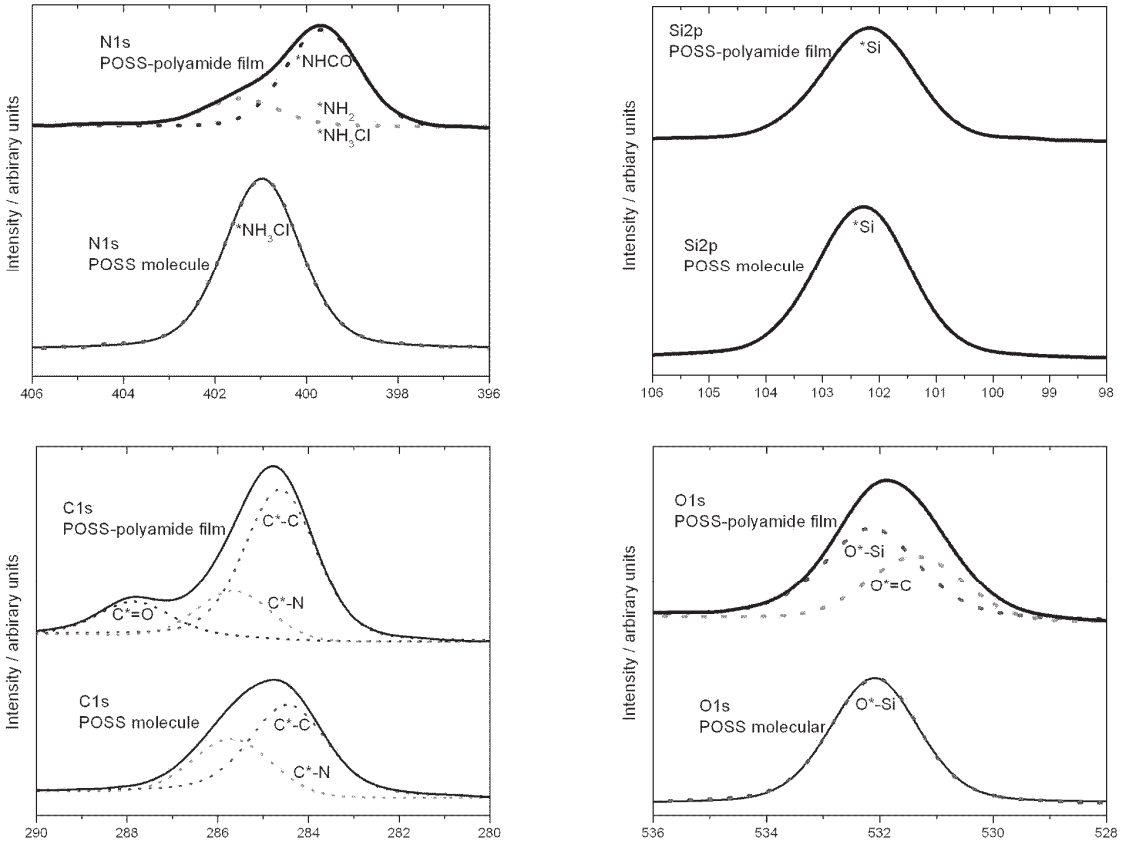

Figure 2: XPS spectra of a POSS-polyamide hybrid film prepared at a pH of 8.7 (pH modulated using NaOH)

Properties of the ultra-thin POSS-polyamide hybrid films are significantly affected by the pH at which the reaction is performed. The effect of alkaline additives is illustrated by Attenuated Total Reflection Fourier Transform Infrared Spectroscopy (ATR-FTIR) analysis (Figure 3). The spectra in figure 3 indicate that a minimum pH is required to allow film formation. For too low pH values the extent of conversion of POSS-$NH_3^+Cl^-$ functional groups into cross-linkable primary amines is probably insufficient. Comprehensive investigations have confirmed that an alkaline pH modulated between 8 and 11 is vital for film formation during the IP process. In this pH range the conversion of ammonium chloride groups to primary amines is

adequate. In addition, the alkaline additives also act as acid acceptors, neutralizing the HCl produced during polycondensation reaction.[42-45] At pH values exceeding 11 film formation is hampered due to either hydrolysis of TMC, inhibiting the IP reaction[42, 43, 46], or hydrolysis of the silsesquioxane cage under highly alkaline conditions.[47] The band at 2240 cm^{-1}, present in all the ATR-FTIR spectra, represents the -C≡N stretching vibration from the underlying PAN ultra-porous support. The sharp bands 1125 and 1040 cm^{-1} can be attributed to the Si-O-Si asymmetric stretching vibrations of polyhedral and ladder silsesquioxan structures, respectively.[48-50] With increasing pH the intensity of the peak at 1125 cm^{-1} decreases and that at 1040 cm^{-1} increases. This indicates that at mild pH conditions the hybrid film comprises mainly polyhedral silsesquioxans whereas under highly alkaline conditions a ladder silsesquioxane network structure emerges.

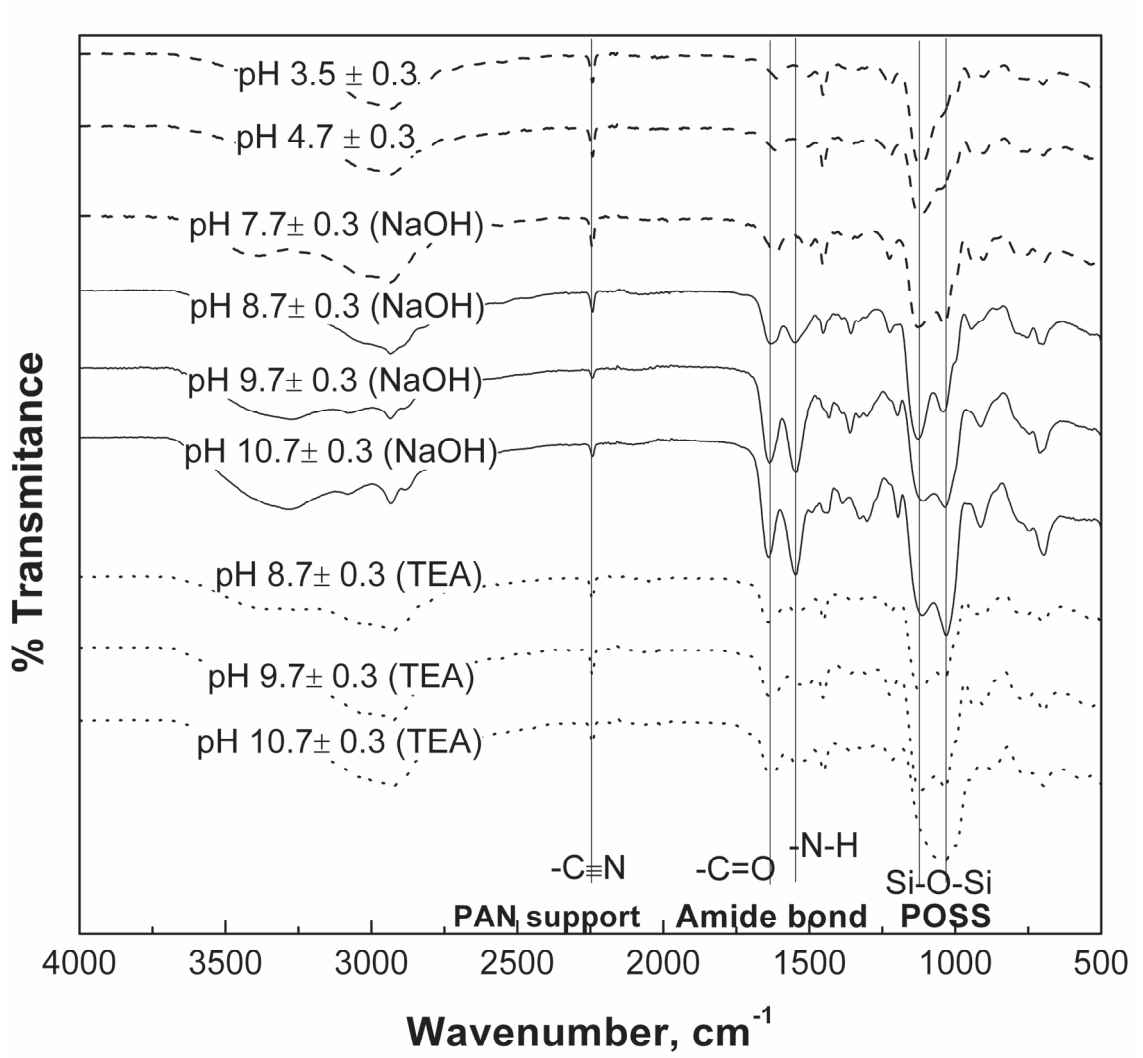

Figure 3: FTIR spectra of the composite POSS-polyamide-PAN films as a function of aqueous phase pH.

The macroscopic integrity of the ultra-thin hybrid films becomes apparent from their substantial molecular selectivity in liquid permeation experiments, in which supported hybrid films were exposed to pressurized (10 bar) solutions of polyethylene glycols in water, and to solutions of polystyrene in toluene. The compositions of the feed and permeated solutions were analyzed with gel permeation chromatography. Figure 4 shows the extent of solute retention of a hybrid film fabricated at pH of 9.7±0.3, with a reaction time of 5 minutes. The molecular weight of molecules which are 90 % retained by the films is referred to as molecular weight cut off. Any molecule smaller than the MWCO can pass the film to a certain percentage. The lines shown in Figure x are obtained from a polydisperse polymer solutions of polyethylenglycol in water or polystyrene in toluene. For the aqueous solution the molecular weight cut off is ~200 g mol^{-1}, for the toluene solution ~1000 g mol^{-1}. The permeance of water and toluene is 0.3 and 0.6 $L.m^{-2}.hr^{-1}.bar^{-1}$ respectively. The high retention for small solute molecules proofs of a highly crosslinked polyamide network and the absence of surface defects.

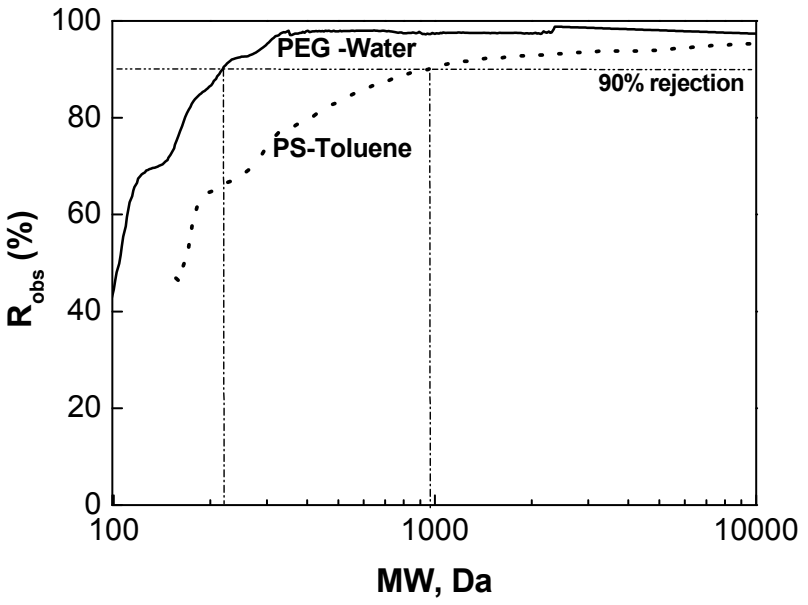

Figure 4: Molecular sieving characteristics of the Hybrid composite films

The reaction conditions strongly affect the degree of crosslinking in the hybrid material, illustrated by the well known tradeoff between permeance and selectivity

in Figure 5.[51] The data indicate that a minimum reaction time of 5 minutes is required to achieve formation of a defect free film. The most pronounced correlation between trade-off and pH of the POSS solution is observed in the case of NaOH. The highest selectivity, combined with lowest permeance, is observed for a pH of 9.7±0.3, indicating that this pH facilitates a highly crosslinked hybrid network. For a pH of 10.7±0.3 the trade-off shifts towards lower selectivity and higher permeance. The high value of the pH probably results in hydrolysis of TMC or the polyamide bond,[42] and a consequent lower degree of cross-linking. At a pH of 8.7±0.3, lower conversion of the ammonium chloride groups decreases the extent of crosslinking. When TEA is added as a base the trade-off between permeance and selectivity is less pronounced. When the pH of the aqueous POSS solution is changed from mild to strong alkaline conditions, a reduction in the selectivity is observed, while the change in permeance is less pronounced. Different performance trends at similar pH could be attributed to a higher TEA diffusion rate relative to NaOH in the organic phase, causing a pronounced TEA induced TMC hydrolysis.

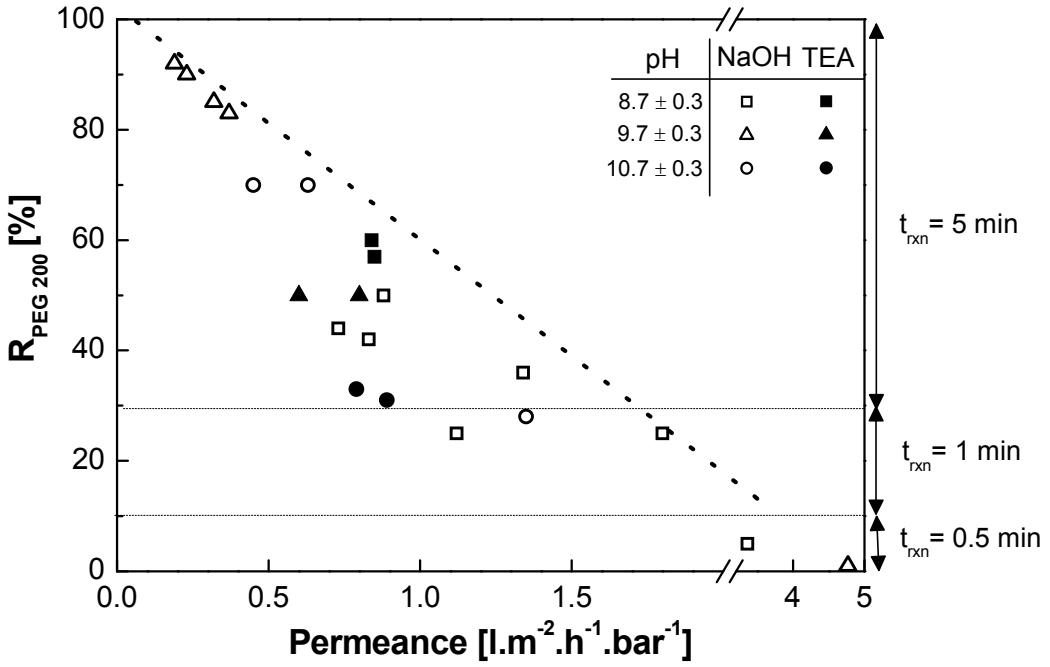

Figure 5: Comparison of mass transport property with molecular separation performance of different membrane prepared at varying reaction conditions

In summary, a method is presented for preparation of ultrathin hybrid films by interfacial polycondensation of polyhedral oligomeric silsesquioxane with a trifunctional acid chloride. The reaction forces an intrinsic homogeneous distribution of inorganic and organic constituents on the molecular scale. Confinement of the reaction to a liquid-liquid inter-phase region allows facile preparation of self-supporting and supported hybrid films with virtually unlimited macroscopic dimensions. The thin films are robust and flexible, and exhibit molecular selectivity in liquid permeation experiments. The presented strategy for film formation can easily be extended to other organic reactants, and to silsesquioxanes decorated with a variety of functional groups. This allows development of a new generation of quasi 2-D hybrid macromolecular networks with amendable chain conformation, and tailored chemical affinity via appropriate choice of the silsesquioxane functional groups.

TABLE S.1: XPS analysis of POSS-polyamide hybrid film

	C				N			O			Si	Cl
	Total C conc. %				**Total N conc. %**			**Total O conc. %**			**Total Si conc. %**	**Total Cl conc. %**
POSS-$NH_3^+Cl^-$ (calculated)	**40**				**13.3**			**20**			**13.3**	**13.3**
POSS-$NH_3^+Cl^-$ (exp.)	**43.4**				**12.95**			**20.18**			**12.29**	**11.18**
Binding energy (BE)		284.8 **(C-C)**	286 **(C-N)**			401.0 **(NH_3Cl)**			532.1 **Si-O-Si)**		102.3 **O-Si-O)**	197.2
% of the total elem. conc. at identified BE.		70%	30%			100%			100%		100%	100%
POSS-polyamide (exp)	**57.40**				**7.78**			**24.84**			**8.07**	**1.91**
Binding energy (BE)		284.7 **(C-C)**	286.0 **(C-N)**	287.9 **(C=O)**		401.3 **(NH_3Cl) / (NH_2)**	399.6 **(NH-C=O)**		532.1 **Si-O-Si)**	531.3 **(O=C)**	102.2 **O-Si-O)**	198.1
% of the total elem. conc. at identified BE.		80.1%	8.2%	11.7%		19.7%	80.3%		63.3 %	36.7%	100%	100%

$C_{calculated} \approx C_{experimental}$, $N_{calculated} \approx N_{experimental}$, $O_{calculated} \approx O_{experimental}$, $Si_{calculated} \approx Si_{experimental}$ & $Cl_{calculated} \approx Cl_{experimental}$

Methods

Scanning electron microscopy (SEM) images were taken using LEO-1550 Schottky field emission scanning electron microscope (Carl–Zeiss, Germany). X-ray photonelectron spectroscopy measurements were performed on Quantera SXM (scanning XPS microprobe) from Physical Electronics. A monochromatic Al Kα source (1486.6 eV) was used at a base pressure less than 10^{-8} torr. XPS peak positions were energy referenced to the C1s peak of aliphatic carbon at 284.8 eV. Attenuated Total Reflection Fourier Transform Infrared Spectroscopy (ATR FT-IR) was done using an ALPHA FT-IR Spectrometer (Bruker Optics Inc, Germany) which is equipped with an ATR diamond crystal. Permeation experiments performed at room temperature in a dead-end filtration setup described previously.[52, 53] The permeance was calculated as the ratio of the flux over the trans-membrane pressure difference (Δp in [bar]):

$$\text{permeance} = \frac{J}{\Delta p} = \frac{V}{At\Delta p}$$

where J is the permeate flux in [L m^{-2} hr^{-1}], V is the permeate volume [L], A is the membrane area in [m^2] and t is the permeation time [hr].

The observed retention R was calculated from

$$R = \frac{c_b - c_{permeate}}{c_b}$$

where c_{permeate} is the average permeate concentration and c_b is the average bulk concentration inside the test cell over the total permeation time t, measured as in our previous work.[52, 53]

References

[1] P. Prosposito, M. Casalboni, F. De Matteis, R. Pizzoferrato, Thin Solid Films 2000, 373, 150-154.

[2] A. Sellinger, P. M. Weiss, A. Nguyen, Y. Lu, R. A. Assink, W. Gong, C. J. Brinker, Nature 1998, 394, 256.

[3] K. Hosono, I. Matsubara, N. Murayama, S. Woosuck, N. Izu, Chemistry of Materials 2004, 17, 349-354.

[4] M. Y. Lo, C. Zhen, M. Lauters, G. E. Jabbour, A. Sellinger, Journal of the American Chemical Society 2007, 129, 5808-5809.

[5] B.-H. Jeong, E. M. V. Hoek, Y. Yan, A. Subramani, X. Huang, G. Hurwitz, A. K. Ghosh, A. Jawor, Journal of Membrane Science 2007, 294, 1-7.

[6] S.-Y. Kwak, S. H. Kim, S. S. Kim, Environmental Science & Technology 2001, 35, 2388-2394.

[7] M. E. Wright, B. J. Petteys, A. J. Guenthner, S. Fallis, G. R. Yandek, S. J. Tomczak, T. K. Minton, A. Brunsvold, Macromolecules 2006, 39, 4710-4718.

[8] D. B. Mitzi, Chemistry of Materials 2001, 13, 3283-3298.

[9] J.-c. Huang, C.-b. He, Y. Xiao, K. Y. Mya, J. Dai, Y. P. Siow, Polymer 2003, 44, 4491-4499.

[10] D. B. Cordes, P. D. Lickiss, F. Rataboul, Chemical Reviews 2010, 110, 2081-2173.

[11] G. Li, L. Wang, H. Ni, C. U. Pittman, Journal of Inorganic and Organometallic Polymers 2001, 11, 123-154.

[12] H. Ghanbari, A. de Mel, A. M. Seifalian, International Journal of Nanomedicine 2011, 6, 775–786.

[13] K. Pielichowski, J. Njuguna, B. Janowski, J. Pielichowski, in Supramolecular Polymers Polymeric Betains Oligomers, Vol. 201, Springer Berlin / Heidelberg, 2006, pp. 225-296.

[14] D. Xu, L. S. Loo, K. Wang, Journal of Polymer Science Part B: Polymer Physics 2010, 48, 2185-2192.

[15] N. L. Le, Y. Wang, T.-S. Chung, Journal of Membrane Science 2011, In Press, Accepted Manuscript.

[16] K. Madhavan, B. S. R. Reddy, Journal of Membrane Science 2009, 342, 291-299.

[17] P. Iyer, G. Iyer, M. Coleman, Journal of Membrane Science 2010, 358, 26-32.

[18] M. Z. Asuncion, R. M. Laine, Macromolecules 2007, 40, 555-562.

[19] S. Wu, T. Hayakawa, M.-a. Kakimoto, H. Oikawa, Macromolecules 2008, 41, 3481-3487.

[20] M. Oaten, N. R. Choudhury, Macromolecules 2005, 38, 6392-6401.

[21] P.-Y. Mabboux, K. K. Gleason, Journal of The Electrochemical Society 2005, 152, F7-F13.

[22] G. Wu, Z. Su, Chemistry of Materials 2006, 18, 3726-3732.

[23] Y. Kim, F. Zhao, M. Mitsuishi, A. Watanabe, T. Miyashita, Journal of the American Chemical Society 2008, 130, 11848-11849.

[24] P. W. Morgan, Condensation Polymers: By Interfacial and Solution Methods, Wiley-Interscience, New York, 1965.

[25] Y. Yeo, N. Baek, K. Park, Biotechnology and Bioprocess Engineering 2001, 6, 213-230.

[26] Q. Sun, Y. Deng, Journal of the American Chemical Society 2005, 127, 8274-8275.

[27] D. Saihi, I. Vroman, S. Giraud, S. Bourbigot, Reactive and Functional Polymers 2006, 66, 1118-1125.

[28] S. L. Poe, M. KobaÅ¡lija, D. T. McQuade, Journal of the American Chemical Society 2007, 129, 9216-9221.

[29] R. J. Petersen, Journal of Membrane Science 1993, 83, 81-150.

[30] J. Huang, S. Virji, B. H. Weiller, R. B. Kaner, Journal of the American Chemical Society 2002, 125, 314-315.

[31] D. D. Sawall, R. M. Villahermosa, R. A. Lipeles, A. R. Hopkins, Chemistry of Materials 2004, 16, 1606-1608.

[32] H. Gao, T. Jiang, B. Han, Y. Wang, J. Du, Z. Liu, J. Zhang, Polymer 2004, 45, 3017-3019.

[33] S. Yang, H. Liu, Journal of Materials Chemistry 2006, 16, 4480-4487.

[34] J. Lei, W. Liang, C. J. Brumlik, C. R. Martin, Synthetic Metals 1992, 47, 351-359.

[35] M. Fathizadeh, A. Aroujalian, A. Raisi, Journal of Membrane Science 2011, 375, 88-95.

[36] M. L. Lind, A. K. Ghosh, A. Jawor, X. Huang, W. Hou, Y. Yang, E. M. V. Hoek, Langmuir 2009, 25, 10139-10145.

[37] H. S. Lee, S. J. Im, J. H. Kim, H. J. Kim, J. P. Kim, B. R. Min, Desalination 2008, 219, 48-56.

[38] S. Y. Lee, H. J. Kim, R. Patel, S. J. Im, J. H. Kim, B. R. Min, Polymers for Advanced Technologies 2007, 18, 562-568.

[39] K. Mallick, M. J. Witcomb, R. Erasmus, M. S. Scurrell, Materials Science and Engineering: B 2007, 140, 166-171.

[40] G. L. Jadav, P. S. Singh, Journal of Membrane Science 2009, 328, 257-267.

[41] R. Vendamme, S.-Y. Onoue, A. Nakao, T. Kunitake, Nat Mater 2006, 5, 494-501.

[42] B. Tang, Z. Huo, P. Wu, Journal of Membrane Science 2008, 320, 198-205.

[43] J.-Q. Liu, Z.-L. Xu, X.-H. Li, Y. Zhang, Y. Zhou, Z.-X. Wang, X.-J. Wang, Separation and Purification Technology 2007, 58, 53-60.

[44] I.-C. Kim, J. Jegal, K.-H. Lee, Journal of Polymer Science Part B: Polymer Physics 2002, 40, 2151-2163.

[45] A. K. Ghosh, B.-H. Jeong, X. Huang, E. M. V. Hoek, Journal of Membrane Science 2008, 311, 34-45.

[46] H. Wang, Q. Zhang, S. Zhang, Journal of Membrane Science 2011, In Press, Corrected Proof.

[47] F. J. Feher, R. Terroba, J. W. Ziller, Chemical Communications 1999, 2309-2310.

[48] S. Wu, T. Hayakawa, R. Kikuchi, S. J. Grunzinger, M.-a. Kakimoto, H. Oikawa, Macromolecules 2007, 40, 5698-5705.

[49] H. Cai, X. Zhang, K. Xu, H. Liu, J. Su, X. Liu, Z. Fu, Y. Guo, M. Chen, Polymers for Advanced Technologies 2010, n/a-n/a.

[50] Z. Zhang, G. Liang, T. Lu, Journal of Applied Polymer Science 2007, 103, 2608-2614.

[51] H. B. Park, B. D. Freeman, Z.-B. Zhang, M. Sankir, J. E. McGrath, Angewandte Chemie 2008, 120, 6108-6113.

[52] M. Dalwani, N. E. Benes, G. Bargeman, D. Stamatialis, M. Wessling, Journal of Membrane Science 2010, 363, 188-194.

[53] M. Dalwani, N. E. Benes, G. Bargeman, D. Stamatialis, M. Wessling, Journal of Membrane Science 2011, 372, 228-238.

Conclusions, Implications and future perspectives

6.1 Conclusions

In **Chapter 2** a new method based on Gel permeation chromatography (GPC) has been presented that allows molecular weight cut off (MWCO) analysis of nanofiltration (NF) membranes as a function of pH. It is elucidated that by appropriate modification of the ion content of GPC samples obtained at various pH, changes in membrane performance with respect to pH can be monitored quantitatively. The significance of the method has been illustrated by applying it to a commercially available NF membrane (NF-270, DOW FILMTEC™) in the pH range of 2-12. Reversible changes with respect to pH have been observed that could be related qualitatively to the ionic strength of the feed solution and the zeta potential curve of the membrane.

Chapter 3 illustrates the effect of pH on the performance of in-house developed thin film composite (TFC) NF membranes. TFC polyamide NF membranes in this chapter have been fabricated on a polyacrylonitrile support via interfacial polymerization (IP) between piperazine and trimesoyl chloride. Effects of some fabrication parameters that were found to have a crucial effect on the membrane NF performance are discussed. Membranes prepared using the most optimal parameters showed NF performance comparable to commercially available, IP based, NF membranes like NF-270 (DOW FILMTEC™) and Desal-5DK. The MWCO of the developed membranes was determined in the pH range of 1-13 using the method developed in Chapter 2. The cut-off appeared to be practically constant in acidic and neutral conditions. At extremely alkaline conditions (pH > 11) an increase in MWCO and a reduction in membrane flux were observed. In order to relate the changes in performance to changes in the structural properties of the membranes, the Donnan steric partitioning pore model (DSPM) was applied to the permeation data. The model suggests that these membranes have a higher effective average pore size and a lower effective porosity in alkaline conditions as compared to the other pH conditions. These changes in the pore size and porosity are attributed to the higher surface charge and presence of Na^+ and OH^- in alkaline conditions.

Chapter 4 diverts from IP based membranes and explores the feasibility of sulfonated poly (ether ether ketone) (SPEEK) membranes in applications involving extreme pH conditions. Here TFC's were prepared by spin coating SPEEK solutions on polyethersulfone (PES) supports, followed by appropriate thermal curing. The developed membranes revealed excellent stability in the entire pH range from 0- 14, even under prolonged exposure (up to several weeks). An evaluation of the membrane fabrication parameters shows that post treatment via thermal curing is vital. A set of membranes prepared using the most optimal fabrication conditions demonstrates at neutral pH a molecular weight cut-off of ~ 500 g mol^{-1} and a divalent salt retention of 85-95%, which is characteristic of tight nanofiltration membranes. The water permeance of this set is higher than commercially available pH stable membranes (MPF-34 and NP030P) and similar to Desal-5-DK, a commercial high performance IP based membrane. Permeance and MWCO analysis at varying pH indicates that charge effects induce reversible changes in the membrane properties. Especially at strongly alkaline conditions the developed membrane appears to be more open. These performance variations are explained by changes in membrane due to different interactions between the ions in the feed solutions and the resulting membrane charge density at different pH. Further in this chapter the possibility to crosslink the SPEEK network to develop even tighter NF membranes has been addressed. However covalent cross linking by the Friedel-Crafts route at higher temperatures was prohibited by the limited thermal stability of the polymeric ultrafiltration supports used in this work.

Chapter 5 exploits the IP technique to create novel hybrid TFCs with Polyhedral oligomeric silsesquioxanes (POSS) as the primary building blocks. POSS cages have been linked together via the classical polycondensation chemistry widely used for IP polyamide membrane fabrication. The concept was illustrated using a water soluble quaternary ammonium chloride salt functionalized POSS (POSS-$NH_3^+Cl^-$) as the aqueous phase monomer, and trimesoyl chloride (TMC) as the organic phase (hexane) monomer. The complete reaction synthesis was completed in a two steps. In the first step POSS-$NH_3^+Cl^-$ was converted to POSS-NH_2 (Octa(aminopropyl)silsesquioxane) via dilute alkaline solutions. In the second step the IP reaction was performed between POSS-NH_2 in the aq. phase and TMC in

the organic (hexane) phase resulting in a thin film POSS-polyamide hybrid network. Both, free standing as well as substrate supported films could be obtained. In depth analysis to prove the chemistry was carried out via Fourier transform infrared spectrometry and X-ray photoelectron spectroscopy. The effect of fabrication parameters like the reaction time and the amount / type of base in the reaction mixture was evaluated by permeation experiments on the substrate supported films. The tightest hybrid matrix revealed a MWCO of 200 g mol^{-1} in polyethylene glycol - water system and 1000 g mol^{-1} in polystyrene – toluene system.

6.2 Implications and future perspectives

Several huge industries like the chlor alkali, paper and pulp and mining industries involve acidic and alkaline aqueous effluents where nanofiltration membranes are frequently applied. The molecular weight cut-off method developed in **chapter 2** allows in-situ characterization at conditions in which membranes are likely to be applied. In subsequent chapters (**Chapter 3 and 4**) it has been shown that the method is in fact applicable to a range of commercial to in-house made membranes. Reversible changes in the performance could be observed for many membranes with the help of this method, and could be correlated to variation in membrane morphology at different pH conditions. Such dependence of the membrane performance on pH of the feed solution could be crucial, and therefore must be taken into account while using the membranes in applications involving operation at extreme pH conditions. Such a tool can further aid development of new membranes for the above mentioned applications, since performance in the final application can easily be predicted via these simulated measurements. Moreover the application window of numerous presently available membranes can be broadened by using this method to determine how these would perform during extreme pH conditions.

Well established theoretical models can make use of the performance data obtained from such an in-situ method to interpret the change in membrane performance as a function of pH. **Chapter 2** demonstrates how the Donnan

Sterric Partitionaing Pore model (DSPM) can relate changes in flux and uncharged molecules retention to theoretical pore size and porosity at respective pH. Further study could benefit from use or development of advanced models that also incorporate the variation of surface charge during filtration with acidic or alkaline feeds.

Fabrication of membranes via IP can be complicated by the surface properties and the broad pore size distribution of the ultrafiltration support membranes. A uniform impregnation of the aqueous phase monomer throughout the ultra-porous surface is vital for defect free membrane fabrication, since these will be the sites where the organic phase monomer attaches to form the layer responsible for nanofiltration. The vacuum and surfactant SDS employed during membrane fabrication in **chapter 3** ensures complete impregnation of large as well as small pores, thereby eliminating creation of any vacant sites that could cause these defects. Such approaches help to attain a very precise control on the IP fabrication procedure, making it more or less independent of the support membrane. Using the described procedure, investigation of completely different supports for the IP reaction could be performed, for e.g. the use of structured membranes (Figure 1) as supports which would provide a much higher surface to length ratio [1].

a)

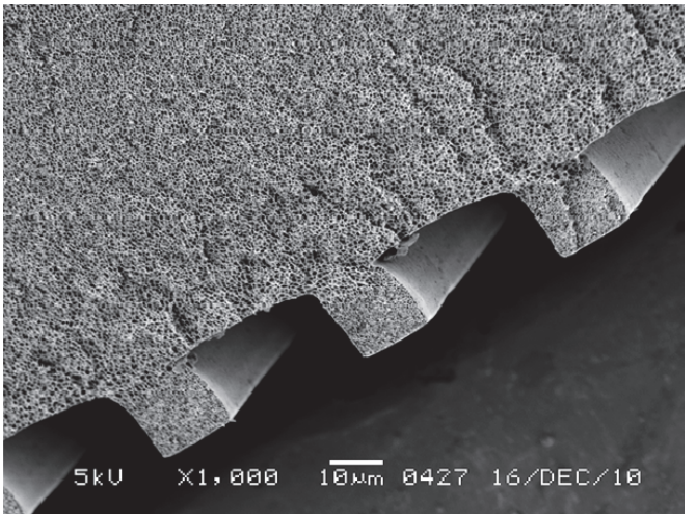

b)

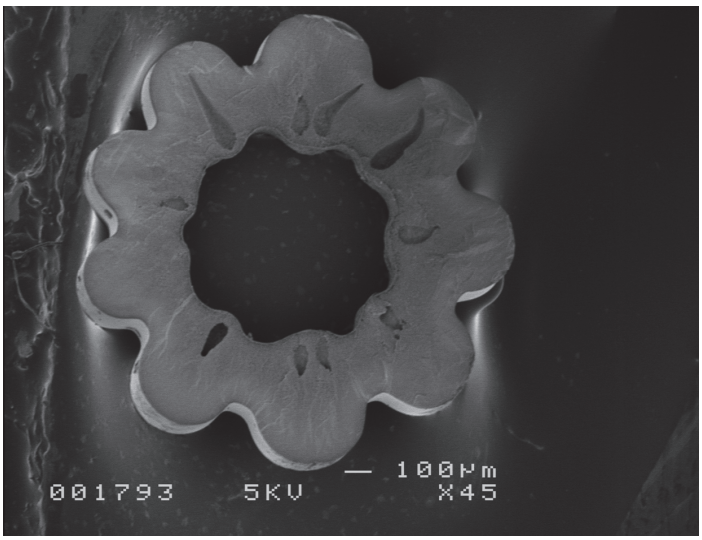

c)

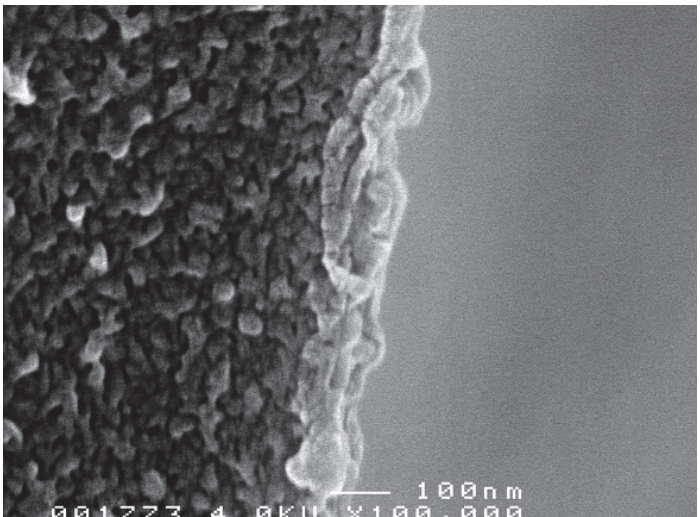

Figure 1 : Structured membranes fabricated via phase separation microfabrication a) Flat sheet configeration b) Hollow fiber configeration (fibers kindly obtained from Dr. P.Z. Çulfaz) c) IP layer on a structured support

The use of vacuum in such supports could be vital since this would ensure a homogeneous layer in the ridges and valleys of the microscopic structure, since the valleys would normally tend to encompass a thicker aqueous phase layer on the membrane surface, as compared to the ridges. When IP is performed on this thicker aqueous phase layer the resulting nanometer scale IP film will probably

not laminate directly on the support. A preliminary study of IP reaction on such supports also concluded that a relatively homogenous and defect free layer could be formed when vacuum was employed during fabrication.

The IP process however is restricted by the fact that it requires two highly reactive monomers which have to be soluble individually in two immiscible phases. This limits the use of copiously available chemistry that could generate cross-linked polymer networks capable of substantial pH stability. This is probably the reason that although membranes fabricated via the IP process are available since 1980's, all new "recipes" still revolve around the polyamide chemistry. Even though these IP based membranes have a proven good track record of performance in NF, and some improvements can still be made by altering the fabrication parameters, the pH stability of any polyamide is unlikely to exceed a value of 13 or 14. Thus for applications involving harsher alkaline conditions, completely new materials that are inert to hydrolysis should be sought. Sulfonated polymers which have established significant utility as membranes for fuel cells [2] and electrodialysis [3] applications could become excellent alternatives to traditional polyamides in NF. Such materials can simply be coated on suitable substrates to generate high performance TFC membranes. Although this concept is proved on SPEEK based TFCs (**Chapter 4**) which show sufficient permeance compared to polyamides, there is still room for improvement in retention characteristics, by for e.g. crosslinking the SPEEK layer. However a crosslinking approach, such as the one addressed in **Chapter 4**, requires thermal curing at high temperatures. Accordingly thermal stable substrates such as inorganic membranes could be thought as suitable support membranes for such processing. Inorganic membranes with high porosity but low pore size such as γ-alumina membranes coated on α-alumina supports (Figure 2) could be suitable alternatives to the polyethersulfone membranes used in **Chapter 4**.

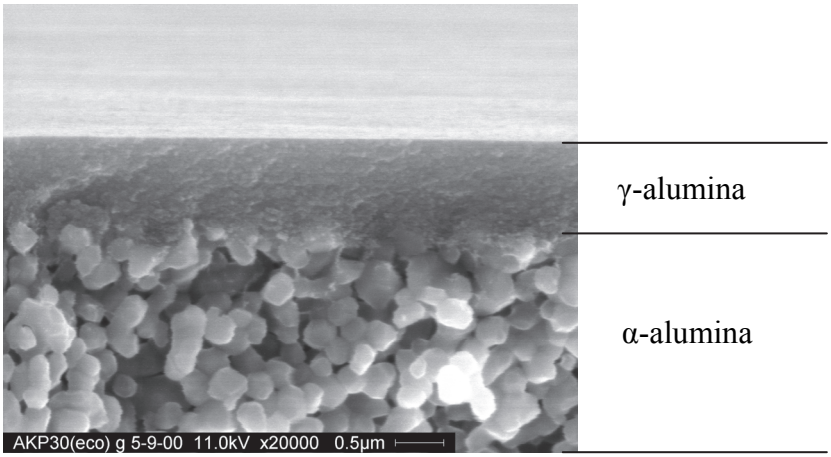

Figure 2: Thermal stable supports: highly porous γ-alumina coated on α-alumina supports

Alternatively SPEEK could be prepared by direct polymerization of sulfonated monomers instead of the traditional post sulfonation route [4]. Such a process would give different polymer matrix that is devoid of problems side reactions or molecular weight degradation which would help in improving the retention as well as flux. In addition such synthesis also allows incorporation of photo-initiator groups in the monomers before SPEEK formation that allows crosslinking of the final matrix via mild conditions like UV irradiation [5]. Further optimization of the polymer matrix to enhance the NF performance could also be achieved using a variety of techniques like blending SPEEK with non sulfonated polymers [6, 7] or inorganic particles [8, 9]. Thus after the proof of principle demonstrated in **Chapter 4,** all the above mentioned sulfonated polymer systems could become potential candidates for pH stable NF applications.

The technique of IP on the other hand can be utilized to explore options to fabricate novel thin layers with new monomers. The concept illustrated in **chapter 5** unlocks one such possibility, by fabrication of a hybrid layer comprising of inorganic cage like materials (POSS) linked together via amide bonds. Studies have already demonstrated advantages of incorporating particles like zeolite [10-12], titanium dioxide [13], silver [14], gold [15], silica [16] etc. within thin IP layer. However in all these cases the inorganic nanoparticles are primarily inert fillers which do not participate in IP reaction, but are just physically dispersed within the matrix. Consequently the problem of leaking via interstitial voids cannot be

completely ruled out [10, 11]. Thus connecting functionalized inorganic POSS molecules via polyamide linkages by IP could be a suitable solution to fill up possible interstitial voids or defects. Such hybrid films could have remarkably different properties compared to pure polyamide films prepared via IP. Pure polyamide films result in hydrophilic surfaces and thereby primarily used in aqueous applications. Hybrid films prepared via the same technique encompass hydrophobic hard segments (POSS), and consequently allow permeation of even hydrophobic solvents such as toluene. Further the charge behavior of the hybrid films also seems to be considerably unusual. Figure 3 shows that the isolectric point of one the POSS-polyamide films are significantly higher as compared to other polyamide films, possibly due a few of the unreacted NH_3^+ groups still present on the T8 POSS structure. Presumably if all the NH_3^+ groups are converted to NH_2 the IEP would shift to a lower value close the standard polyamides. Nevertheless this extra degree of freedom to modify the surface charge could be utilized for different applications for e.g. retention of positively charged anions.

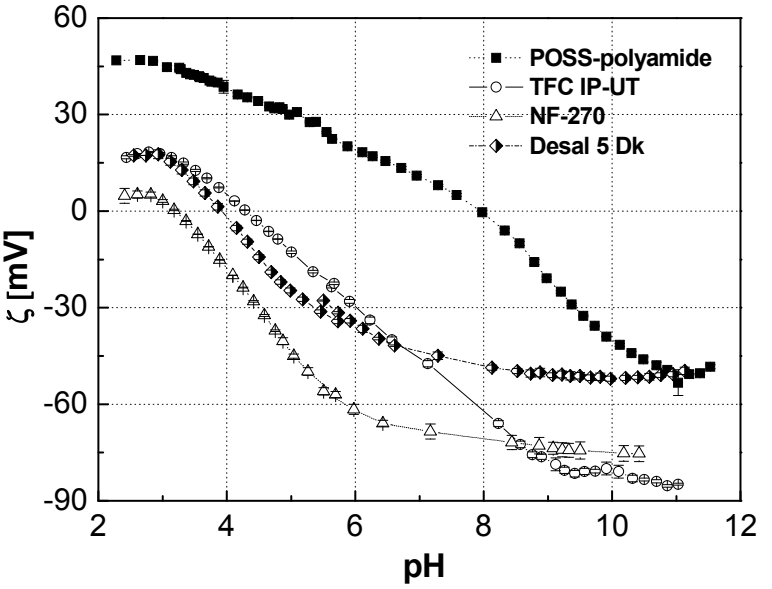

Figure 3: Zeta potential curves of POSS-polyamide compared to standard polyamide membranes

The basic concept illustrated in **chapter 5** could be extended to a variety of widely available POSS molecules and different crosslinkers (depending on functional groups on POSS). Thus a complete new range of hybrid free standing or substrate supported films could be developed for a variety of applications even beyond membrane technology. Use of such hybrid films in microelectromechanical devices in the form of sensors or actuators, coatings in the automobile industry or microencapsulation for drug delivery could become directions for future research.

References

[1] P.Z. Çulfaz, Microstructured hollow fibers and microsieves; fabrication, characterization and filtration applications, Ph.D. thesis, University of Twente, 2011.

[2] A.J. Appleby, J. Twidell, Recent Developments and Applications of the Polymer Fuel Cell [and Discussion], Philosophical Transactions: Mathematical, Physical and Engineering Sciences, 354 (1996) 1681-1693.

[3] E. Vallejo, G. Pourcelly, C. Gavach, R. Mercier, M. Pineri, Sulfonated polyimides as proton conductor exchange membranes. Physicochemical properties and separation H+/Mz+ by electrodialysis comparison with a perfluorosulfonic membrane, Journal of Membrane Science, 160 (1999) 127-137.

[4] H.B. Park, B.D. Freeman, Z.-B. Zhang, M. Sankir, J.E. McGrath, Highly Chlorine-Tolerant Polymers for Desalination, Angewandte Chemie, 120 (2008) 6108-6113.

[5] S. Zhong, C. Liu, H. Na, Preparation and properties of UV irradiation-induced crosslinked sulfonated poly(ether ether ketone) proton exchange membranes, Journal of Membrane Science, 326 (2009) 400-407.

[6] H. Zhang, X. Li, C. Zhao, T. Fu, Y. Shi, H. Na, Composite membranes based on highly sulfonated PEEK and PBI: Morphology characteristics and performance, Journal of Membrane Science, 308 (2008) 66-74.

[7] O.D. Thomas, T.J. Peckham, U. Thanganathan, Y. Yang, S. Holdcroft, Sulfonated polybenzimidazoles: Proton conduction and acid–base crosslinking, Journal of Polymer Science Part A: Polymer Chemistry, 48 (2010) 3640-3650.

[8] M.L. Di Vona, E. Sgreccia, A. Donnadio, M. Casciola, J.F. Chailan, G. Auer, P. Knauth, Composite polymer electrolytes of sulfonated poly-ether-ether-ketone (SPEEK) with organically functionalized TiO2, Journal of Membrane Science, 369 (2010) 536-544.

[9] S. Feng, Y. Shang, G. Liu, W. Dong, X. Xie, J. Xu, V.K. Mathur, Novel modification method to prepare crosslinked sulfonated poly(ether ether ketone)/silica hybrid membranes for fuel cells, Journal of Power Sources, 195 (2010) 6450-6458.

[10] M. Fathizadeh, A. Aroujalian, A. Raisi, Effect of added NaX nano-zeolite into polyamide as a top thin layer of membrane on water flux and salt rejection in a reverse osmosis process, Journal of Membrane Science, 375 (2011) 88-95.

[11] M.L. Lind, A.K. Ghosh, A. Jawor, X. Huang, W. Hou, Y. Yang, E.M.V. Hoek, Influence of Zeolite Crystal Size on Zeolite-Polyamide Thin Film Nanocomposite Membranes, Langmuir, 25 (2009) 10139-10145.

[12] B.-H. Jeong, E.M.V. Hoek, Y. Yan, A. Subramani, X. Huang, G. Hurwitz, A.K. Ghosh, A. Jawor, Interfacial polymerization of thin film nanocomposites: A new concept for reverse osmosis membranes, Journal of Membrane Science, 294 (2007) 1-7.

[13] H.S. Lee, S.J. Im, J.H. Kim, H.J. Kim, J.P. Kim, B.R. Min, Polyamide thin-film nanofiltration membranes containing TiO2 nanoparticles, Desalination, 219 (2008) 48-56.

[14] S.Y. Lee, H.J. Kim, R. Patel, S.J. Im, J.H. Kim, B.R. Min, Silver nanoparticles immobilized on thin film composite polyamide membrane: characterization, nanofiltration, antifouling properties, Polymers for Advanced Technologies, 18 (2007) 562-568.

[15] K. Mallick, M.J. Witcomb, R. Erasmus, M.S. Scurrell, Hydrophilic behaviour of gold-poly (o-phenylenediamine) hybrid nanocomposite, Materials Science and Engineering: B, 140 (2007) 166-171.

[16] G.L. Jadav, P.S. Singh, Synthesis of novel silica-polyamide nanocomposite membrane with enhanced properties, Journal of Membrane Science, 328 (2009) 257-267.

Summary

The research presented in this thesis focuses on development and performance evaluation of thin film composite (TFC) nanofiltration (NF) membranes, with special attention to extreme pH applications.

Chapter 1 gives a general introduction to the topic, highlighting a list of applications that can benefit from development and performance evaluation of pH stable membranes. The different fabrication methods that are exploited in this work for fabrication of TFC membranes are introduced, including their respective adjustable parameters.

In **Chapter 2** a new method that allows molecular weight cut off (MWCO) characterization of NF membranes as a function of pH is presented. It is elucidated that by appropriate modification of the ion content of GPC samples obtained at various pH, changes in membrane performance with respect to pH can be monitored quantitatively. Performance evaluation of a well-known commercial NF membrane (NF-270, Dow Filmtec™) via this method reveals reversible changes with respect to pH, signifying the relevance of performance characterization at the relevant conditions. The developed method is thus also used in the following chapters for characterization of in-house developed NF membranes.

In **Chapter 3** the above mentioned method illustrates the effect of pH on the performance of in-house developed polyamide TFC NF membranes, fabricated via the interfacial polymerization (IP) route. Following an investigation of optimal fabrication parameters the performance of the developed membranes has been compared to commercial NF membranes currently used in the industry. Using the Donnan steric partitioning pore model, the pH induced performance changes have been correlated to morphological changes in the membrane matrix, i.e., changes in the effective average pore size and effective porosity of the membrane.

TFC's presented in **Chapter 4** were prepared by spin coating sulfonated poly (ether ether ketone) (SPEEK) solutions on ultraporous polyethersulfone (PES) supports. The optimal fabrication parameters required for obtaining stable membranes were determined and the resulting performance was benchmarked

against several commercial NF membranes. Additionally in this chapter a technique to crosslink SPEEK to enhance membrane retention is briefly addressed. The developed membranes reveal excellent stability in the entire pH range from 0-14, even under prolonged exposure (up to several weeks). Permeance and MWCO analysis at varying pH (via method of **Chapter 1**) indicate that charge effects induce reversible changes in the membrane properties.

In **Chapter 5** novel hybrid TFC membranes containing Polyhedral oligomeric silsesquioxanes (POSS) are presented. Inorganic POSS cages have been linked together via the classical polycondensation chemistry widely used for IP polyamide membrane fabrication. Both, free standing as well as substrate supported films could be obtained. In depth analysis to confirm the chemistry was carried out via Fourier transform infrared spectrometry and X-ray photoelectron spectroscopy. NF permeation experiments were performed on the substrate supported films and the effect of some important fabrication parameters are discussed.

Samenvatting

Het onderzoek in dit proefschrift richt zich op de ontwikkeling en evaluatie van de prestaties van dunne film composiet (TFC) nanofiltratie (NF) membranen, met speciale aandacht voor toepassingen bij extreme pH.

Hoofdstuk 1 geeft een algemene inleiding op het onderwerp. Een aantal toepassingen wordt geïntroduceerd waarvoor pH stabiele membranen van grote toegevoegde waarde zouden zijn. Verschillende fabricagemethodes, geselecteerd voor de vervaardiging van TFC membranen, worden geïntroduceerd. Het effect van de instelbare parameters wordt besproken.

In **Hoofdstuk 2** wordt een nieuwe methode gepresenteerd die het mogelijk maakt om de bepaling van de moleculaire gewicht afsnede (MWCO) van NF membranen als functie van de pH uit te voeren. Bij de methode worden de iongehaltes van het eluent en geneutraliseerde GPC monsters op elkaar afgestemd. Met de methode kunnen veranderingen in membraanprestaties als functie van de pH kwantitatief worden bepaald. Evaluatie van de prestaties van een bekend commercieel verkrijgbaar membraan (NF-270, Dow Filmtec™) als functie van de pH laat omkeerbare veranderingen zien. Dit benadrukt de relevantie van de prestatie-evaluatie onder relevante condities. De ontwikkelde methode wordt gebruikt in de volgende hoofdstukken voor de karakterisering van de in die hoofdstukken ontwikkelde membranen.

In **Hoofdstuk 3** illustreert de bovenstaande methode het effect van de pH op de ontwikkelde polyamide TFC-NF membranen die middels grensvlakpolymerisatie (IP) zijn gemaakt. Na het in kaart brengen van de optimale fabricageparameters zijn de prestaties van de ontwikkelde membranen vergeleken met industrieel toegepaste commercieel verkrijgbare NF membranen. Middels het Donnan sterische verdelingsmodel zijn de door de pH geïnduceerde prestatieveranderingen gecorreleerd aan de morfologische veranderingen in de matrix, d.w.z. veranderingen in de effectieve poriegrootte en effectieve porositeit van het membraan.

De TFC's gepresenteerd in **Hoofdstuk 4** werden gemaakt door middel van spin-coating van gesulfoneerd poly (ether ether keton) (SPEEK) oplossingen op ultra-

poreuze polyethersulfon (PES) steunlagen. De geoptimaliseerde fabricageparameters, benodigd om stabiele membranen te verkrijgen, zijn bepaald. De resulterende membraanprestaties zijn afgezet tegen verschillende commercieel verkrijgbare NF membranen. Daarnaast wordt in dit hoofdstuk een techniek aangestipt om SPEEK te cross-linken. De ontwikkelde membranen laten een uitmuntende stabiliteit zien in het volledige pH bereik van 0-14, zelfs onder langdurige blootstelling (tot enkele weken). De permeatie en MWCO analyse bij variërende pH (via de methode van **Hoofdstuk 1**) geven aan dat ladingseffecten omkeerbare veranderingen in membraaneigenschappen veroorzaken.

In **Hoofdstuk 5** worden nieuw ontwikkelde hybride TFC membranen met polyhedrale oligomere silsesquioxanen (POSS) gepresenteerd. Anorganische POSS kooien werden aan elkaar verbonden via klassieke polycondensatiechemie die breed verbreid gebruikt wordt voor IP polyamide membraanbereiding. Zowel vrijstaande als substraat-ondersteunde films konden worden verkregen. Diepgaande analyse om de chemie te bevestigen werd uitgevoerd via Fourier getransformeerde infrarood-spectroscopie en Röntgen fotoelectron-spectroscopie. NF permeatie-experimenten werden uitgevoerd op de substraat gedragen films en het effect van enkele belangrijke fabricageparameters wordt bediscussieerd.

Acknowledgements

The last 4 years have truly been the most remarkable ones of my life. Looking back I'm convinced that doing a PhD was the one of the best decisions I've made (including my marriage, ofcourse ☺). Although at times it was a rollercoaster ride, I have been very lucky with friends and colleagues who helped me enjoy this journey. So I would like to thank everyone who helped making my stay in Enschede an incredible one.

Matthias: I would like to thank you for giving me the opportunity to work in Twente. I still remember our conversation on the phone, while rushing to catch my last train after my interview. Over the years we have had many formal and informal conversations. Thank you for all your PhD-related as well as personal advices and for always believing in me. I appreciate all the efforts that you put in my development and supervision. I've learnt a lot from you and it was a pleasure to work with you.

Nieck: I am grateful for all the help and guidance you have given me in the last years. I have great respect for you in both aspects; as a researcher as well as a person. Dr. Benes you have been crucial in building my self-confidence in these eventful years. As I have often told you that after our weekly meetings I used to feel extremely relaxed, which helped me enjoy my work. Thanks your constant confidence in my work and for encouraging me to start writing while measuring. I think I could not have completed my PhD so smoothly in time without your help and supervision. I value your efforts in improving my writing (I hope you finally feel that you have succeeded☺) and your advice in dealing with scientific, non-scientific, bureaucratic and personal issues. I appreciate the fact that you think from a student's point of view. It was fun partying & drinking with you in Amsterdam this summer, but we have to still take our drinking to the next level. So be prepared for 11/11/11.

In the last months I worked closely with Jumeng (cool name: Dr. Zheng). Dr Zheng thanks for your efforts and time (long evenings). Please pass my apologies to your wife who thought you were having an affair with someone instead of

working with me in the lab. It was a lot of fun working with you and thanks for your constant motivation and support.

I would also like to thank Mark Hempenius for his help with the POSS chemistry and for several other scientific discussions. Another person who contributed to this work in the last months is Marcel Boerrigter. Thanks for all your efforts in the measurements and your smart ideas to do things more efficiently. I would also like to thank Marcel Beijeman for his contribution with to this work. It was great to have an independent student like you. Jonathan (Tingle.nl ☺) thanks for spicing up this work with your animations and drawings.

I was working in a DSTI project where I worked closely with many people. Gerrald I would like to thank you for all your help and support all these years. Your scientific input has been very crucial in my PhD work. I appreciate the time you spent on fruitful scientific discussions and in refining my publications. Dimitris thanks for guiding me in the initial years and for your support throughout as a project leader. Arian, thanks for all the inputs in the last four years and for your confidence in my work. I would also like to thank Petrus Cuperus, Menno Plantenga, Rob Kreiter, Louis Winnubst and Jaap Vente for their support and encouragement.

I would like to thank all the members in the MTG group for making it a fun place in addition to a high quality scientific environment. John thanks your help with building my setups and numerous things in the lab. Harmen, thanks for all the scientific and social discussions. From the very beginning I learnt a lot from you (dispensation, experimental procedures, safety rules…) and I am grateful for all your help. Greet thank you very much for guiding me through the procedures and paperwork. I also appreciate your help that you have given on a personal level. I would also like to thank all my officemates including Jorrit, Hans, Szymon and Irdham for creating a fantastic atmosphere to work. Szymon you have been my partner in this crime. Thanks for all your help, especially with the cover. It was great to have worked so closely with you and finally also defend with you on the same day.

I would like to thank Joris and Alisia for many scientific discussions and filling out tax forms (I don't know who will help me out next April); Enver, Olga, Christina,

Jeroen, Marcel ten Hove, Emiel and Anne Corine for an excellent working and partying atmosphere ☺; Wojciech for several discussions on ellipsometry and spin coating; Al-Hadidi for sharing a common love for the SURPASS and for your company on weekends; Erik, Herman, Wika and Rob Betlman for the help with GPC, SEM and many other things in the lab. Harro & Imre, Nico & Caro, Can & Laura, Nazeley and Ana, thanks for the nice times we have had together. Harro & Imre thanks for helping us with the couch hunting and other shopping. Maik, Hakan (non-smoker), Jens, Matias, Gerard, Elif, Nilesh and Can for the entertaining "rauchen" breaks. Can it was great to have you as a companion these years especially in the concept submission phase. Mieke thanks for your help in so many things in the lab from inorganic supports to SEM pictures and also for the nice time together at the conferences. Hammad, Martin, Frank, Sander, Joao, David-Yuja, Gregory, Susanne and Henny, thanks for the discussions and great time we have had together. I would like to thank Kitty, Zandrie and Antoine for a pleasant and safe working atmosphere.

Jigar & Falguni, Pravin uncle & Seema aunty and Srivatsa you have been like my family here in the Netherlands. Thank you for the nice dinners, outings and events. I was never home sick thanks to the Indian community in Enschede. Thanks to all of you especially Jeetu-Lavanya, Sandeep-Jalaja, Chandu-Meenakshi, Pallavi-Reddy, Anindita-Supriyo, Giri-Varsha, Shodhan-Chaithanya, Dhaval-Hinal, Shilpa, Omkar, Shashank and Hemant.

My family has been very important as a moral support at every stage of my PhD, even if they were continents away. Mama and Papa thanks for the continuous encouragement and motivation. Although I understand your old age and the strong Dutch winter, I will miss you both a lot during the defence. Sandeep my brother: thank you for all the help, encouragement and moral support. I want to also thank Shraddha's parents and Tamz for their constant support.

And now the most important person of my life: my wife Tina. How can I ever thank you for all that you have done for me? I am very lucky to have you in my life. You have been my strength in these years. Motivating me when things are rough, cheering me up me when I've had a bad day in the lab, taking care that I've

had my food ☺, sacrificing everything in India and starting a new life here with me. Thank you for everything. I love you baby!